NASA Contractor Report 166025

(NASA-CR-166025) A STUDY OF AERODYNAMIC HEATING DISTRIBUTIONS ON A TIP-FIN CONTROLLER INSTALLED ON A SPACE SHUTTLE ORBITER MODEL Final Report (Calspan Advanced Technology Center) 102 p

N83-20997

Unclas
G3/18 03179

A STUDY OF AERODYNAMIC HEATING DISTRIBUTIONS ON A TIP-FIN CONTROLLER INSTALLED ON A SPACE SHUTTLE ORBITER MODEL

Charles E. Wittliff

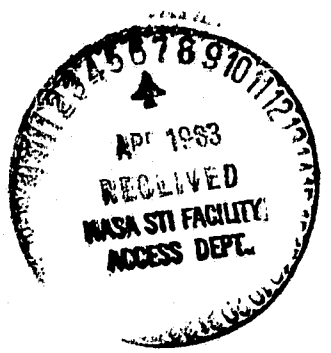

CALSPAN ADVANCED TECHNOLOGY CENTER
Buffalo, New York 14225

Contract NAS1-16618
August 1982

National Aeronautics and
Space Administration

Langley Research Center
Hampton, Virginia 23665

FOREWORD

This is the Final Report on a study of aerodynamic heating distributions on a tip-fin controller installed on a Space Shuttle Orbiter model. This study was conducted by the Aerodynamic Research Department of the Calspan Advanced Technology Center and was sponsored by the Langley Research Center of the National Aeronautics and Space Administration under Contract NAS 1-16618. Mr. Charles E. Wittliff of Calspan ATC was the Project Engineer on this program which was monitored by Mr. Delma C. Freeman, Jr. and Ms. Kathryn E. Wurster of NASA LaRC.

TABLE OF CONTENTS

LIST OF TABLES

LIST OF FIGURES

LIST OF FIGURES (Cont'd)

SUMMARY

The aerodynamic heating of a tip-fin controller mounted on a Space Shuttle Orbiter model has been studied experimentally in the Calspan Advanced Technology Center 96-inch Hypersonic Shock Tunnel. A 0.0175-scale model was tested at Mach numbers from 10 to 17.5 at angles of attack typical of a shuttle entry. The study was conducted in two phases. In Phase I testing a thermographic phosphor technique was used to qualitatively determine the areas of high heat-transfer rates. Based on the results of this phase, the model was instrumented with 40 thin-film resistance thermometers to obtain quantitative measurements of the aerodynamic heating.

The results of the Phase II testing indicate that the highest heating rates, which occur on the leading edge of the tip-fin controller, are very sensitive to angle of attack for $\alpha \leq 30°$. The shock wave from the leading edge of the orbiter wing impinges on the leading edge of the tip-fin controller resulting in peak values of h/h_{Ref} in the range from 1.5 to 2.0. Away from the leading edge, the heat-transfer rates never exceed $h/h_{Ref} = 0.25$ when the control surface is not deflected. With the control surface deflected 20°, the heat-transfer rates had a maximum value of $h/h_{Ref} = 0.3$. The heating rates are quite nonuniform over the outboard surface and are sensitive to angle of attack.

INTRODUCTION

As part of a NASA program to investigate improvements to the Space Shuttle Orbiter, the Langley Research Center has conducted preliminary studies which have shown that a tip-fin controller has potential for enhancing the controllability and improving the performance of the orbiter vehicle by providing positive yaw control in the low hypersonic and supersonic speed regime (ref. 1). A potential problem area that must be addressed, as part of a feasibility study of the tip-fin controller application, is the determination of the aerodynamic heating of the controller during entry. Because of the complexity of the flow field, wind-tunnel tests were required to define the aerodynamic heating

distributions. These tests were conducted in the Calspan Hypersonic Shock Tunnel (ref. 2) which provides a unique capability for measuring detailed heating distributions over a range of hypersonic Mach numbers and Reynolds numbers. The results of this experimental heat-transfer investigation are the subject of this report.

Prior to instrumenting a tip-fin controller model with heat-transfer gauges, an initial test phase was undertaken to qualitatively determine the regions of high heat transfer. This Phase I testing utilized a thermographic mapping technique (ref. 3). Aside from the anticipated high heat transfer at the leading edge of the controller, several regions of high and low heat transfer were detected on the outboard surface (ref. 4). The thermographic phosphor technique did not detect variations in heat transfer on the inboard surface even though a region of separated flow was known to exist there. The Phase I test results were used to determine the location of the heat-transfer gauges. The tip-fin model was instrumented with a total of 40 gauges. In addition, two gauges were located on the upper wing surface just inboard of the controller, and there were two gauges on the bottom centerline of the body.

The objective of the Phase II tests was to experimentally measure the aerodynamic heating in sufficient detail to define the tip-fin heating environment and to determine the thermal-protection system requirements. The test program involved 37 test runs at five test conditions and included angles of attack from 25° to 40°. A limited number of runs at small sideslip angles were included also. Tests were conducted with 0° and 20° tip-fin controller deflection.

For the test conditions at nominal Mach numbers of 10, 12.5 and 15, the flight Reynolds number (based on free-stream conditions and body length) was matched in the present tests. At the highest test Mach number of 17.5, the flight Reynolds number could not be duplicated. At this Mach number, tests were performed at two different Reynolds number to provide a basis for extrapolating to the flight condition. The model used in this program was a 0.0175-scale simulation of the Space Shuttle Orbiter.

In the following sections of this report, the Calspan 96-inch Hypersonic Shock Tunnel is described first and is followed by a description of the model and heat-transfer instrumentation. The test conditions and data reduction procedures are discussed prior to presenting and discussing the test results.

In the discussion of the test results, comparisons are made between the thermographic phosphor results of Phase I and the detailed heat-transfer measurements of Phase II. The variations in heat transfer on the outboard surface, that were evident in the qualitative Phase I results, have been quantified by the Phase II results. The aerodynamic heating rate varies by as much as an order of magnitude over this surface in a nonuniform manner. The highest heat transfer occurs, however, along the leading edge of the tip-fin. This heat transfer is strongly influenced by the impingement of the shock wave generated by the leading edge of the orbiter wing. The peak heating on the tip-fin leading edge is sensitive to the angle of attack at $\alpha \leq 30°$.

SYMBOLS

a	speed of sound, ft/s
c	specific heat, BTU/slug-°R
c_p	specific heat at constant pressure, ft-lb/slug-°R
C_H	Stanton number
g	gravitational acceleration, ft/s^2
h	heat-transfer coefficient, lb/ft^2-s
H	enthalpy, ft-lb/slug = ft^2/s^2
J	mechanical equivalent of heat, ft-lb/BTU
k	thermal conductivity, BTU/ft-s-°R

K	gauge sensitivity, Ω/°R
L	length, ft
Le	Lewis number
M	Mach number
p	pressure, psia
P	static-to-total pressure ratio, p/p_o
Pr	Prandtl number
q	dynamic pressure, psia
$\dot{q}$	heat-transfer rate, BTU/ft^2-s
r	recovery factor
R	resistance, Ω, or gas constant, ft-lb/slug-°R
R_N	nose radius, ft
t	time, s
T	temperature, °R
U	velocity, ft/s
x	distance along surface, ft
y	distance normal to surface, ft
Z	compressibility factor
α	angle of attack, deg.
β	sideslip angle, deg.

γ specific heat ratio

δ deflection angle, deg.

μ viscosity, slugs/ft-s

ρ density, slugs/ft^3

ϕ roll angle, deg.

ψ yaw angle, deg.

Subscripts

D dissociation

e edge of boundary layer

i incident shock wave

p perfect gas

Ref stagnation point for a sphere having R_N = 0.0175 ft

w cold wall conditions ($T_w = T_1$)

o free-stream stagnation conditions

1 initial conditions in driven tube

5 theoretical conditions behind a reflected normal shock wave

∞ free-stream conditions

Superscript

' conditions at stagnation point on model

TEST FACILITY

The basic components of the Calspan 96-inch Hypersonic Shock Tunnel (HST) are shown in figure 1. The tunnel employs a chambered shock tube with an area ratio (driver/driven) of 1.56. The 5-inch I.D. driver is 16 feet long and is externally heated by a resistance heater to 1210°R (750°F). The driver gas is a mixture of helium and nitrogen where the ratio of the two gases is varied to achieve tailored-interface operation at different shock wave speeds. The tailored-interface mode of operation (ref. 5) is used to maximize the steady-state test time.

The driven tube is 4 inch I.D. and 48.5 feet long. Three ports along this tube contain instrumentation to detect and time the passage of the incident shock wave. Air is used in the driven tube as the test gas.

A contoured, axisymmetric convergent-divergent nozzle connects the shock tube to the 96-inch diameter test section. The nozzle used in this test program has a 48-inch exit diameter and was designed to provide parallel, uniform flow at $M_\infty = 16$. It can be operated off-design over the Mach number range from 9 to 19.5 by means of interchangeable throats of various diameters. Throat diameters of 1.843, 1.125, 0.660 and 0.400 inches were used to provide nominal free-stream Mach numbers of 10, 12.5, 15 and 17.5, respectively.

The 96-inch diameter test section contains a model support system for sting-mounting the model and pitching the model up to 55 degrees. Combined pitch and sideslip (or yaw) are achieved by the conventional pitch-and-roll technique. For model angles of attack α and yaw ψ (where $\psi = -\beta$, the sideslip angle), the model is rolled to angle ϕ and then pitched to an angle α' given by the following expressions.

$$\alpha' = \sin^{-1} \left[1 - (\cos \alpha \cos \psi)^2\right]^{1/2} \qquad (1)$$

$$\phi = -\tan^{-1} (\tan \psi / \sin \alpha) \qquad (2)$$

The angles α' and ϕ were set to within $\pm 1'$.

The fundamental instrumentation associated with the 96-inch HST includes sensors for measuring the initial pressure and temperature in both the driver and driven portions of the shock tube, detectors and counters for measuring the speed of the incident shock waves in the driven tube, and transducers for measuring the pressure behind the reflected shock wave. The pitot-pressure probe was mounted in the test section above the model to monitor the test flow.

The data from the model, the test section pitot-pressure probe, and the pressures behind the reflected shock wave were recorded on a 49-channel Navigation Computer Corporation (NAVCOR) MCL-100 data acquisiton system. The NAVCOR system simultaneously samples the inputs to each data channel at 50 μsec intervals and records the signal levels in digital form on a magnetic drum. The available recording time is 15 msec. The readout cycle after a test run involves transferring the data to a digital-to-analog converter at a speed compatible with a direct-writing strip chart recorder. The steady-state levels on the analog records are then marked and read for each channel.

MODEL AND HEAT-TRANSFER INSTRUMENTATION

The model used for this test is a 0.0175-scale simulation of the Space Shuttle Orbiter. The model, designated as 92-0, was originally a pressure model built to OV102 (Vehicle 5) lines. Elevon and body-flap surfaces are simulated on the model; however, they were not deflected during this test program. The OMS and SSME nozzles are not simulated on the model. A photograph of the model installed in the HST is shown in figure 2.

For these tests the vertical tail was removed and a tip-fin controller was added to the left wing. The tip-fin controller was designed and fabricated at Calspan to dimensions supplied by NASA-LaRC. Deflection of the control surface was simulated by a bolted on part. The basic configuration of the tip-fin controller is shown in figure 3. Photographs of the controller are shown in figures 4 and 5.

The identification and location of the heat-transfer gauges are given in Table I and shown in figure 6. The scale of the model restricted the total number of gauges that could be installed on the tip-fin controller and the deflected surface. There are 12 gauges located on the outboard surface, 9 gauges on the inboard surface, and 5 gauges on the leading and top edge of the basic tip fin. The 20° deflected surface contains 14 gauges, and two gauges were mounted on the upper surface of the orbiter wing just inboard of the tip-fin controller.

The measurement of heat-transfer rate relied on sensing the transient surface temperature of the model by means of thin-film resistance thermometers. (See, for example, refs. 6 to 9.) These gauges were fabricated either on small Pyrex 7740 glass buttons 1/8-inch in diameter or on contoured strips of Pyrex. The gauge consists of a thin platinum film (approximately 0.1 micron thick) painted and baked on the Pyrex substrate. A thin dielectric coating of magnesium fluoride was vapor deposited on the surface of the gauge to provide insulation from any flow-field ionization.

Because the heat capacity of the platinum film is negligible, the resistance thermometer measures the instantaneous surface temperature of the Pyrex substrate. The heat-transfer rate can be deduced from the measured surface temperature history from the equation for heat conduction in a semi-infinite solid of known thermal properties. An analysis (ref. 6) has shown that this technique is valid for these gauges and the short duration of shock tunnel tests. The thin-film gauges were calibrated prior to their installation in the model. The calibration procedure amounts simply to measuring the electrical resistance of the gauge at various temperatures. The measurements were made at room temperature, at approximately 110°F, and at approximately 160°F. Over this temperature range the calibration factor $K = dR/dT$ ($\Omega/°R$) was constant for each gauge, although it varies from gauge to gauge.

During the test program the gauges most directly exposed to the airflow suffered some erosion because of minute particles in the air. This erosion resulted in an increased gauge resistance. Prior to each test run, the gauge resistances were measured, and the calibration factor was adjusted for those gauges exhibiting a change in room temperature resistance.

The thin-film gauges were operated in a constant current circuit so that any change in resistance of the gauge during a test run was detected as a change in voltage drop across the element.

TEST CONDITIONS

The objective of this program was to obtain heat-transfer data at nominal Mach numbers of 10, 12.5, 15, and 17.5 at flight Reynolds numbers. This was accomplished at the three lowest Mach numbers; however, at Mach 17.5 the flight Reynolds number of 2.1×10^6 (based on free-stream conditions and vehicle length) could not be attained. At this Mach number, tests were conducted at Reynolds numbers of 0.987×10^6 and 1.44×10^6 in order to provide a basis for an extrapolation to the flight value. The test values of Reynolds number and Mach number are listed in the following table and are compared with the corresponding parameters from flight STS-1 in figure 7. The detailed test conditions are listed in Table III for both the Phase I and Phase II tests.

Average Test Conditions

Test Condition	Mach Number	Reynolds Number
1	17.5	1.44×10^6
2	14.9	3.33×10^6
3	12.5	4.36×10^6
4	10.1	5.96×10^6
5	17.3	9.87×10^5

Free-stream test conditions were computed assuming an isentropic expansion of the air from conditions behind the reflected shock wave to the free-stream Mach number. In the test section, the flow has expanded sufficiently so that the air was cool enough to obey the perfect gas equation of state. However, real-gas effects in the isentropic expansion were taken into account. The procedure used in determining the test conditions is described in the following paragraphs.

Normally, the values of the free-stream Mach number in the test section are determined from correlations of M_∞ with the incident shock wave Mach number M_i and the nozzle reservoir pressure p_o based on extensive airflow calibrations of the nozzle with each of the various size throats. This procedure was used for the present test for Test Conditions 3 and 4 (M_∞ = 12.5 and 10.1). At the other test conditions, the airflow calibrations (with the 0.660-inch and 0.400-inch throats) did not extend to the high values of p_o used here. For the runs at these Test Conditions (1, 2 and 5), the pitot pressure measured during each test run was used to calculate the free-stream Mach number M_∞.

Starting with the measured incident shock wave speed U_i, the initial air pressure in the driven tube p_1, and the initial air temperature in the driven tube T_1, the reservoir (or stagnation) enthalpy H_o and temperature T_o of the air behind the reflected shock wave were calculated from

$$H_o = H_1 \ (H_5/H_1) \tag{3}$$

and

$$T_o = T_1 \ (T_5/T_1) \tag{4}$$

where H_5/H_1 and T_5/T_1 are functions of U_i, p_1, and T_1 (ref. 10) for reflected normal shock waves. The value of H_1 is taken from reference 11 knowing p_1 and T_1.

Knowing the value of M_∞ (from the airflow correlations), the free-stream static temperature was obtained from

$$T_\infty = \frac{H_o}{c_{p_\infty}} \left(1 + \frac{\gamma_\infty - 1}{2} M_\infty^2 \right)^{-1} \tag{5}$$

with $c_{p_\infty} = 6006\ ft^2/sec^2\text{-}°R$ and $\gamma_\infty = 1.40$.

Free-stream static pressure was calculated from

$$p_\infty = p_o \left(\frac{p}{P_p} \right) \left(1 + \frac{\gamma_\infty - 1}{2} M_\infty^2 \right)^{\frac{-\gamma_\infty}{\gamma_\infty - 1}} \tag{6}$$

where

$$\frac{p}{P_p} = \frac{(p_\infty/p_o)_{Real}}{(p_\infty/p_o)_{Perfect}}$$

is the real-gas correction to the perfect gas static-to-total pressure ratio as described in reference 12. The sources for the real-gas data used in this procedure were references 13 and 14.

The free-stream velocity was determined from

$$U_\infty = M_\infty a_\infty \tag{7}$$

where $a_\infty = 49.01\sqrt{T_\infty}$, the speed of sound.

The free-stream dynamic pressure was found from

$$q_\infty = 1/2 \left(\gamma_\infty p_\infty M_\infty^2 \right) \tag{8}$$

The free-stream density was obtained from the ideal-gas equation of state

$$\rho_\infty = 144\ p_\infty / RT_\infty \tag{9}$$

where R = 1716 ft-lb/slug-°R, the gas constant.

Values of the absolute viscosity μ, used to compute the free-stream Reynolds number, were obtained from reference 11.

The test-section pitot-pressure p_o' was calculated from

$$p_o' = q_\infty \left(p_o'/q_\infty\right) \tag{10}$$

where the ratio p_o'/q_∞ has been correlated as a function of M_∞ and H_o for normal shock waves in air in thermodynamic equilibrium. Because this ratio is a weak function of p_o and M_∞, it is possible to represent all cases of interest to within 0.5% by two curves for $M_\infty < 7.5$ and $M_\infty \geq 7.5$.

For Test Conditions 1, 2, and 5, the above procedure was used in an iterative manner. First, a value of M_∞ was estimated, and the procedure carried out through equation 8. The calculated value of p_o' was compared to the measured value and the procedure was repeated using a new value of M_∞ until the calculated and measured values agreed to within 0.1 per cent.

For Test Conditions 3 and 4, where the correlations of airflow calibrations were used to specify M_∞, the validity of the procedure can be seen in the following comparison of some of the measured and calculated values of p_o'.

Comparison of Measured and Calculated Pitot Pressures

Run No.	Test Condition	Measured p_o'	Calculated p_o'
42	4	15.98	16.13
43	"	16.09	16.23
44	"	16.20	16.26
45	"	16.27	16.30
46	3	9.840	9.353
47	"	9.373	8.973
48	"	9.887	9.378
49	"	9.502	9.064

At Test Condition 4 the agreement between the measured pitot pressures and those obtained from the airflow calibrations was always within 1 per cent. For Test Condition 3 the measured pitot pressures were about 5 per cent higher than the calculated values. Such differences were considered acceptable because they correspond to only a 1 per cent difference in free-stream Mach number.

HEAT TRANSFER DATA REDUCTION

The thin-film heat-transfer gauge is a resistance thermometer which reacts to the local surface temperature of the model. The theory of heat conduction is used to relate the surface temperature history to the rate of heat transfer. Because the platinum resistance element has negligible heat capacity and, hence, negligible effect on the Pyrex substrate surface temperature, the substrate can be characterized as being homogeneous and isotropic. Furthermore, because of the short duration of a shock tunnel test, the substrate can be treated as a semi-infinite body. The one-dimensional heat conduction equation is

$$\rho c(T) \frac{\partial T}{\partial t} = \frac{\partial}{\partial y}\left(k(T) \frac{\partial T}{\partial y}\right) \tag{11}$$

where ρ, c, and k are the substrate density, specific heat and thermal conductivity, respectively; y is the distance normal to the substrate surface; and T(t) is the transient surface temperature rise (T(o) = 0).

If the substrate properties are independent of temperature, a closed-form solution of equation 11 can be obtained for the heat-transfer rate

$$\dot{q}(t) = 1/2\sqrt{\frac{\pi \rho c k}{t}}\left[T(t) + \frac{1}{\pi}\int_0^t \frac{\tau\, T(t) - t\, T(\tau)}{(t-\tau)^{3/2}}\, d\tau\right] \tag{12}$$

where τ is a dummy variable. Although numerical integration can be used to solve equation 12, in the present test an analog electrical network technique was used.

In cases where the surface temperature rise is less than 50°F, the variation of ρck with temperature is small, and equation (12) may be solved directly by use of a passive analog network termed a $\dot{q}$-meter (ref. 15). The analog is based on the fact that the equation for heat conduction in a semi-infinite solid is identical to that for a semi-infinite electrical transmission line with distributed series resistance and shunt capacitance. In practice, it has been found feasible to construct the analog of a finite number of circuit elements consisting of parallel resistor-capacitor elements in a series arrangement. For surface temperature changes greater than 50°F, the variation of substrate properties with temperature causes a drop of the $\dot{q}$-meter output which is corrected by a time and heat-transfer rate dependent factor. In the present tests the temperature change was such that this correction was necessary only for the three gauges located on the leading edge of the tip-fin controller and the gauge on the bottom edge of the deflected control surface (HT-13, 14, 15 and 29, respectively, in Table I).

As previously mentioned, the voltage signals from the heat-transfer gauges were sampled, digitized, and recorded on the NAVCOR system. After the test run, the data were played back at a slower speed to feed through a digital-to-analog converter. The analog signals were then processed by a $\dot{q}$-meter and recorded on a dual channel strip-chart recorder. Simultaneously, the voltage signal proportional to the surface temperature change was recorded on the other channel. Typical results from the two thin-film gauges located at X/L = 0.1 and 0.4 on the bottom center of the fuselage are shown in figure 8 (These were taken during Run 1 of the Phase I tests, ref. 4). The upper traces are the heat-transfer rates (output of the $\dot{q}$-meter), and the lower traces are the corresponding transient surface temperature histories (input to the $\dot{q}$-meter). In this figure Channel 41 represents the gauge at X/L= 0.1, and Channel 42 is the gauge at X/L = 0.4. The traces for Channel 41 are typical measurements for a laminar boundary layer. The "spikes" observed for Channel 42 are typical of a transitional boundary layer. The very fast-response thin-film gauges are capable of sensing the turbulence bursts occurring in a boundary layer undergoing transition from laminar to turbulent flow.

The heat-transfer rate is a function of the difference between the adiabatic wall (or recovery) temperature and the instantaneous wall temperature (or, alternatively, the recovery and wall enthalpies). In a typical hypersonic flow the recovery temperature is much larger than the wall temperature, and the change in wall temperature during a test run has no significant effect on the difference in these two temperatures (or corresponding enthalpies). However, large heat-transfer rates are accompanied by large changes in the wall temperature. In such cases, the following correction for the wall temperature is applied to obtain the equivalent, cold-wall, heat-transfer rate based on the initial wall temperature T_w.

$$\dot{q}_w = \dot{q}_{(T)} \quad \frac{rH_o - H(T_w)}{rH_o - H(T)} \tag{13}$$

The recovery factor r varies from 1.0 for a stagnation point flow to typically 0.85 for a laminar boundary layer well removed from the stagnation point. In the present tests the only gauges for which this correction was required were the gauges on the leading edge of the tip fin and the bottom edge of the deflected control surface (HT-13, 14, 15 and 29, respectively). Because these gauges were most probably always in a laminar boundary layer, the recovery factor was taken as $r = \sqrt{Pr_w}$ where the Prandtl number was evaluated at the initial wall temperature.

The heat-transfer data were normalized in terms of a heat-transfer coefficient h and a Stanton number C_H, based on free-stream conditons. The relations used were

$$h = Jg\ \dot{q}_w/(rH_o - H_w) \tag{14}$$

where J = 778.26 ft-lb/BTU and g = 32.17 ft/sec^2, and

$$C_H = J\dot{q}_w/\rho_\infty U_\infty (rH_o - H_w) \tag{15}$$

The heat-transfer data were also normalized by $\dot{q}_{Ref}$, the stagnation-point heat-transfer rate for a sphere of radius 0.0175 feet. This reference heat-transfer rate was calculated from the Fay and Riddell formula (ref. 16)

$$\dot{q}_{Ref} = \frac{0.76}{(Pr_w)^{0.6}} (\rho_w \mu_w)^{0.1} (\rho_o' \mu_o')^{0.4} \left[1 + (Le^{.52} - 1) \frac{H_D}{H_o} \right] (H_o - H_w) \left(\frac{dU_e}{dx} \right)_o \qquad (16)$$

where the Lewis number Le = 1.40, H_D is the dissociation enthalpy, and $(dU_e/dx)_o$ is the stagnation point velocity gradient. For the present test conditions, the dissociation energy $H_D << H_o$ (the total enthalpy) and the bracketed term in equation (16) was taken as unity. The stagnation point velocity gradient was calculated from the modified Newtonian flow relation for axisymmetric bodies

$$\left(\frac{dU_e}{dx} \right)_o = \frac{1}{R_N} \sqrt{\frac{2(p_o' - p_\infty) \times 144}{\rho_o'}} \qquad (17)$$

where R_N is the radius of the sphere. Equation (17) can be rewritten as

$$\left(\frac{dU_e}{dx} \right)_o = \frac{1}{R_N} \sqrt{2 Z_o' R T_o' (1 - p_\infty / p_o')} \qquad (18)$$

where R = 1716 ft-lb/slug°R, the gas constant for air, and $Z_o' = 1.0$ for the present test conditions.

The heat-transfer coefficient h were also normalized by h_{Ref}, where

$$h_{Ref} = Jg \, \dot{q}_{Ref} / (H_o - H_w) \qquad (19)$$

In summary the measured heat-transfer rates are presented as $\dot{q}_w$, $\dot{q}_w/\dot{q}_{Ref}$, h/h_{Ref} and C_H and are listed in Table IV.

RESULTS AND DISCUSSION

Before discussing the more significant features of the heat-transfer measurements, a few comments on the sequence of the test program are in order. In general, the tip-fin controller would not be used for aerodynamic control at speeds above Mach 10; therefore most of the test runs at $\delta = 20°$ were at that test condition. At Mach 12.5 only angles of attack of 28° and 40° were run with $\delta = 20°$. Initially, the lowest angle of attack was to be 25°; however, shortly after the beginning of the test program this was changed to 28° on the basis of altered mission requirements. Early in the test program the sensitivity of the leading-edge heat transfer to angle of attack was noted. This led to modifying the test matrix to better define this variation by including test runs at $\alpha = 29°$, 30°, and 31° at Mach 10.

Four repeat runs were made during the test. In each case, the loss of important data was the reason for repeating the run. However, these runs serve also to indicate the general repeatability of the flow and heat-transfer data.

The Phase I thermal mapping tests using thermographic phosphor (Runs 1-12) were reported in reference 4. The present Phase II tests consisted of 23 tests (Runs 13-35) without the control surface deflected and 14 tests (Runs 36-49) with controller deflected 20°. During these latter tests some of the gauges on the outboard surface (HT-7,8 and 9 see figure 6) were covered by the bolted-on flap (figure 5) and no data were acquired during Runs 36-49. On the other hand, gauges HT-10, 11 and 12 yielded data in the cavity region behind the deflected control surface.

In the remainder of this section, the heat-transfer results for the various regions of the tip-fin controller (i.e., leading, top, and bottom edges, and the outboard and inboard surfaces) will be discussed. The discussion will be in terms of the normalized heat-transfer coefficient h/h_{Ref} rather than the heat-transfer rate $\dot{q}_w$ or the Stanton number C_H.

LEADING, TOP, AND BOTTOM EDGES

There are three gauges located along the straight leading edge (HT-13, 14 and 15) at 25-, 50-, and 75-percent span. A fourth gauge was located at 97% span (HT-16) on the radius that faired the leading edge into the top edge, and a fifth gauge (HT-17) was located on the top edge at 80% of the tip chord. When 20° deflection of the controller was simulated, there was a gauge (HT-29) located at 55% of the chord of the deflected surface along the bottom edge. This bottom edge and the straight leading edge experienced the highest heat transfer rates on the fin, and they will be discussed first.

The variation of h/h_{Ref} with angle of attack at M_∞ = 10.1 and 12.5 is shown in figure 9 for the three locations along the leading edge. Data for both 0° and 20° deflections are shown. At 25% of the span (figure 9a) a peak value of h/h_{Ref} = 1.57 occurred at α = 28°; at 50% of the span (figure 9b) the peak value of h/h_{Ref} = 1.92 also occurred at α = 28°; and at 75% of the span (figure 9c) the peak value of h/h_{Ref} = 1.73 occurred at α = 29°. At all three spanwise locations the variation of h/h_{Ref} with angle of attack is similar. At α = 25°, h/h_{Ref} ranges from 0.93 to 1.25, whereas at α = 28° the values of h/h_{Ref} lie in the range 1.5 to 2, except at the 75% span where the peak heating occurs at α = 29°. After peak heating occurs, the value of h/h_{Ref} decreases rapidly with increasing angle of attack. At angles of attack of 35° and 40°, h/h_{Ref} lies in the range 0.7 to 1.0. In figure 9 the data for δ = 20° tend to be greater than for δ = 0°, with the largest differences near the peak heating values. The differences in heating at M_∞ = 10.1 and 12.5 are quite small.

The spanwise distribution of h/h_{Ref} is shown in figure 10 for the various angles of attack at M_∞ = 10.1. At α = 25°, the lowest heating occurs at 50% span, whereas this location experiences the highest heating at α = 28°. For angles of attack from 29° to 35°, h/h_{Ref} increases monotonically with increasing span, although the levels are decreasing with increasing angle of attack. At α = 40°, the heating rate is nearly constant along the leading edge. Data from both δ = 0° and δ = 20° are included in this figure.

The variation with Mach number of heat transfer to the leading edge is illustrated in figure 11 for an angle of attack of 28°. The parameter h/h_{Ref} is relatively insensitive to Mach number at all three spanwise locations. However, at the highest Mach number the normalized heating is generally lower than at the three lower Mach numbers.

The influence of sideslip angle β on the heat transfer to the leading edge is most pronounced at angles of attack below 30°. At α = 35° and 40° there is no significant change with sideslip angle. A typical effect at α = 28° is shown in figure 12 at M_∞ = 12.5 with δ = 0° and 20°. The effect is significant at the 25% and 50% spanwise locations, but is negligible at 75% of the span.

The heat transfer measured at the 55% chord on the deflected control surface is shown in figure 13 as a function of angle of attack and sideslip angle at M_∞ = 10.1 and 12.5. At β = 0°, the highest heating occurs at $\alpha \leq 30°$ and there is little variation with Mach number. At a sidelsip angle β = -2° (which puts the outboard surface to the windward) the heat transfer at α = 28° and 40° is nearly the same. At α = 28°, h/h_{Ref} has decreased noticably from the β = 0° values whereas at α = 40°, there has been an increase in h/h_{Ref} over the β = 0° levels.

Near and on the top edge of the tip-fin controller (97% and 100% span, HT-16 and 17), the heating rates were relatively low for all test conditions. On the leading-edge radius at 97% span the normalized parameter h/h_{Ref} varied from a low value of 0.0277 to a maximum value of 0.0506. On the top of the controller at 80% of the tip chord, h/h_{Ref} ranged from 0.00645 to 0.0296. These heating levels are more than an order of magnitude lower than the heating rates on the leading edge.

OUTBOARD SURFACE

$\delta = 0°$

During the Phase I tests with an undeflected controller, a single band of higher heating rate appeared to extend across the outboard surface at $M_\infty = 14.8$ and $\alpha = 40°$. At $M_\infty = 17.2$, however, this feature could not be distinguished clearly. This band of higher heat transfer is illustrated in figures 14 and 15. Figure 14 (also figure 12 of reference 4) shows (a) the pre-run tare picture and (b) the test picture taken during Run 9 at $M_\infty = 14.8$ and $\alpha = 40°$. In figure 14a, where the model is at a uniform (room) temperature, a variation in shading between the lower and upper portions of the controller is observed. Such variations are due to a combined nonuniformity of the thermographic coating and the UV light intensity. The same pattern can be observed in the test picture (figure 14b). It is evident that the highest measured heat-transfer rates coincide with the dark band and that outside this band the heat-transfer rates are always lower. Figure 15 is an enlargement of the test picture. The test picture exposure was approximately 2.8 ms and was taken during the period of steady flow conditions. During the exposure time, the surface temperature was continuously increasing (typically from 543°R to 547°R). In figure 15, the dark band extending across the control fin from near the root at the leading edge to the trailing edge at about 2/3 of the span represents a true region of higher temperature and higher heat transfer. The Phase II tests provided quantitative verification of this feature. Figure 16 shows a schametic representation of figure 15 with specific values of h/h_{Ref} (Run 30 of Phase II) indicated at discrete locations.

In all of the Phase II tests at $\delta = 0°$, the maximum measured value of h/h_{Ref} was 0.1575 (HT-4 on Run 21 at $M_\infty = 10.1$, $\alpha = 40°$, $\beta = -2°$). The minimum value of h/h_{Ref} was .00850 (HT-8 on Run 19 at $M_\infty = 10.1$, $\alpha = 40°$, $\beta = 0°$). On the average h/h_{Ref} varied from about 0.017 to approximately 0.113 over the outboard surface. The distribution of h/h_{Ref} varied with free-stream Mach

number M_∞ and angle of attack, but the overall heating levels remained low relative to the leading-edge heat transfer.

$\delta = 20°$

For the tests with the controller deflected there are three regions of interest: (1) the tip-fin ahead of the hinge line; (2) the deflected controller; (3) the cavity behind the deflected controller. On the tip-fin ahead of the controller the heating rates were generally the same as at $\delta = 0°$ except near the hinge line. On the deflected controller, the heat transfer was 2 or 3 times greater than at $\delta = 0°$. In the cavity behind the deflected controller the heat transfer was very low.

The Phase I tests indicated a more complex pattern of heat-transfer distribution at $\delta = 20°$ as compared to $\delta = 0°$. Figure 17 shows (a) the pre-run tare and (b) the test picture taken during Phase I Run 5 at $M_\infty = 10$ and $\alpha = 40°$. Again, note the nonuniformity in intensity in the tare picture. Comparing the tare and test pictures, one observes two streaks of higher heat transfer sweeping across the controller and a region of higher heat transfer just downstream of the hinge line. These features are seen better in figure 18, which is an enlargement of the test picture (figure 16b). Figure 18 is represented schematically in figure 19 and values of h/h_{Ref} are noted at various locations. Again, in general, the qualitative Phase I results are verified by the quantitative Phase II data. However, there are some minor anomalies: For example, note that at 75% span (approximately 0.4 in. on the vertical scale) $h/h_{Ref} = 0.145$ (HT-39) in the area between the two shaded regions and 0.114 (HT-40) in the downstream shaded region. Figure 18 would indicate that the former value should be lower than the latter value. Also, the value of $h/h_{Ref} = 0.076$ (HT-36) indicated in the lower shaded area is about one-half the value of 0.145 shown in the clear area at 75%. No explanation has been found for these discrepancies between the Phase I and Phase II results. In general, however, the results from the two phases are consistent.

On the portion of the tip-fin forward of the hinge line h/h_{Ref} varied from a minimum value of 0.0125 to a maximum of 0.161. These levels are comparable to those observed at $\delta = 0°$. However, near the hinge line (HT-5 and -6) the heat transfer was always lower at $\delta = 20°$ than at $\delta = 0°$. The magnitude of the differences clearly indicate a region of separated flow in the vicinity of the hinge line. Oil-flow tests at $M_\infty = 10$ at NASA LaRC also indicate such a separated flow region. This separated region does not appear to extend very far downstream of the hinge line for the conditions on the present test.

On the 20° deflected surface, the values of h/h_{Ref} ranged from 0.0341 to 0.3078. On the average, the variation over the surface for a given test was from 0.049 to 0.25. For $\delta = 0°$ and 20°, the chordwise heat-transfer distributions at 50% span for $M_\infty = 10.1$ and $\alpha = 28°$ are shown in figure 20. The large decrease in h/h_{Ref} ahead of the hinge line and the large increase behind the hinge line are clearly evident.

At $M_\infty = 10.1$ the model was pitched through the angle of attack range from 28° to 40° with the control surface deflected 20°. Typical chordwise distributions of heat transfer are shown in figure 21 at $\alpha = 28°$ and 40° for the 50% and 75% spanwise locations. At any given location large changes in h/h_{Ref} are observed although the maximum and minimum values overall are rather insensitive to angle of attack.

INBOARD SURFACE

There were two arrays of heat-transfer gauges on the inboard surface of the tip-fin controller. One array extended chordwise from 10% to 80% of the local chord at 17% of the span. The second array extended spanwise from 17% to 83% at the 80% chord position. For the entire test matrix the values of

h/h_{Ref} measured on the inboard surface ranged from a maximum of 0.228 to a minimum of 0.0013. The highest heating rates were always measured at the location nearest the leading edge (HT-20 at x/c = 0.10 and Z/b = 0.17). Oil-flow pictures taken previously at NASA LaRC indicate the existence of a region of separated flow in the aft corners of the tip-fin/wing junction. At large angles of attack the flow over the surface of the wing separates and the separation line extends across the inboard surface of the tip-fin. The extent of the separated flow region increases with increasing angle of attack. The heat-transfer distributions and the nature of the transient heat-transfer records support the existence of the separated flow region and its variation with angle of attack.

Deflection of the controller does not affect the heat transfer on the inboard surface ahead of the region of separated flow. Within the separated flow region there are some differences from test to test that are more likely due to the unsteady nature of the flow than to deflection of the controller.

Typical heat-transfer distributions at M_∞ = 10.1 for angles of attack of 28° and 40° are shown in figures 22 and 23 for the constant span (Z/b = 0.17) and constant chord (x/c = 0.80) arrays, respectively. In both figures 22 and 23 data from repeat runs are shown. With a few exceptions (which generally occur at very low heating rates) the repeatability is very good. The chordwise distribution (figure 22) shows a monotonic decrease in h/h_{Ref} at α = 28°. However, at α = 40° where the separated flow region is larger, h/h_{Ref} decreases monotonically only over the forward 50% to 60% of the chord. Comparing the relative levels of h/h_{Ref} at $x/c \leq .6$, it is noted that the heat transfer decreases by a factor of 2 or more as α is increased from 28° to 40°.

The spanwise distribution (figure 23) shows a monotonic increase in h/h_{Ref} with increasing Z/b at α = 28°. At α = 40°, the region of separated flow would

appear to extend up to somewhere between Z/b = 0.4 and Z/b = 0.6 at this chord position (x/c = 0.80). Also note that differences between α = 28° and 40° are much smaller along this constant-chord plot than they were in figure 22.

At the higher Mach numbers the heat-transfer distributions are similar to those shown in figures 22 and 23. The largest differences occur in the separated flow region where h/h_{Ref} increases with increasing Mach number. This is best illustrated in figure 24 which, shows the spanwise distribution at x/c = 0.80 for M_∞ = 17.5. It can be seen that the heat transfer is higher near the root of the tip-fin and at α = 28° is nearly constant across the span. It is noted also in figure 24 that the heating at x/c = 0.80 is relatively insensitive to angle of attack at both Z/b = 0.63 and 0.83.

WING UPPER SURFACE

The two heat-transfer gauges on the wing upper surface are located opposite the 25% and 75% chord positions of the tip-fin controller and are about 2% of the wing half-span inboard from the controller. The heat-transfer rates measured at these two positions are comparable to, but slightly lower than, those measured at similar chordwise locations of the inboard surface of the tip-fin controller (e.g. figure 22). At the 25% chord location, h/h_{Ref} ranged from 0.01201 to 0.06289, while at 75% chord the range was from 0.00064 to 0.00622. At the aft position the value of h/h_{Ref} typically was an order of magnitude lower than at the forward location. At the forward location h/h_{Ref} decreased with increasing angle of attack. Average values at α = 28° were 0.0356 and at α = 40° were 0.0137. At the aft position, h/h_{Ref} was relatively insensitive to angle of attack. However, the values measured at M_∞ = 17.5 and α = 28° and 35° were higher than at other Mach numbers. The gauge at the 75% chord position was most likely always in a region of separated flow, while separation never extended forward to the 25% chord location.

CONCLUSIONS

An experimental investigation of the aerodynamic heating of a tip-fin controller on a Space Shuttle orbiter model has been conducted at Mach numbers from 10 to 17.5. At all but the highest Mach number, the Reynolds number based on free-stream conditions at body length matched that of the STS-1 entry. The angle of attack was varied from 25° to 40°. The effect of small sideslip angles ($\beta = -2°$) was investigated at selected test conditions.

The Phase I thermal mapping tests indicated that the outboard surface experienced regions of higher heat-transfer that swept across the surface. The quantitative Phase II tests have confirmed this finding. The Phase I tests were successful in their goal of defining the areas of high heat transfer and in selecting the locations for the heat-transfer gauges used during the Phase II program.

As would be expected, the leading edge of the tip fin experienced the highest heating rates. Furthermore, the heat transfer to the leading edge was sensitive to the angle of attack in the range $25° < \alpha < 35°$. At the lower angles of attack, the shock wave from the leading edge of wing impinged on the leading edge of the tip-fin controller. This shock interaction resulted in peak values of h/h_{Ref} in the range 1.5 to 2 at $\alpha = 28°$.

Elsewhere on the tip fin, the heat-transfer rates were generally an order of magnitude or more smaller than the leading-edge heat transfer. Deflecting the controller 20° produced local values of h/h_{Ref} of approximately 0.3; a factor of 3 to 10 increase over the heat transfer at $\delta = 0°$. When the controller was deflected 20°, values of h/h_{Ref} approaching 1.0 were measured on the bottom edge.

The variation of h/h_{Ref} with free-stream Mach number was relatively minor. At Mach numbers of 17.3 and 17.5 the variation of h/h_{Ref} with Reynolds number was insignificant.

REFERENCES

1. Powell, R. W.; and Freeman, D. C., Jr.: Application of a Tip-Fin Controller to the Shuttle Orbiter for Improved Yaw Control. AIAA Paper 81-0074, Jan. 1981.

2. Hypersonic Shock Tunnel - Description and Capabilities. Calspan ATC, Sept. 1975.

3. Rogers, C. E.; Bogdan, L.; Kingly, R. E.; and Stratton, J. E.: A Thermal Mapping Technique for Shock Tunnels and a Practical Data-Reduction Procedure. AIAA Paper 72-1031, Sept. 1972.

4. Wittliff, C. E.; and Hilton, J.H.: A Thermal Mapping Investigation of a Tip-Fin Controller on a Space Shuttle Orbiter Model. Calspan Rept. No. 6912-A-1, March 1982.

5. Wittliff, C.E.; Wilson, M. R.; and Hertzberg, A.: The Tailored-Interface Hypersonic Shock Tunnel. J. Aero/Space Sci., Vol. 26, No. 4, April 1959, pp. 219-228.

6. Vidal, R. J.: Model Instrumentation Techniques for Heat Transfer and Force Measurements in a Hypersonic Shock Tunnel. WADC Tech. Note 56-315, AD-97238, U.S. Air Force (also Calspan Rept. No. AD-917-A), Feb. 1956.

7. Bogdan, L.; and Garberoglio, J. E.: Transient Heat Transfer Measurements with Thin-Film Resistance Thermometers - Fabrication and Application Technology. AFAPL-TR-67-72, U.S. Air Force, June 1967.

8. Schultz, D.L.; and Jones, T.V.: Heat Transfer Measurements in Short-Duration Hypersonic Facilities, AGARD-AG-165, Feb. 1973.

9. Miller, Charles G., III: Comparison of Thin-Film Resistance Heat-Transfer Gages with Thin-Skin Transient Calorimeter Gages in Conventional Hypersonic Wind Tunnels. NASA TM-83197, Dec. 1981.

10. Lewis, Clark H.; and Burgess, E. G., III: Charts of Normal Shock Wave Properties in Imperfect Air (Supplement: M_s = 1 to 10). AEDC-TR-65-196, U.S. Air Force, Sept. 1965.

11. Hilsenrath, J.; et al.: Tables of Thermal Properties of Gases. NBS Circular 565, 1955.

12. Reece, J. W.: Test Section Conditions Generated in the Supersonic Expansion of Real Air. J. Aero/Space Sci., Vol. 29, No. 5, May 1962, pp. 617,618.

13. Hilsenrath, J.; et al.: Tables of Thermodynamic Properties of Air Including Dissociation and Ionization from 1500 °K to 15,000 °K. AEDC-TR-59-20, U.S. Air Force, Dec. 1959.

14. Neel, C. A.; and Lewis, Clark H.: Interpolations of Imperfect Air Thermodynamic Data II. At Constant Pressure. AEDC-TDR-64-184, U.S. Air Force, Sept. 1964.

15. Skinner, G. T.: Analog Network to Convert Surface Temperature to Heat Flux. ARS J., Vol. 30, No. 6, June 1960, pp. 569-570.

16. Fay, J. A.; and Riddell, F. R.: Theory of Stagnation-Point Heat Transfer in Dissociated Air. J. Aero. Sci., Vol. 25, No. 2, February 1958, pp. 73-85.

Table I

HEAT-TRANSFER INSTRUMENTATION

Gauge Position	R @ 70°F	$\frac{dR/dT}{R_{70°}} \times 10^3$	dR/dT	x/c	Z/b	x/c_f
1	84.85	1.332	.11302	.10	.10	
2	91.51	1.346	.12313	.23	.25	
3	88.19	1.342	.11839	.30	.15	
4	99.58	1.329	.13236	.30	.25	
5	76.68	1.347	.10329	.30	.50	
6	97.21	1.378	.13397	.25	.925	
7	95.59	1.361	.13012	.60	.50	
8	96.75	1.366	.13216	.70	.25	
9	96.97	1.366	.13250	.70	.50	
10	75.69	1.343	.10167	.80	.50	
11	77.45	1.332	.10317	.80	.75	
12	90.64	1.331	.12063	.80	.925	
13	81.95	1.342	.10997	0	.25	
14	95.72	1.351	.12936	0	.50	
15	94.73	1.332	.12617	0	.75	
16	79.93	1.327	.10607	0	.97	
17	82.16	1.343	.11032	.80	1.00	
18	87.70	1.347	.11814			
19	85.94	1.338	.11502			
20	90.00	1.350	.12151	.10	.17	
21	73.22	1.344	.09843	.23	.17	
22	92.18	1.347	.12413	.40	.17	
23	80.81	1.342	.10841	.50	.17	
24	89.74	1.335	.11976	.60	.17	
25	86.90	1.355	.11776	.80	.17	
26	110.51	1.340	.14808	.80	.37	
27	105.20	1.334	.14030	.80	.63	
28	91.36	1.366	.12480	.80	.83	
29	81.49	1.334	.10867	.75	.184	.55
30	80.16	1.292	.10359	.47	.25	.06
31	83.87	1.342	.11256	.66	.25	.40
32	90.54	1.363	.12344	.83	.25	.70
33	83.97	1.284	.10778	.43	.50	.06
34	85.61	1.325	.11340	.55	.50	.25
35	102.68	1.362	.13985	.64	.50	.40
36	99.83	1.329	.13272	.82	.50	.70
37	85.52	1.298	.11100	.39	.75	.06
38	79.44	1.327	.10538	.51	.75	.25
39	86.41	1.338	.11564	.61	.75	.40
40	93.71	1.305	.12231	.71	.75	.55
41	102.66	1.335	.13702	.81	.75	.70
42	91.26	1.277	.11651	.36	.925	.06
90(1)	79.65	1.367	.10885	X/L = .10		
90(2)	85.46	1.336	.11417	X/L = .10		
91	81.73	1.348	.11021	X/L = .40		

(1) Runs 13-32
(2) Runs 36-49

b = span of controller
c = local chord of controller
c_f = local chord of deflected surface

Table II-1

PHASE I - RUN SCHEDULE

Run No.	α deg	β deg	δ deg	TEST CONDITION	NOMIMAL M_∞	NOMIMAL $Re_{\infty,L}$	REMARKS
1	40	0	0	3	12.6	4.57×10^6	Viewed Inboard Surface
2	40	0	0	4	10.0	5.59×10^6	" " "
3	40	0	0	4	"	"	" " "
4	40	0	20	4	"	"	Viewed Outboard Surface
5	40	0	20	4	"	"	" " "
6	40	-2	20	4	"	"	" " "
7	40	+2	20	4	"	"	" " "
8	30	0	20	4	"	"	" " "
9	40	0	0	2	14.8	3.17×10^6	" " "
10	40	0	0	1	17.2	1.34×10^6	" " "
11	40	-2	0	1	"	"	" " "
12	40	+2	0	3	12.6	4.57×10^6	Viewed Inboard Surface

Table II-2

PHASE II - RUN SCHEDULE

Run No.	α deg	β deg	δ deg	TEST CONDITION	NOMINAL M_∞	NOMINAL $Re_{\infty,L}$	REMARKS
13	25°	0°	0°	4	10.1	5.96×10^6	
14	25°	0°	"	"	"	"	Repeat of Run 13
15	25°	-2°	"	"	"	"	
16	25°	+2°	"	"	"	"	
17	35°	0°	"	"	"	"	
18	35°	0°	"	"	"	"	Repeat of Run 17
19	40°	0°	"	"	"	"	
20	35°	-2°	"	"	"	"	
21	40°	-2°	"	"	"	"	
22	40°	-2°	"	3	12.5	4.36×10^6	
23	40°	0°	"	"	"	"	
24	35°	0°	"	"	"	"	
25	28°	0°	"	"	"	"	
26	28°	-2°	"	"	"	"	
27	28°	-2°	"	2	14.9	3.33×10^6	
28	28°	0°	"	"	"	"	
29	35°	0°	"	"	"	"	
30	40°	0°	"	"	"	"	

Table II-2 (Cont'd)

PHASE II - RUN SCHEDULE

Run No.	α deg	β deg	δ deg	TEST CONDITION	NOMINAL M_∞	NOMINAL $Re_{\infty,L}$	REMARKS
31	40°	0°	0°	1	17.5	1.44×10^6	
32	35°	0°	"	"	"	"	
33	28°	0°	"	"	"	"	
34	28°	0°	"	5	17.3	0.987×10^6	
35	28°	0°	"	4	10.1	5.96×10^6	
36	28°	0°	20°	"	"	"	
37	28°	0°	"	"	"	"	Repeat of Run 36
38	30°	0°	"	"	"	"	
39	35°	0°	"	"	"	"	
40	40°	0°	"	"	"	"	
41	31°	0°	"	"	"	"	
42	31°	0°	"	"	"	"	Repeat of Run 41
43	29°	0°	"	"	"	"	
44	28°	-2°	"	"	"	"	
45	40°	-2°	"	"	"	"	
46	40°	-2°	"	3	12.5	4.36×10^6	
47	28°	-2°	"	"	"	"	
48	28°	0°	"	"	"	"	
49	40°	0°	"	"	"	"	

Table III-1

PHASE I TEST CONDITIONS

RUN NO.	1	2	3	4	5	6
α	40°	40°	40°	40°	40°	40°
β	0°	0°	0°	0°	0°	+2°
δ	0°	0°	0°	20°	20°	20°
M_i	3.689	3.533	3.499	3.528	3.528	3.506
p_o	9212	4564	5476	5377	5441	5566
H_o	2.138E+7	1.949E+7	1.930E+7	1.944E+7	1.944E+7	1.951E+7
T_o	3120	2906	2883	2900	2900	2911
M_∞	12.58	9.990	10.05	10.04	10.04	10.05
U_∞	6442	6096	6067	6089	6089	6100
T_∞	109.1	154.8	151.6	153.1	153.0	153.1
p_∞	4.432E-2	9.902E-2	1.171E-1	1.155E-1	1.169E-1	1.186E-1
q_∞	4.912	6.925	8.291	8.154	8.252	8.398
ρ_∞	3.409E-5	5.366E-5	6.486E-5	6.334E-5	6.410E-5	6.499E-5
μ_∞	9.179E-8	1.297E-7	1.270E-7	1.283E-7	1.282E-7	1.283E-7
Re/ft	2.392E+6	2.522E+6	3.098E+6	3.006E+6	3.044E+6	3.089E+6
p_o'	9.126	12.85	15.38	15.13	15.31	15.58
T_w	532	529	531	529	529	533
H_w	3.195E+6	3.177E+6	3.189E+6	3.177E+6	3.177E+6	3.201E+6
$\dot{q}_{Ref}$	169.1	178.5	192.6	193.0	194.1	196.4
h_{Ref}	.2328	.2739	.2992	.2970	.2987	.3014

Table III-1

PHASE I TEST CONDITIONS

RUN NO.	7	8	9	10	11	12
α	40°	30°	40°	40°	40°	40°
β	-2°	0°	0°	0°	+2°	-2°
δ	20°	20°	0°	0°	0°	0°
M_i	3.481	3.499	4.369	4.629	4.836	3.598
p_o	5431	5333	18,550	15,400	18,728	8527
H_o	1.927E+7	1.958E+7	2.921E+7	3.200E+7	3.546E+7	2.014E+7
T_o	2880	2922	4014	4369	4762	2969
M_∞	10.06	10.05	14.84	17.17	17.34	12.61
U_∞	6062	6112	7562	7937	8357	6252
T_∞	151.1	153.9	108.0	89.07	96.59	102.2
p_∞	1.156E-1	1.134E-1	2.595E-2	7.262E-3	7.776E-3	4.113E-2
q_∞	8.193	8.017	4.005	1.497	1.638	4.583
ρ_∞	6.420E-5	6.181E-5	2.017E-5	6.842E-6	6.756E-6	3.377E-5
μ_∞	1.267E-7	1.290E-7	9.083E-8	7.493E-8	8.126E-8	8.599E-8
Re/ft	3.073E+6	2.929E+6	1.679E+6	7.248E+5	6.948E+5	2.455E+6
p_o'	15.20	14.87	7.484	2.802	3.073	8.506
T_w	533	537	532	530	536	528
H_w	3.201E+6	3.225E+6	3.195E+6	3.183E+6	3.219E+6	3.171E+6
$\dot{q}_{Ref}$	191.0	192.6	223.1	151.9	178.6	151.8
h_{Ref}	.2975	.2948	.2147	.1319	.1387	.2239

Table III-2
PHASE II TEST CONDITIONS

RUN NO.	13	14	15	16	17	18	19	20	21	22	23
α	25°	25°	25°	25°	35°	35°	40°	35°	40°	40°	40°
β	0°	0°	-2°	+2°	0°	0°	0°	-2°	-2°	-2°	0°
δ	0°	0°	0°	0°	0°	0°	0°	0°	0°	0°	0°
M_i	3.607	3.458	3.381	3.499	3.496	3.508	3.482	3.500	3.474	3.674	3.705
p_o	5375	5343	5021	5654	5639	5623	5659	5621	5588	8598	9167
H_o	2.049E+7	1.891E+7	1.846E+7	1.954E+7	1.957E+7	1.979E+7	1.916E+7	1.947E+7	1.936E+7	2.115E+7	2.174E+7
T_o	3038	2832	2773	2910	2916	2945	2860	2901	2888	3091	3167
M_∞	9.995	10.07	10.08	10.06	10.06	10.05	10.07	10.06	10.07	12.55	12.56
U_∞	6250	6006	5935	6105	6111	6145	6046	6095	6077	6407	6496
T_∞	162.6	148.1	144.2	153.2	153.5	155.3	149.9	152.8	151.5	108.4	111.2
p_∞	1.159E-1	1.138E-1	1.060E-1	1.201E-1	1.197E-1	1.191E-1	1.203E-1	1.197E-1	1.181E-1	4.184E-2	4.396E-2
q_∞	8.116	8.076	7.549	8.514	8.486	8.433	8.550	8.482	8.393	4.618	4.863
ρ_∞	5.984E-5	6.447E-5	6.172E-5	6.579E-5	6.545E-5	6.432E-5	6.737E-5	6.576E-5	6.544E-5	3.240E-5	3.319E-5
μ_∞	1.361E-7	1.242E-7	1.210E-7	1.284E-7	1.286E-7	1.301E-7	1.257E-7	1.280E-7	1.270E-7	9.116E-8	9.349E-8
Re/ft	2.748E+6	3.118E+6	3.029E+6	3.129E+6	3.109E+6	3.037E+6	3.241E+6	3.131E+6	3.133E+6	2.277E+6	2.306E+6
p_o'	15.07	14.98	13.99	15.80	15.74	15.65	15.86	15.74	15.57	8.579	9.038
T_w	533	531	535	534	535	536.5	531	533	535	531	534.5
H_w	3.201E+6	3.189E+6	3.213E+6	3.207E+6	3.213E+6	3.222E+6	3.189E+6	3.201E+6	3.213E+6	3.189E+6	3.210E+6
$\dot{q}_{Ref}$	205.4	185.3	173.4	198.0	198.1	200.2	193.8	196.9	194.3	161.9	171.7
h_{Ref}	.2974	.2951	.2847	.3035	.3032	.3025	.3038	.3030	.3013	.2257	.2320

Table III-2
PHASE II TEST CONDITIONS

RUN NO.	24	25	26	27	28	29	30	31	32	33	34
α	35°	28°	28°	28°	28°	35°	40°	40°	35°	28°	28°
β	0°	0°	-2°	-2°	0°	0°	0°	0°	0°	0°	0°
δ	0°	0°	0°	0°	0°	0°	0°	0°	0°	0°	0°
M_i	3.786	3.749	3.756	4.300	4.246	4.254	4.198	4.648	4.601	4.584	4.463
P_o	9456	9227	9125	18,030	18,210	18,260	17.490	17,990	17,490	17,300	10,850
H_o	2198E+7	2.192E+7	2.183E+7	2.839E+7	2.828E+7	2.755E+7	2.759E+7	3.350E+7	3.189E+7	3.239E+7	3.086E+7
T_o	3192	3188	3176	3919	3907	3815	3827	4540	4356	4419	4310
M_∞	12.51	12.54	12.52	14.92	14.92	15.06	14.72	17.48	17.62	17.38	17.31
U_∞	6530	6521	6508	7456	7441	7546	7347	8123	7927	7986	7796
T_∞	113.3	112.5	112.4	103.8	103.4	98.95	103.6	89.80	84.17	87.81	84.34
P_∞	4.658E-2	4.479E-2	4.470E-2	2.471E-2	2.508E-2	2.403E-2	2.669E-2	7.356E-3	7.004E-3	7.510E-3	4.787E-3
q_∞	5.108	4.932	4.910	3.855	3.912	3.819	4.053	1.575	1.524	1.590	1.005
ρ_∞	3.450E-5	3.340E-5	3.338E-5	1.997E-5	2.035E-5	2.038E-5	2.162E-5	6.874E-6	6.983E-6	7.178E-6	4.763E-6
μ_∞	9.528E-8	9.465E-8	9.450E-8	8.735E-8	8.701E-8	8.325E-8	8.715E-8	7.555E-8	7.080E-8	7.387E-8	7.095E-8
Re/ft	2.365E+6	2.301E+6	2.299E+6	1.705E+6	1.740E+6	1.799E+6	1.823E+6	7.391E+5	7.819E+5	7.760E+5	5.234E+5
P_o'	9.496	9.168	9.125	7.200	7.305	7.129	7.565	2.951	2.852	2.976	1.880
T_w	527	531	529	532	537	529	536	540	532	538	534
H_w	3.165E+6	3.189E+6	3.177E+6	3.195E+6	3.225E+6	3.177E+6	3.219E+6	3.243E+6	3.195E+6	3.231E+6	3.249E+6
$\dot{q}_{Ref}$	178.8	174.8	173.7	211.6	211.8	203.3	209.3	163.8	152.6	158.4	118.9
h_{Ref}	.2379	.2336	.2331	.2103	.2116	.2088	.2150	.1355	.1331	.1360	.1078

Table III-2
PHASE II TEST CONDITIONS

RUN NO.	35	36	37	38	39	40	41	42	43	44	45
α	28°	28°	28°	30°	35°	40°	31°	31°	29°	28°	40°
β	0°	0°	0°	0°	0°	0°	0°	0°	0°	-2°	-2°
δ	0°	20°	20°	20°	20°	20°	20°	20°	20°	20°	20°
M_i	3.488	3.540	3.460	3.426	3.475	3.463	3.346	3.478	3.502	3.480	3.516
p_o	5839	5728	5568	5311	5543	5433	5049	5755	5821	5842	5805
H_o	1.943E+7	1.944E+7	1.868E+7	1.850E+7	1.923E+7	1.891E+7	1.801E+7	1.919E+7	1.956E+7	1.941E+7	1.941E+7
T_o	2896	2893	2795	2773	2870	2828	2712	2865	2914	2895	2892
M_∞	10.07	10.04	10.08	10.08	10.07	10.07	10.09	10.07	10.07	10.08	10.06
U_∞	6088	6089	5969	5941	6057	6007	5862	6052	6110	6086	6086
T_∞	151.9	152.9	146.0	144.6	150.6	148.1	140.3	150.1	153.1	151.5	152.2
p_∞	1.237E-1	1.237E-1	1.190E-1	1.133E-1	1.177E-1	1.158E-1	1.068E-1	1.223E-1	1.231E-1	1.230E-1	1.239E-1
q_∞	8.792	8.735	8.465	8.057	8.355	8.222	7.625	8.695	8.747	8.764	8.786
ρ_∞	6.831E-5	6.786E-5	6.842E-5	6.575E-5	6.558E-5	6.562E-5	6.391E-5	6.837E-5	6.749E-5	6.814E-5	6.832E-5
μ_∞	1.273E-7	1.282E-7	1.224E-7	1.213E-7	1.262E-7	1.242E-7	1.177E-7	1.258E-7	1.283E-7	1.270E-7	1.275E-7
Re/ft	3.266E+6	3.224E+6	3.336E+6	3.220E+6	3.147E+6	3.175E+6	3.182E+6	3.288E+6	3.215E+6	3.265E+6	3.260E+6
p_o'	16.31	16.20	15.69	14.93	15.50	15.25	14.13	16.13	16.23	16.26	16.30
T_w	537	527	527	529	533	530	533	532	534	535	530
H_w	3.207E+6	3.165E+6	3.165E+6	3.177E+6	3.201E+6	3.183E+6	3.201E+6	3.195E+6	3.207E+6	3.213E+6	3.183E+6
$\dot{q}_{Ref}$	199.8	199.8	187.0	180.0	192.4	187.0	168.9	195.8	201.1	199.2	199.9
h_{Ref}	.3084	.3074	.3018	.2941	.3005	.2977	.2856	.3065	.3079	.3079	.3084

Table III-2
PHASE II TEST CONDITIONS

RUN NO.	46	47	48	49							
α	40°	28°	28°	40°							
β	-2°	-2°	0°	0°							
δ	20°	20°	20°	20°							
M_i	3.733	3.731	3.715	3.742							
p_o	9490	9148	9415	9195							
H_o	2.190E+7	2.220E+7	2.141E+7	2.208E+7							
T_o	3187	3228	3124	3210							
M_∞	12.57	12.55	12.57	12.55							
U_∞	6519	6564	6446	6545							
T_∞	111.9	113.8	109.4	113.2							
p_∞	4.548E-2	4.374E-2	4.562E-2	4.421E-2							
q_∞	5.032	4.826	5.048	4.876							
ρ_∞	3.410E-5	3.226E-5	3.499E-5	3.278E-5							
μ_∞	9.415E-8	9.567E-8	9.204E-8	9.519E-8							
Re/ft	2.361E+6	2.213E+6	2.450E+6	2.254E+6							
p_o'	9.353	8.973	9.378	9.064							
T_w	533	537	529	534							
H_w	3.201E+6	3.225E+6	3.177E+6	3.207E+6							
$\dot{q}_{Ref}$	176.3	175.4	171.9	174.7							
h_{Ref}	.2361	.2314	.2360	.2318							

Table IV

HEAT-TRANSFER DATA

RUN	POS	Q	Q/Q(REF)	C(H)	H/H(REF)
13	1	19.249	9.371E-02	2.850E-03	1.153E-01
	2	10.813	5.264E-02	1.601E-03	6.479E-02
	3	12.720	6.193E-02	1.884E-03	7.621E-02
	4	7.826	3.810E-02	1.159E-03	4.689E-02
	5	9.665	4.706E-02	1.431E-03	5.791E-02
	6	13.803	6.720E-02	2.044E-03	8.271E-02
	7	3.508	1.708E-02	5.194E-04	2.102E-02
	8	13.465	6.555E-02	1.994E-03	8.068E-02
	9	3.578	1.742E-02	5.298E-04	2.144E-02
	10	5.877	2.861E-02	8.703E-04	3.521E-02
	11	2.796	1.361E-02	4.140E-04	1.675E-02
	12	6.771	3.296E-02	1.003E-03	4.057E-02
	13	198.503	9.664E-01	2.939E-02	1.189E 00
	14	163.890	7.979E-01	2.427E-02	9.820E-01
	16	6.705	3.265E-02	9.929E-04	4.018E-02
	19	0.374	1.819E-03	5.533E-05	2.239E-03
	21	10.672	5.196E-02	1.580E-03	6.394E-02
	22	5.384	2.621E-02	7.972E-04	3.226E-02
	23	3.622	1.763E-02	5.363E-04	2.170E-02
	24	2.178	1.060E-02	3.225E-04	1.305E-02
	26	1.731	8.425E-03	2.563E-04	1.037E-02
	27	2.411	1.174E-02	3.570E-04	1.445E-02
	28	3.152	1.534E-02	4.667E-04	1.888E-02
	90	19.781	9.630E-02	2.929E-03	1.185E-01
	91	12.693	6.180E-02	1.880E-03	7.605E-02

Table IV

HEAT-TRANSFER DATA

RUN	POS	Q	Q/Q(REF)	C(H)	H/H(REF)
14	1	17.293	9.332E-02	2.729E-03	1.152E-01
	3	9.386	5.065E-02	1.481E-03	6.254E-02
	3	10.845	5.852E-02	1.711E-03	7.226E-02
	4	6.840	3.691E-02	1.079E-03	4.558E-02
	5	8.555	4.617E-02	1.350E-03	5.700E-02
	6	12.745	6.878E-02	2.011E-03	8.492E-02
	7	2.961	1.598E-02	4.673E-04	1.973E-02
	8	12.200	6.584E-02	1.925E-03	8.129E-02
	9	2.747	1.483E-02	4.335E-04	1.831E-02
	10	5.002	2.699E-02	7.894E-04	3.333E-02
	11	2.291	1.236E-02	3.615E-04	1.526E-02
	12	6.273	3.385E-02	9.899E-04	4.180E-02
	13	177.540	9.581E-01	2.802E-02	1.183E 00
	14	140.101	7.561E-01	2.211E-02	9.335E-01
	15	185.479	1.001E 00	2.927E-02	1.236E 00
	16	5.971	3.222E-02	9.422E-04	3.979E-02
	17	3.156	1.703E-02	4.980E-04	2.103E-02
	19	0.296	1.598E-03	4.674E-05	1.974E-03
	20	31.593	1.705E-01	4.986E-03	2.105E-01
	21	10.038	5.417E-02	1.584E-03	6.688E-02
	22	4.612	2.489E-02	7.278E-04	3.073E-02
	23	3.384	1.826E-02	5.341E-04	2.255E-02
	24	2.251	1.215E-02	3.552E-04	1.500E-02
	25	0.707	3.814E-03	1.115E-04	4.710E-03
	26	1.190	6.421E-03	1.878E-04	7.928E-03
	27	1.737	9.376E-03	2.742E-04	1.158E-02
	28	2.722	1.469E-02	4.296E-04	1.814E-02
	90	16.830	9.083E-02	2.656E-03	1.121E-01
	91	11.329	6.114E-02	1.788E-03	7.549E-02

Table IV

HEAT-TRANSFER DATA

RUN	POS	Q	Q/Q(REF)	C(H)	H/H(REF)
15	1	18.051	1.041E-01	3.111E-03	1.288E-01
	2	10.963	6.322E-02	1.889E-03	7.822E-02
	3	9.579	5.524E-02	1.651E-03	6.835E-02
	4	8.106	4.675E-02	1.397E-03	5.783E-02
	5	9.925	5.724E-02	1.710E-03	7.081E-02
	6	14.620	8.431E-02	2.520E-03	1.043E-01
	7	3.398	1.959E-02	5.856E-04	2.424E-02
	8	11.892	6.858E-02	2.049E-03	8.485E-02
	9	2.340	1.350E-02	4.033E-04	1.670E-02
	10	3.784	2.182E-02	6.521E-04	2.700E-02
	11	4.255	2.454E-02	7.333E-04	3.036E-02
	12	6.235	3.596E-02	1.075E-03	4.448E-02
	13	219.607	1.266E 00	3.785E-02	1.567E 00
	14	150.565	8.683E-01	2.595E-02	1.074E 00
	15	172.246	9.933E-01	2.968E-02	1.229E 00
	16	7.092	4.090E-02	1.222E-03	5.060E-02
	17	3.194	1.842E-02	5.505E-04	2.279E-02
	18	8.815	5.084E-02	1.519E-03	6.289E-02
	19	0.304	1.752E-03	5.237E-05	2.168E-03
	20	28.627	1.651E-01	4.933E-03	2.042E-01
	21	8.621	4.972E-02	1.486E-03	6.151E-02
	22	4.030	2.324E-02	6.945E-04	2.875E-02
	23	2.642	1.524E-02	4.554E-04	1.885E-02
	24	1.753	1.011E-02	3.022E-04	1.251E-02
	25	0.505	2.915E-03	8.710E-05	3.606E-03
	26	0.726	4.186E-03	1.251E-04	5.179E-03
	27	1.606	9.264E-03	2.768E-04	1.146E-02
	28	2.251	1.298E-02	3.880E-04	1.606E-02
	90	15.765	9.092E-02	2.717E-03	1.125E-01
	91	10.297	5.938E-02	1.775E-03	7.347E-02

Table IV

HEAT-TRANSFER DATA

RUN	POS	Θ	Q/Q(REF)	C(H)	H/H(REF)
16	1	19.049	9.621E-02	2.787E-03	1.187E-01
	2	8.436	4.261E-02	1.234E-03	5.256E-02
	3	11.236	5.675E-02	1.644E-03	7.000E-02
	4	5.528	2.792E-02	8.087E-04	3.444E-02
	5	7.194	3.633E-02	1.052E-03	4.482E-02
	6	12.219	6.171E-02	1.788E-03	7.613E-02
	7	2.596	1.311E-02	3.798E-04	1.617E-02
	8	14.321	7.233E-02	2.095E-03	8.922E-02
	9	3.718	1.878E-02	5.439E-04	2.316E-02
	10	5.793	2.926E-02	8.475E-04	3.609E-02
	11	1.736	8.767E-03	2.539E-04	1.081E-02
	12	3.846	1.942E-02	5.627E-04	2.396E-02
	13	203.195	1.026E 00	2.973E-02	1.266E 00
	14	141.299	7.136E-01	2.067E-02	8.803E-01
	15	167.472	8.458E-01	2.450E-02	1.043E 00
	16	6.838	3.453E-02	1.000E-03	4.260E-02
	17	3.002	1.516E-02	4.392E-04	1.871E-02
	18	8.745	4.417E-02	1.279E-03	5.448E-02
	19	0.480	2.422E-03	7.015E-05	2.988E-03
	20	36.564	1.847E-01	5.349E-03	2.278E-01
	21	10.869	5.489E-02	1.590E-03	6.772E-02
	22	5.494	2.775E-02	8.038E-04	3.423E-02
	23	3.834	1.936E-02	5.609E-04	2.389E-02
	24	2.430	1.227E-02	3.555E-04	1.514E-02
	25	0.697	3.523E-03	1.020E-04	4.345E-03
	26	1.411	7.127E-03	2.064E-04	8.791E-03
	27	1.873	9.460E-03	2.740E-04	1.167E-02
	28	2.987	1.508E-02	4.370E-04	1.861E-02
	90	18.707	9.448E-02	2.737E-03	1.165E-01
	91	11.646	5.882E-02	1.704E-03	7.255E-02

Table IV

HEAT-TRANSFER DATA

RUN	POS	Q	Q/Q(REF)	C(H)	H/H(REF)
17	1	12.669	6.395E-02	1.859E-03	7.890E-02
	2	9.749	4.921E-02	1.430E-03	6.071E-02
	3	14.333	7.235E-02	2.103E-03	8.926E-02
	4	13.646	6.888E-02	2.002E-03	8.498E-02
	5	7.022	3.544E-02	1.030E-03	4.373E-02
	6	11.540	5.826E-02	1.693E-03	7.187E-02
	7	8.825	4.455E-02	1.295E-03	5.496E-02
	8	3.163	1.597E-02	4.641E-04	1.970E-02
	12	6.594	3.329E-02	9.674E-04	4.107E-02
	13	128.455	6.484E-01	1.885E-02	8.000E-01
	14	144.742	7.307E-01	2.124E-02	9.014E-01
	15	146.558	7.398E-01	2.150E-02	9.127E-01
	16	5.561	2.807E-02	8.159E-04	3.463E-02
	17	3.869	1.953E-02	5.677E-04	2.410E-02
	18	4.519	2.281E-02	6.630E-04	2.814E-02
	19	0.318	1.606E-03	4.667E-05	1.981E-03
	20	20.324	1.026E-01	2.982E-03	1.266E-01
	21	6.052	3.055E-02	8.880E-04	3.769E-02
	22	2.551	1.288E-02	3.742E-04	1.589E-02
	23	1.914	9.663E-03	2.808E-04	1.192E-02
	24	0.628	3.170E-03	9.213E-05	3.911E-03
	25	0.564	2.846E-03	8.273E-05	3.512E-03
	26	0.858	4.330E-03	1.259E-04	5.342E-03
	27	1.487	7.504E-03	2.181E-04	9.258E-03
	28	2.200	1.110E-02	3.227E-04	1.370E-02
	90	36.899	1.863E-01	5.414E-03	2.298E-01
	91	24.389	1.231E-01	3.578E-03	1.519E-01

Table IV

HEAT-TRANSFER DATA

RUN	POS	Q	Q/Q(REF)	C(H)	H/H(REF)
18	1	13.155	6.571E-02	1.928E-03	8.105E-02
	2	10.390	5.190E-02	1.523E-03	6.402E-02
	3	14.736	7.361E-02	2.160E-03	9.079E-02
	4	13.308	6.647E-02	1.950E-03	8.200E-02
	5	6.549	3.271E-02	9.597E-04	4.035E-02
	6	11.469	5.729E-02	1.681E-03	7.067E-02
	7	9.010	4.500E-02	1.320E-03	5.551E-02
	8	2.894	1.445E-02	4.241E-04	1.783E-02
	9	11.936	5.962E-02	1.749E-03	7.354E-02
	10	19.469	9.725E-02	2.853E-03	1.200E-01
	11	7.687	3.840E-02	1.127E-03	4.736E-02
	12	6.772	3.382E-02	9.924E-04	4.172E-02
	13	132.748	6.631E-01	1.945E-02	8.179E-01
	14	140.578	7.022E-01	2.060E-02	8.662E-01
	15	145.532	7.269E-01	2.133E-02	8.967E-01
	16	5.568	2.781E-02	8.160E-04	3.431E-02
	17	3.792	1.894E-02	5.557E-04	2.336E-02
	18	4.739	2.367E-02	6.945E-04	2.920E-02
	19	0.325	1.623E-03	4.762E-05	2.002E-03
	20	21.769	1.087E-01	3.190E-03	1.341E-01
	21	6.149	3.071E-02	9.011E-04	3.789E-02
	22	2.538	1.268E-02	3.719E-04	1.564E-02
	23	1.786	8.922E-03	2.618E-04	1.101E-02
	24	0.477	2.385E-03	6.996E-05	2.941E-03
	25	0.621	3.100E-03	9.097E-05	3.824E-03
	26	0.870	4.347E-03	1.275E-04	5.362E-03
	27	1.342	6.705E-03	1.967E-04	8.271E-03
	28	2.074	1.036E-02	3.039E-04	1.278E-02
	90	24.809	1.239E-01	3.636E-03	1.529E-01
	91	17.949	8.966E-02	2.630E-03	1.106E-01

Table IV

HEAT-TRANSFER DATA

RUN	POS	Q	Q/Q(REF)	C(H)	H/H(REF)
19	1	10.695	5.519E-02	1.578E-03	6.810E-02
	2	10.310	5.320E-02	1.521E-03	6.564E-02
	3	5.479	2.827E-02	8.086E-04	3.489E-02
	4	20.112	1.038E-01	2.968E-03	1.281E-01
	5	10.656	5.498E-02	1.573E-03	6.785E-02
	6	8.765	4.523E-02	1.294E-03	5.581E-02
	7	8.434	4.352E-02	1.245E-03	5.370E-02
	8	1.335	6.889E-03	1.970E-04	8.501E-03
	9	14.883	7.680E-02	2.196E-03	9.477E-02
	10	8.932	4.609E-02	1.318E-03	5.687E-02
	11	9.336	4.817E-02	1.378E-03	5.944E-02
	12	10.640	5.490E-02	1.570E-03	6.775E-02
	13	119.641	6.173E-01	1.766E-02	7.618E-01
	14	126.675	6.536E-01	1.869E-02	8.066E-01
	15	115.032	5.936E-01	1.698E-02	7.324E-01
	16	5.813	2.999E-02	8.578E-04	3.701E-02
	17	3.992	2.060E-02	5.891E-04	2.542E-02
	18	2.103	1.085E-02	3.104E-04	1.339E-02
	19	0.215	1.108E-03	3.168E-05	1.367E-03
	20	14.250	7.353E-02	2.103E-03	9.073E-02
	21	3.420	1.765E-02	5.047E-04	2.178E-02
	22	0.672	3.469E-03	9.922E-05	4.281E-03
	23	0.336	1.734E-03	4.960E-05	2.140E-03
	24	0.333	1.718E-03	4.914E-05	2.120E-03
	25	0.351	1.813E-03	5.185E-05	2.237E-03
	26	0.289	1.492E-03	4.268E-05	1.841E-03
	27	0.562	2.898E-03	8.287E-05	3.575E-03
	28	1.714	8.843E-03	2.529E-04	1.091E-02
	90	27.922	1.441E-01	4.121E-03	1.778E-01
	91	19.558	1.009E-01	2.886E-03	1.245E-01

Table IV

HEAT-TRANSFER DATA

RUN	POS	Q	Q/Q(REF)	C(H)	H/H(REF)
20	1	14.159	7.191E-02	2.084E-03	8.870E-02
	2	10.560	5.363E-02	1.554E-03	6.615E-02
	3	18.248	9.268E-02	2.686E-03	1.143E-01
	4	14.667	7.449E-02	2.159E-03	9.188E-02
	5	8.428	4.280E-02	1.240E-03	5.279E-02
	6	13.192	6.700E-02	1.941E-03	8.264E-02
	7	10.006	5.082E-02	1.473E-03	6.268E-02
	8	4.410	2.240E-02	6.490E-04	2.762E-02
	9	10.056	5.107E-02	1.480E-03	6.300E-02
	10	16.199	8.227E-02	2.384E-03	1.015E-01
	11	8.536	4.335E-02	1.256E-03	5.347E-02
	12	6.118	3.107E-02	9.004E-04	3.833E-02
	13	133.160	6.763E-01	1.960E-02	8.342E-01
	14	143.591	7.293E-01	2.113E-02	8.995E-01
	15	142.284	7.226E-01	2.094E-02	8.913E-01
	16	5.603	2.846E-02	8.246E-04	3.510E-02
	17	3.359	1.706E-02	4.943E-04	2.104E-02
	18	4.882	2.479E-02	7.184E-04	3.058E-02
	19	0.380	1.931E-03	5.595E-05	2.382E-03
	20	20.085	1.020E-01	2.956E-03	1.258E-01
	21	5.581	2.835E-02	8.214E-04	3.496E-02
	22	2.349	1.193E-02	3.457E-04	1.471E-02
	23	1.616	8.206E-03	2.378E-04	1.012E-02
	24	0.451	2.288E-03	6.631E-05	2.823E-03
	25	0.690	3.506E-03	1.016E-04	4.324E-03
	26	0.726	3.685E-03	1.068E-04	4.545E-03
	27	1.106	5.615E-03	1.627E-04	6.926E-03
	28	1.874	9.518E-03	2.758E-04	1.174E-02

Table IV

HEAT-TRANSFER DATA

RUN	POS	Q	Q/Q(REF)	C(H)	H/H(REF)
21	1	12.379	6.371E-02	1.851E-03	7.865E-02
	2	10.594	5.452E-02	1.584E-03	6.730E-02
	3	7.097	3.653E-02	1.061E-03	4.509E-02
	4	24.791	1.276E-01	3.708E-03	1.575E-01
	5	11.457	5.896E-02	1.714E-03	7.279E-02
	6	9.992	5.142E-02	1.494E-03	6.348E-02
	7	11.059	5.692E-02	1.654E-03	7.026E-02
	8	1.954	1.006E-02	2.922E-04	1.241E-02
	9	19.883	1.023E-01	2.974E-03	1.263E-01
	10	18.212	9.373E-02	2.724E-03	1.157E-01
	11	10.625	5.468E-02	1.589E-03	6.750E-02
	12	6.734	3.466E-02	1.007E-03	4.279E-02
	13	115.049	5.921E-01	1.721E-02	7.309E-01
	14	112.173	5.773E-01	1.678E-02	7.127E-01
	15	106.974	5.506E-01	1.600E-02	6.796E-01
	16	5.377	2.767E-02	8.042E-04	3.416E-02
	17	2.862	1.473E-02	4.280E-04	1.818E-02
	18	2.398	1.234E-02	3.586E-04	1.523E-02
	19	0.416	2.143E-03	6.227E-05	2.645E-03
	20	12.627	6.499E-02	1.889E-03	8.022E-02
	21	3.158	1.625E-02	4.723E-04	2.006E-02
	22	0.727	3.744E-03	1.088E-04	4.621E-03
	23	0.392	2.016E-03	5.860E-05	2.489E-03
	24	0.401	2.063E-03	5.996E-05	2.547E-03
	25	0.565	2.910E-03	8.456E-05	3.592E-03
	26	0.529	2.725E-03	7.919E-05	3.364E-03
	27	0.585	3.010E-03	8.746E-05	3.715E-03
	28	1.469	7.558E-03	2.196E-04	9.330E-03
	90	27.903	1.436E-01	4.173E-03	1.773E-01
	91	48.458	2.494E-01	7.248E-03	3.079E-01

Table IV

HEAT-TRANSFER DATA

RUN	POS	Q	Q/Q(REF)	C(H)	H/H(REF)
22	1	13.081	8.080E-02	3.354E-03	9.927E-02
	2	12.071	7.456E-02	3.095E-03	9.161E-02
	3	6.016	3.716E-02	1.542E-03	4.565E-02
	4	19.695	1.216E-01	5.049E-03	1.495E-01
	5	10.371	6.406E-02	2.659E-03	7.870E-02
	6	9.609	5.935E-02	2.464E-03	7.292E-02
	7	11.224	6.933E-02	2.878E-03	8.518E-02
	8	1.896	1.171E-02	4.862E-04	1.439E-02
	9	19.857	1.226E-01	5.091E-03	1.507E-01
	10	13.801	8.524E-02	3.538E-03	1.047E-01
	11	9.521	5.881E-02	2.441E-03	7.226E-02
	12	6.609	4.082E-02	1.694E-03	5.016E-02
	13	104.814	6.474E-01	2.687E-02	7.954E-01
	14	103.552	6.396E-01	2.655E-02	7.859E-01
	15	98.853	6.106E-01	2.534E-02	7.502E-01
	16	5.298	3.272E-02	1.358E-03	4.020E-02
	17	1.913	1.181E-02	4.904E-04	1.452E-02
	18	2.083	1.287E-02	5.340E-04	1.581E-02
	19	0.243	1.503E-03	6.240E-05	1.847E-03
	20	12.894	7.964E-02	3.306E-03	9.785E-02
	21	3.127	1.931E-02	8.016E-04	2.373E-02
	22	1.369	8.459E-03	3.511E-04	1.039E-02
	23	0.468	2.889E-03	1.199E-04	3.550E-03
	24	0.236	1.460E-03	6.059E-05	1.793E-03
	25	0.382	2.362E-03	9.803E-05	2.902E-03
	26	0.344	2.126E-03	8.825E-05	2.612E-03
	27	0.718	4.433E-03	1.840E-04	5.446E-03
	28	1.435	8.864E-03	3.679E-04	1.089E-02
	90	38.797	2.396E-01	9.947E-03	2.944E-01
	91	16.785	1.037E-01	4.303E-03	1.274E-01

Table IV

HEAT-TRANSFER DATA

RUN	POS	Q	Q/Q(REF)	C(H)	H/H(REF)
23	1	11.143	6.490E-02	2.665E-03	7.969E-02
	2	11.147	6.492E-02	2.666E-03	7.972E-02
	3	5.002	2.913E-02	1.196E-03	3.578E-02
	4	18.020	1.049E-01	4.309E-03	1.289E-01
	5	10.436	6.078E-02	2.496E-03	7.464E-02
	6	8.656	5.041E-02	2.070E-03	6.191E-02
	7	9.974	5.809E-02	2.385E-03	7.134E-02
	8	1.346	7.842E-03	3.220E-04	9.630E-03
	9	15.930	9.278E-02	3.810E-03	1.139E-01
	10	7.488	4.361E-02	1.791E-03	5.355E-02
	11	8.976	5.228E-02	2.147E-03	6.420E-02
	12	9.043	5.266E-02	2.163E-03	6.467E-02
	13	108.218	6.303E-01	2.588E-02	7.740E-01
	14	115.664	6.736E-01	2.766E-02	8.273E-01
	15	109.881	6.400E-01	2.628E-02	7.859E-01
	16	6.217	3.621E-02	1.487E-03	4.447E-02
	17	2.797	1.629E-02	6.688E-04	2.000E-02
	18	1.890	1.101E-02	4.521E-04	1.352E-02
	19	0.294	1.713E-03	7.035E-05	2.104E-03
	20	13.912	8.103E-02	3.327E-03	9.950E-02
	21	3.253	1.894E-02	7.779E-04	2.326E-02
	22	1.540	8.969E-03	3.683E-04	1.101E-02
	23	0.687	4.003E-03	1.644E-04	4.916E-03
	24	0.286	1.663E-03	6.830E-05	2.043E-03
	25	0.551	3.207E-03	1.317E-04	3.938E-03
	26	0.464	2.705E-03	1.111E-04	3.322E-03
	27	1.008	5.871E-03	2.411E-04	7.209E-03
	28	1.798	1.047E-02	4.300E-04	1.286E-02
	90	30.779	1.793E-01	7.361E-03	2.201E-01
	91	18.412	1.072E-01	4.403E-03	1.317E-01

Table IV

HEAT-TRANSFER DATA

RUN	POS	Q	Q/Q(REF)	C(H)	H/H(REF)
24	1	13.983	7.821E-02	3.146E-03	9.587E-02
	2	10.222	5.717E-02	2.300E-03	7.008E-02
	3	11.787	6.592E-02	2.652E-03	8.081E-02
	4	14.248	7.969E-02	3.206E-03	9.768E-02
	5	7.787	4.355E-02	1.752E-03	5.339E-02
	6	12.196	6.821E-02	2.744E-03	8.361E-02
	7	9.722	5.437E-02	2.187E-03	6.665E-02
	8	2.933	1.640E-02	6.598E-04	2.011E-02
	9	11.247	6.290E-02	2.531E-03	7.711E-02
	10	20.345	1.138E-01	4.577E-03	1.395E-01
	11	7.989	4.468E-02	1.797E-03	5.477E-02
	12	6.552	3.664E-02	1.474E-03	4.492E-02
	13	132.081	7.387E-01	2.972E-02	9.055E-01
	14	146.001	8.166E-01	3.285E-02	1.001E 00
	15	146.449	8.191E-01	3.295E-02	1.004E 00
	16	6.045	3.381E-02	1.360E-03	4.144E-02
	17	3.043	1.702E-02	6.848E-04	2.087E-02
	18	3.797	2.123E-02	8.542E-04	2.603E-02
	19	0.308	1.723E-03	6.930E-05	2.112E-03
	20	21.523	1.204E-01	4.842E-03	1.476E-01
	21	5.914	3.307E-02	1.331E-03	4.054E-02
	22	2.333	1.305E-02	5.250E-04	1.600E-02
	23	1.793	1.003E-02	4.034E-04	1.229E-02
	24	0.801	4.480E-03	1.802E-04	5.492E-03
	25	0.450	2.515E-03	1.012E-04	3.083E-03
	26	0.762	4.260E-03	1.714E-04	5.222E-03
	27	1.475	8.252E-03	3.320E-04	1.012E-02
	28	2.082	1.164E-02	4.684E-04	1.427E-02
	90	27.865	1.558E-01	6.269E-03	1.910E-01
	91	16.773	9.381E-02	3.774E-03	1.150E-01

Table IV

HEAT-TRANSFER DATA

RUN	POS	Q	Q/Q(REF)	C(H)	H/H(REF)
25	1	16.454	9.413E-02	3.850E-03	1.155E-01
	2	8.969	5.131E-02	2.099E-03	6.295E-02
	3	15.344	8.778E-02	3.590E-03	1.077E-01
	4	6.987	3.997E-02	1.635E-03	4.904E-02
	5	8.738	4.999E-02	2.044E-03	6.133E-02
	6	16.010	9.159E-02	3.746E-03	1.124E-01
	7	3.937	2.252E-02	9.213E-04	2.764E-02
	8	12.034	6.884E-02	2.816E-03	8.446E-02
	9	5.955	3.407E-02	1.393E-03	4.180E-02
	10	6.393	3.658E-02	1.496E-03	4.487E-02
	11	2.663	1.523E-02	6.230E-04	1.869E-02
	12	2.953	1.690E-02	6.910E-04	2.073E-02
	13	175.996	1.007E 00	4.118E-02	1.235E 00
	14	239.673	1.371E 00	5.608E-02	1.682E 00
	15	149.191	8.535E-01	3.491E-02	1.047E 00
	16	6.866	3.928E-02	1.607E-03	4.820E-02
	17	2.750	1.573E-02	6.434E-04	1.930E-02
	18	6.194	3.543E-02	1.449E-03	4.347E-02
	19	0.334	1.910E-03	7.812E-05	2.344E-03
	20	27.730	1.586E-01	6.488E-03	1.946E-01
	21	8.680	4.966E-02	2.031E-03	6.092E-02
	22	3.627	2.075E-02	8.486E-04	2.546E-02
	23	2.591	1.482E-02	6.063E-04	1.819E-02
	24	1.763	1.009E-02	4.126E-04	1.238E-02
	25	0.546	3.123E-03	1.277E-04	3.831E-03
	26	1.135	6.492E-03	2.655E-04	7.965E-03
	27	1.520	8.695E-03	3.556E-04	1.067E-02
	28	2.117	1.211E-02	4.954E-04	1.486E-02
	90	21.534	1.232E-01	5.038E-03	1.511E-01
	91	12.674	7.250E-02	2.965E-03	8.896E-02

Table IV

HEAT-TRANSFER DATA

RUN	POS	Q	Q/Q(REF)	C(H)	H/H(REF)
26	1	17.211	9.908E-02	4.053E-03	1.215E-01
	2	11.301	6.506E-02	2.661E-03	7.980E-02
	3	15.037	8.657E-02	3.541E-03	1.062E-01
	4	7.247	4.172E-02	1.707E-03	5.118E-02
	5	10.650	6.131E-02	2.508E-03	7.521E-02
	6	16.616	9.566E-02	3.913E-03	1.173E-01
	7	3.565	2.052E-02	8.395E-04	2.517E-02
	8	11.682	6.726E-02	2.751E-03	8.250E-02
	9	5.228	3.010E-02	1.231E-03	3.692E-02
	10	6.448	3.712E-02	1.519E-03	4.553E-02
	11	3.129	1.801E-02	7.368E-04	2.209E-02
	12	4.398	2.532E-02	1.036E-03	3.106E-02
	13	143.117	8.239E-01	3.371E-02	1.011E 00
	14	183.653	1.057E 00	4.325E-02	1.297E 00
	15	155.163	8.933E-01	3.654E-02	1.096E 00
	16	5.216	3.003E-02	1.228E-03	3.683E-02
	17	2.298	1.323E-02	5.412E-04	1.623E-02
	18	6.323	3.640E-02	1.489E-03	4.465E-02
	19	0.421	2.426E-03	9.923E-05	2.975E-03
	20	24.814	1.429E-01	5.844E-03	1.752E-01
	21	7.584	4.366E-02	1.786E-03	5.356E-02
	22	3.313	1.907E-02	7.802E-04	2.339E-02
	23	2.303	1.326E-02	5.423E-04	1.626E-02
	25	0.294	1.691E-03	6.919E-05	2.075E-03
	26	0.794	4.568E-03	1.869E-04	5.604E-03
	27	1.381	7.950E-03	3.252E-04	9.752E-03
	28	2.070	1.192E-02	4.875E-04	1.462E-02
	90	21.964	1.264E-01	5.173E-03	1.551E-01
	91	12.768	7.350E-02	3.007E-03	9.016E-02

Table IV

HEAT-TRANSFER DATA

RUN	POS	Q	Q/Q(REF)	C(H)	H/H(REF)
27	1	21.439	1.013E-01	5.410E-03	1.233E-01
	2	13.607	6.430E-02	3.434E-03	7.824E-02
	3	14.059	6.644E-02	3.548E-03	8.084E-02
	4	9.150	4.324E-02	2.309E-03	5.261E-02
	5	12.570	5.940E-02	3.172E-03	7.228E-02
	6	16.042	7.581E-02	4.048E-03	9.225E-02
	7	4.556	2.153E-02	1.150E-03	2.620E-02
	8	10.722	5.067E-02	2.706E-03	6.166E-02
	9	5.338	2.522E-02	1.347E-03	3.069E-02
	10	6.873	3.248E-02	1.734E-03	3.952E-02
	11	4.328	2.046E-02	1.092E-03	2.489E-02
	12	6.023	2.846E-02	1.520E-03	3.463E-02
	13	190.525	9.004E-01	4.808E-02	1.096E 00
	14	169.953	8.032E-01	4.289E-02	9.773E-01
	15	190.162	8.987E-01	4.799E-02	1.093E 00
	16	6.501	3.073E-02	1.641E-03	3.739E-02
	17	2.249	1.063E-02	5.676E-04	1.293E-02
	18	5.928	2.801E-02	1.496E-03	3.409E-02
	19	0.471	2.227E-03	1.189E-04	2.710E-03
	20	29.801	1.408E-01	7.520E-03	1.714E-01
	21	8.509	4.021E-02	2.147E-03	4.893E-02
	22	3.569	1.687E-02	9.006E-04	2.052E-02
	23	2.462	1.164E-02	6.213E-04	1.416E-02
	24	1.709	8.078E-03	4.313E-04	9.829E-03
	25	0.767	3.624E-03	1.935E-04	4.410E-03
	26	1.496	7.069E-03	3.775E-04	8.602E-03
	27	1.643	7.766E-03	4.146E-04	9.449E-03
	28	2.408	1.138E-02	6.076E-04	1.385E-02
	90	27.990	1.323E-01	7.063E-03	1.610E-01
	91	14.479	6.843E-02	3.654E-03	8.326E-02

Table IV

HEAT-TRANSFER DATA

RUN	POS	Q	Q/Q(REF)	C(H)	H/H(REF)
28	1	19.338	9.130E-02	4.830E-03	1.112E-01
	2	10.508	4.961E-02	2.624E-03	6.043E-02
	3	13.013	6.144E-02	3.250E-03	7.483E-02
	4	7.959	3.758E-02	1.988E-03	4.577E-02
	5	9.912	4.680E-02	2.476E-03	5.700E-02
	6	17.766	8.388E-02	4.437E-03	1.022E-01
	7	4.281	2.021E-02	1.069E-03	2.462E-02
	8	10.063	4.751E-02	2.513E-03	5.787E-02
	9	6.029	2.847E-02	1.506E-03	3.467E-02
	10	7.144	3.373E-02	1.784E-03	4.108E-02
	11	3.497	1.651E-02	8.734E-04	2.011E-02
	12	3.874	1.829E-02	9.676E-04	2.228E-02
	13	200.573	9.470E-01	5.009E-02	1.153E 00
	14	289.532	1.367E 00	7.231E-02	1.665E 00
	15	176.912	8.353E-01	4.418E-02	1.017E 00
	16	7.084	3.344E-02	1.769E-03	4.073E-02
	17	1.986	9.379E-03	4.961E-04	1.142E-02
	18	5.325	2.514E-02	1.330E-03	3.062E-02
	19	0.632	2.982E-03	1.577E-04	3.632E-03
	20	29.961	1.415E-01	7.483E-03	1.723E-01
	21	8.687	4.102E-02	2.170E-03	4.995E-02
	22	3.775	1.782E-02	9.428E-04	2.171E-02
	23	2.532	1.195E-02	6.323E-04	1.456E-02
	24	1.752	8.273E-03	4.376E-04	1.008E-02
	25	1.131	5.340E-03	2.825E-04	6.504E-03
	26	1.523	7.189E-03	3.803E-04	8.756E-03
	27	1.759	8.304E-03	4.392E-04	1.011E-02
	28	2.461	1.162E-02	6.146E-04	1.415E-02
	90	29.198	1.379E-01	7.292E-03	1.679E-01
	91	16.233	7.664E-02	4.054E-03	9.334E-02

Table IV

HEAT-TRANSFER DATA

RUN	POS	Q	Q/Q(REF)	C(H)	H/H(REF)
29	1	16.584	8.157E-02	4.304E-03	9.929E-02
	2	11.187	5.503E-02	2.903E-03	6.698E-02
	3	9.755	4.798E-02	2.532E-03	5.840E-02
	4	15.066	7.411E-02	3.910E-03	9.020E-02
	5	8.006	3.938E-02	2.078E-03	4.794E-02
	6	12.409	6.104E-02	3.221E-03	7.430E-02
	7	10.023	4.930E-02	2.601E-03	6.001E-02
	8	2.894	1.423E-02	7.509E-04	1.732E-02
	9	11.775	5.792E-02	3.056E-03	7.050E-02
	10	16.564	8.148E-02	4.299E-03	9.917E-02
	11	8.923	4.389E-02	2.316E-03	5.342E-02
	12	7.049	3.468E-02	1.830E-03	4.221E-02
	13	135.066	6.644E-01	3.505E-02	8.087E-01
	14	151.807	7.467E-01	3.940E-02	9.089E-01
	15	155.653	7.656E-01	4.040E-02	9.319E-01
	16	7.175	3.529E-02	1.862E-03	4.296E-02
	17	1.938	9.534E-03	5.030E-04	1.160E-02
	18	3.702	1.821E-02	9.607E-04	2.216E-02
	19	0.341	1.678E-03	8.855E-05	2.043E-03
	20	21.882	1.076E-01	5.679E-03	1.310E-01
	21	6.011	2.957E-02	1.560E-03	3.599E-02
	22	2.618	1.288E-02	6.795E-04	1.567E-02
	23	1.760	8.657E-03	4.568E-04	1.054E-02
	24	1.320	6.491E-03	3.425E-04	7.901E-03
	25	0.832	4.091E-03	2.158E-04	4.979E-03
	26	1.354	6.660E-03	3.514E-04	8.107E-03
	27	1.640	8.068E-03	4.257E-04	9.820E-03
	28	2.254	1.109E-02	5.850E-04	1.350E-02
	90	42.379	2.085E-01	1.100E-02	2.537E-01
	91	21.319	1.049E-01	5.533E-03	1.276E-01

Table IV

HEAT-TRANSFER DATA

RUN	POS	Q	Q/Q(REF)	C(H)	H/H(REF)
30	1	13.811	6.599E-02	3.382E-03	8.041E-02
	2	13.889	6.636E-02	3.401E-03	8.086E-02
	3	4.655	2.224E-02	1.140E-03	2.710E-02
	4	16.787	8.020E-02	4.111E-03	9.773E-02
	5	11.786	5.631E-02	2.886E-03	6.862E-02
	6	9.974	4.765E-02	2.443E-03	5.807E-02
	7	12.154	5.807E-02	2.976E-03	7.076E-02
	8	1.590	7.597E-03	3.894E-04	9.257E-03
	9	13.920	6.651E-02	3.409E-03	8.104E-02
	10	6.378	3.047E-02	1.562E-03	3.713E-02
	11	10.318	4.930E-02	2.527E-03	6.007E-02
	12	9.589	4.582E-02	2.348E-03	5.583E-02
	13	113.589	5.427E-01	2.782E-02	6.613E-01
	14	119.041	5.688E-01	2.915E-02	6.931E-01
	15	122.461	5.851E-01	2.999E-02	7.130E-01
	16	7.259	3.468E-02	1.778E-03	4.226E-02
	17	2.069	9.887E-03	5.068E-04	1.205E-02
	18	2.063	9.859E-03	5.053E-04	1.201E-02
	19	0.244	1.167E-03	5.981E-05	1.422E-03
	20	15.248	7.285E-02	3.734E-03	8.877E-02
	21	3.785	1.809E-02	9.270E-04	2.204E-02
	22	1.558	7.443E-03	3.815E-04	9.069E-03
	23	1.247	5.958E-03	3.054E-04	7.260E-03
	24	0.536	2.563E-03	1.314E-04	3.123E-03
	25	0.730	3.486E-03	1.787E-04	4.247E-03
	26	0.732	3.496E-03	1.792E-04	4.261E-03
	27	1.410	6.735E-03	3.452E-04	8.207E-03
	28	1.911	9.129E-03	4.679E-04	1.112E-02
	90	45.413	2.170E-01	1.112E-02	2.644E-01
	91	21.722	1.038E-01	5.320E-03	1.265E-01

Table IV

HEAT-TRANSFER DATA

RUN	POS	Q	Q/Q(REF)	C(H)	H/H(REF)
31	1	12.207	7.452E-02	6.820E-03	9.041E-02
	2	11.041	6.741E-02	6.169E-03	8.178E-02
	3	3.638	2.221E-02	2.032E-03	2.694E-02
	4	10.456	6.384E-02	5.842E-03	7.745E-02
	5	9.269	5.659E-02	5.179E-03	6.865E-02
	6	8.565	5.229E-02	4.785E-03	6.344E-02
	7	10.087	6.158E-02	5.635E-03	7.471E-02
	8	1.281	7.823E-03	7.159E-04	9.491E-03
	9	8.432	5.148E-02	4.711E-03	6.245E-02
	10	4.525	2.763E-02	2.528E-03	3.352E-02
	11	9.742	5.948E-02	5.443E-03	7.216E-02
	12	6.834	4.172E-02	3.818E-03	5.062E-02
	13	84.887	5.182E-01	4.742E-02	6.287E-01
	14	87.868	5.364E-01	4.909E-02	6.508E-01
	15	78.550	4.795E-01	4.388E-02	5.818E-01
	16	6.452	3.939E-02	3.605E-03	4.779E-02
	17	0.871	5.317E-03	4.866E-04	6.451E-03
	18	1.676	1.023E-02	9.363E-04	1.241E-02
	19	0.299	1.826E-03	1.671E-04	2.216E-03
	20	9.746	5.950E-02	5.445E-03	7.218E-02
	21	2.491	1.521E-02	1.391E-03	1.845E-02
	22	1.068	6.519E-03	5.965E-04	7.908E-03
	23	0.813	4.962E-03	4.541E-04	6.020E-03
	24	0.513	3.133E-03	2.867E-04	3.800E-03
	25	0.818	4.992E-03	4.569E-04	6.057E-03
	26	0.803	4.900E-03	4.485E-04	5.945E-03
	27	1.145	6.991E-03	6.397E-04	8.481E-03
	28	1.578	9.633E-03	8.816E-04	1.169E-02
	90	29.639	1.809E-01	1.656E-02	2.195E-01
	91	15.853	9.678E-02	8.857E-03	1.174E-01

Table IV

HEAT-TRANSFER DATA

RUN	POS	Q	Q/Q(REF)	C(H)	H/H(REF)
32	1	13.629	8.931E-02	8.099E-03	1.084E-01
	2	8.730	5.721E-02	5.187E-03	6.940E-02
	3	6.590	4.318E-02	3.916E-03	5.239E-02
	4	10.474	6.863E-02	6.224E-03	8.326E-02
	5	7.180	4.705E-02	4.266E-03	5.708E-02
	6	8.987	5.889E-02	5.340E-03	7.145E-02
	7	7.920	5.190E-02	4.706E-03	6.297E-02
	8	2.430	1.592E-02	1.444E-03	1.932E-02
	9	9.234	6.051E-02	5.487E-03	7.341E-02
	10	9.088	5.956E-02	5.400E-03	7.225E-02
	11	6.306	4.133E-02	3.747E-03	5.014E-02
	12	4.698	3.079E-02	2.792E-03	3.735E-02
	13	94.391	6.186E-01	5.609E-02	7.504E-01
	14	95.926	6.286E-01	5.700E-02	7.626E-01
	15	108.981	7.142E-01	6.476E-02	8.664E-01
	16	6.252	4.097E-02	3.715E-03	4.970E-02
	17	0.975	6.389E-03	5.794E-04	7.751E-03
	18	2.314	1.517E-02	1.375E-03	1.840E-02
	19	0.608	3.982E-03	3.611E-04	4.831E-03
	20	14.740	9.659E-02	8.759E-03	1.172E-01
	21	4.031	2.642E-02	2.395E-03	3.205E-02
	22	1.606	1.053E-02	9.546E-04	1.277E-02
	23	0.961	6.299E-03	5.711E-04	7.641E-03
	24	0.822	5.388E-03	4.886E-04	6.537E-03
	25	1.160	7.604E-03	6.895E-04	9.225E-03
	26	1.310	8.584E-03	7.784E-04	1.041E-02
	27	1.236	8.100E-03	7.345E-04	9.826E-03
	28	1.664	1.091E-02	9.889E-04	1.323E-02
	90	27.164	1.780E-01	1.614E-02	2.160E-01
	91	15.404	1.009E-01	9.153E-03	1.225E-01

Table IV

HEAT-TRANSFER DATA

RUN	POS	Q	Q/Q(REF)	C(H)	H/H(REF)
33	1	15.217	9.607E-02	8.597E-03	1.166E-01
	2	9.051	5.714E-02	5.113E-03	6.935E-02
	3	8.315	5.249E-02	4.698E-03	6.371E-02
	4	6.593	4.162E-02	3.725E-03	5.052E-02
	5	7.942	5.014E-02	4.487E-03	6.086E-02
	6	12.586	7.946E-02	7.111E-03	9.645E-02
	7	3.335	2.105E-02	1.884E-03	2.556E-02
	8	5.059	3.194E-02	2.858E-03	3.877E-02
	9	3.953	2.496E-02	2.234E-03	3.029E-02
	10	4.928	3.111E-02	2.784E-03	3.776E-02
	11	3.026	1.910E-02	1.710E-03	2.319E-02
	12	3.372	2.129E-02	1.905E-03	2.584E-02
	13	126.191	7.967E-01	7.129E-02	9.670E-01
	14	185.875	1.173E 00	1.050E-01	1.424E 00
	15	125.416	7.918E-01	7.086E-02	9.611E-01
	16	6.216	3.924E-02	3.512E-03	4.763E-02
	17	1.358	8.576E-03	7.675E-04	1.041E-02
	18	3.002	1.895E-02	1.696E-03	2.301E-02
	19	0.702	4.432E-03	3.966E-04	5.380E-03
	20	21.796	1.376E-01	1.231E-02	1.670E-01
	21	5.892	3.720E-02	3.329E-03	4.515E-02
	22	2.487	1.570E-02	1.405E-03	1.906E-02
	23	1.491	9.411E-03	8.422E-04	1.142E-02
	24	1.042	6.577E-03	5.885E-04	7.983E-03
	25	1.542	9.734E-03	8.711E-04	1.182E-02
	26	1.177	7.433E-03	6.652E-04	9.022E-03
	27	1.336	8.437E-03	7.550E-04	1.024E-02
	28	1.893	1.195E-02	1.069E-03	1.451E-02
	91	10.681	6.743E-02	6.035E-03	8.185E-02

Table IV

HEAT-TRANSFER DATA

RUN	POS	Q	Q/Q(REF)	C(H)	H/H(REF)
34	1	11.371	9.564E-02	1.049E-02	1.163E-01
	2	6.629	5.575E-02	6.116E-03	6.779E-02
	3	5.832	4.905E-02	5.380E-03	5.963E-02
	4	5.112	4.300E-02	4.717E-03	5.228E-02
	5	6.013	5.057E-02	5.547E-03	6.148E-02
	6	9.430	7.931E-02	8.700E-03	9.643E-02
	7	2.783	2.341E-02	2.568E-03	2.846E-02
	8	3.638	3.060E-02	3.357E-03	3.720E-02
	9	3.277	2.756E-02	3.024E-03	3.351E-02
	10	3.975	3.343E-02	3.668E-03	4.065E-02
	11	2.396	2.015E-02	2.210E-03	2.450E-02
	12	2.622	2.205E-02	2.419E-03	2.682E-02
	13	96.911	8.151E-01	8.941E-02	9.910E-01
	14	125.446	1.055E 00	1.157E-01	1.283E 00
	15	86.477	7.273E-01	7.979E-02	8.843E-01
	16	5.279	4.440E-02	4.870E-03	5.398E-02
	17	1.065	8.955E-03	9.823E-04	1.089E-02
	18	2.340	1.968E-02	2.159E-03	2.393E-02
	19	0.608	5.117E-03	5.614E-04	6.222E-03
	21	4.416	3.714E-02	4.074E-03	4.516E-02
	22	1.679	1.412E-02	1.549E-03	1.717E-02
	23	1.308	1.100E-02	1.207E-03	1.338E-02
	24	0.878	7.387E-03	8.103E-04	8.981E-03
	25	0.717	6.034E-03	6.619E-04	7.336E-03
	26	0.846	7.116E-03	7.807E-04	8.652E-03
	27	1.113	9.362E-03	1.027E-03	1.138E-02
	28	1.424	1.197E-02	1.313E-03	1.456E-02
	91	9.691	8.150E-02	8.941E-03	9.910E-02

Table IV

HEAT-TRANSFER DATA

RUN	POS	Q	Q/Q(REF)	C(H)	H/H(REF)
35	1	17.666	8.842E-02	2.514E-03	1.091E-01
	2	6.373	3.190E-02	9.068E-04	3.936E-02
	3	19.107	9.563E-02	2.719E-03	1.180E-01
	4	6.643	3.325E-02	9.452E-04	4.102E-02
	5	8.348	4.178E-02	1.188E-03	5.156E-02
	6	14.789	7.402E-02	2.104E-03	9.134E-02
	7	3.955	1.979E-02	5.627E-04	2.442E-02
	8	16.540	8.278E-02	2.354E-03	1.021E-01
	9	6.682	3.344E-02	9.508E-04	4.127E-02
	10	6.800	3.404E-02	9.676E-04	4.200E-02
	11	3.061	1.532E-02	4.355E-04	1.890E-02
	12	2.930	1.466E-02	4.169E-04	1.809E-02
	13	189.390	9.479E-01	2.695E-02	1.170E 00
	14	276.338	1.383E 00	3.932E-02	1.707E 00
	15	155.120	7.764E-01	2.207E-02	9.580E-01
	16	7.022	3.515E-02	9.992E-04	4.337E-02
	17	3.221	1.612E-02	4.584E-04	1.989E-02
	18	7.973	3.991E-02	1.135E-03	4.924E-02
	19	0.352	1.760E-03	5.003E-05	2.171E-03
	20	29.518	1.477E-01	4.200E-03	1.823E-01
	21	9.430	4.720E-02	1.342E-03	5.824E-02
	22	4.195	2.100E-02	5.969E-04	2.591E-02
	23	2.954	1.479E-02	4.204E-04	1.824E-02
	24	1.783	8.925E-03	2.537E-04	1.101E-02
	25	0.558	2.792E-03	7.939E-05	3.446E-03
	26	0.890	4.457E-03	1.267E-04	5.499E-03
	27	1.323	6.622E-03	1.883E-04	8.171E-03
	28	2.008	1.005E-02	2.857E-04	1.240E-02
	91	19.890	9.955E-02	2.830E-03	1.228E-01

Table IV

HEAT-TRANSFER DATA

RUN	POS	Q	Q/Q(REF)	C(H)	H/H(REF)
36	30	49.909	2.498E-01	7.114E-03	3.078E-01
	31	46.187	2.312E-01	6.583E-03	2.848E-01
	32	41.179	2.061E-01	5.870E-03	2.539E-01
	33	24.597	1.231E-01	3.506E-03	1.517E-01
	34	38.345	1.919E-01	5.466E-03	2.365E-01
	35	39.294	1.967E-01	5.601E-03	2.423E-01
	36	22.555	1.129E-01	3.215E-03	1.391E-01
	37	14.236	7.125E-02	2.029E-03	8.779E-02
	38	23.865	1.194E-01	3.402E-03	1.472E-01
	39	46.446	2.325E-01	6.620E-03	2.864E-01
	40	21.362	1.069E-01	3.045E-03	1.317E-01
	41	29.531	1.478E-01	4.209E-03	1.821E-01
	42	11.628	5.820E-02	1.657E-03	7.170E-02
	1	18.271	9.145E-02	2.604E-03	1.127E-01
	2	10.195	5.103E-02	1.453E-03	6.287E-02
	3	20.066	1.004E-01	2.860E-03	1.237E-01
	4	7.738	3.873E-02	1.103E-03	4.772E-02
	5	2.889	1.446E-02	4.119E-04	1.782E-02
	6	5.092	2.549E-02	7.258E-04	3.140E-02
	10	0.221	1.104E-03	3.145E-05	1.361E-03
	11	0.529	2.650E-03	7.547E-05	3.265E-03
	16	7.639	3.823E-02	1.089E-03	4.711E-02
	17	3.135	1.569E-02	4.469E-04	1.933E-02
	18	8.494	4.251E-02	1.211E-03	5.238E-02
	19	0.304	1.522E-03	4.334E-05	1.875E-03
	20	31.869	1.595E-01	4.543E-03	1.965E-01
	21	10.067	5.039E-02	1.435E-03	6.208E-02
	22	4.375	2.190E-02	6.237E-04	2.698E-02
	23	3.062	1.533E-02	4.365E-04	1.888E-02
	24	2.054	1.028E-02	2.927E-04	1.266E-02
	25	0.608	3.043E-03	8.668E-05	3.750E-03
	26	0.849	4.251E-03	1.211E-04	5.238E-03
	27	1.651	8.263E-03	2.353E-04	1.018E-02
	28	2.344	1.173E-02	3.341E-04	1.445E-02

Table IV

HEAT-TRANSFER DATA

RUN	POS	Q	Q/Q(REF)	C(H)	H/H(REF)
37	29	137.516	7.354E-01	2.084E-02	9.077E-01
	30	40.185	2.149E-01	6.090E-03	2.652E-01
	31	35.508	1.899E-01	5.382E-03	2.344E-01
	32	28.804	1.540E-01	4.365E-03	1.901E-01
	33	16.758	8.962E-02	2.540E-03	1.106E-01
	34	28.181	1.507E-01	4.271E-03	1.860E-01
	35	32.746	1.751E-01	4.963E-03	2.161E-01
	36	15.680	8.385E-02	2.376E-03	1.035E-01
	37	11.253	6.018E-02	1.706E-03	7.428E-02
	38	19.663	1.051E-01	2.980E-03	1.298E-01
	39	37.684	2.015E-01	5.711E-03	2.487E-01
	40	16.693	8.927E-02	2.530E-03	1.102E-01
	41	24.433	1.307E-01	3.703E-03	1.613E-01
	42	9.172	4.905E-02	1.390E-03	6.054E-02
	1	16.548	8.849E-02	2.508E-03	1.092E-01
	2	8.593	4.595E-02	1.302E-03	5.672E-02
	3	18.026	9.639E-02	2.732E-03	1.190E-01
	4	6.747	3.608E-02	1.023E-03	4.454E-02
	5	2.023	1.082E-02	3.066E-04	1.335E-02
	6	4.097	2.191E-02	6.209E-04	2.704E-02
	10	0.140	7.464E-04	2.115E-05	9.213E-04
	11	0.551	2.946E-03	8.350E-05	3.637E-03
	12	1.115	5.961E-03	1.689E-04	7.358E-03
	13	237.184	1.268E 00	3.595E-02	1.566E 00
	14	293.156	1.568E 00	4.443E-02	1.935E 00
	15	173.030	9.253E-01	2.622E-02	1.142E 00
	16	6.823	3.649E-02	1.034E-03	4.504E-02
	17	2.744	1.467E-02	4.159E-04	1.811E-02
	18	8.100	4.332E-02	1.228E-03	5.347E-02
	19	0.227	1.215E-03	3.444E-05	1.500E-03
	20	29.762	1.592E-01	4.511E-03	1.965E-01
	21	9.291	4.968E-02	1.408E-03	6.133E-02
	22	4.088	2.186E-02	6.196E-04	2.698E-02
	23	2.998	1.603E-02	4.544E-04	1.979E-02
	24	1.951	1.043E-02	2.957E-04	1.288E-02
	25	0.574	3.068E-03	8.695E-05	3.787E-03
	26	0.800	4.276E-03	1.212E-04	5.278E-03
	27	1.581	8.455E-03	2.396E-04	1.044E-02
	28	2.079	1.112E-02	3.151E-04	1.372E-02
	90	36.321	1.942E-01	5.505E-03	2.397E-01
	91	41.146	2.200E-01	6.236E-03	2.716E-01

Table IV

HEAT-TRANSFER DATA

RUN	POS	Q	Q/Q(REF)	C(H)	H/H(REF)
38	29	124.208	6.900E-01	1.995E-02	8.525E-01
	30	33.309	1.850E-01	5.349E-03	2.286E-01
	31	27.421	1.523E-01	4.404E-03	1.882E-01
	32	16.872	9.373E-02	2.709E-03	1.158E-01
	33	17.975	9.986E-02	2.887E-03	1.234E-01
	34	36.110	2.006E-01	5.799E-03	2.478E-01
	35	24.943	1.386E-01	4.006E-03	1.712E-01
	36	14.473	8.040E-02	2.324E-03	9.934E-02
	37	5.539	3.077E-02	8.895E-04	3.802E-02
	38	19.091	1.061E-01	3.066E-03	1.310E-01
	39	25.684	1.427E-01	4.125E-03	1.763E-01
	40	25.933	1.441E-01	4.165E-03	1.780E-01
	41	17.068	9.482E-02	2.741E-03	1.171E-01
	42	7.811	4.339E-02	1.254E-03	5.361E-02
	1	13.848	7.694E-02	2.224E-03	9.505E-02
	2	8.250	4.584E-02	1.325E-03	5.663E-02
	3	19.281	1.071E-01	3.096E-03	1.323E-01
	4	7.303	4.057E-02	1.173E-03	5.013E-02
	5	1.940	1.078E-02	3.116E-04	1.332E-02
	6	3.344	1.858E-02	5.371E-04	2.296E-02
	10	0.186	1.032E-03	2.984E-05	1.275E-03
	11	0.415	2.308E-03	6.672E-05	2.851E-03
	12	0.808	4.489E-03	1.298E-04	5.546E-03
	13	146.533	8.141E-01	2.353E-02	1.006E 00
	14	194.978	1.083E 00	3.131E-02	1.338E 00
	15	225.468	1.253E 00	3.621E-02	1.548E 00
	16	4.955	2.753E-02	7.956E-04	3.401E-02
	17	2.468	1.371E-02	3.963E-04	1.694E-02
	18	6.711	3.728E-02	1.078E-03	4.606E-02
	19	0.183	1.018E-03	2.942E-05	1.257E-03
	20	24.450	1.358E-01	3.926E-03	1.678E-01
	21	7.870	4.372E-02	1.264E-03	5.402E-02
	22	3.305	1.836E-02	5.308E-04	2.269E-02
	23	2.287	1.271E-02	3.673E-04	1.570E-02
	24	1.501	8.336E-03	2.410E-04	1.030E-02
	25	0.349	1.940E-03	5.609E-05	2.397E-03
	26	0.744	4.131E-03	1.194E-04	5.103E-03
	27	1.419	7.883E-03	2.279E-04	9.739E-03
	28	1.891	1.050E-02	3.036E-04	1.298E-02
	90	22.597	1.255E-01	3.629E-03	1.551E-01
	91	46.764	2.598E-01	7.510E-03	3.210E-01

Table IV

HEAT-TRANSFER DATA

RUN	POS	Q	Q/Q(REF)	C(H)	H/H(REF)
39	29	94.424	4.908E-01	1.424E-02	6.057E-01
	30	33.622	1.747E-01	5.070E-03	2.157E-01
	31	15.878	8.253E-02	2.395E-03	1.019E-01
	32	6.800	3.535E-02	1.026E-03	4.362E-02
	33	28.555	1.484E-01	4.306E-03	1.832E-01
	34	22.711	1.180E-01	3.425E-03	1.457E-01
	35	18.299	9.511E-02	2.760E-03	1.174E-01
	36	30.915	1.607E-01	4.662E-03	1.983E-01
	38	32.338	1.681E-01	4.877E-03	2.074E-01
	39	22.433	1.166E-01	3.383E-03	1.439E-01
	40	17.121	8.899E-02	2.582E-03	1.098E-01
	41	12.223	6.353E-02	1.843E-03	7.841E-02
	42	11.222	5.833E-02	1.692E-03	7.199E-02
	1	12.001	6.238E-02	1.810E-03	7.698E-02
	2	9.732	5.058E-02	1.468E-03	6.243E-02
	3	13.743	7.143E-02	2.073E-03	8.816E-02
	4	13.803	7.174E-02	2.082E-03	8.854E-02
	5	3.857	2.005E-02	5.817E-04	2.474E-02
	6	5.330	2.770E-02	8.038E-04	3.419E-02
	11	1.132	5.883E-03	1.707E-04	7.261E-03
	12	1.004	5.220E-03	1.515E-04	6.442E-03
	13	138.415	7.194E-01	2.087E-02	8.879E-01
	14	145.128	7.543E-01	2.189E-02	9.309E-01
	15	142.550	7.409E-01	2.150E-02	9.144E-01
	16	5.298	2.754E-02	7.990E-04	3.399E-02
	17	1.066	5.539E-03	1.607E-04	6.837E-03
	18	4.518	2.348E-02	6.814E-04	2.898E-02
	19	0.223	1.161E-03	3.369E-05	1.433E-03
	20	21.039	1.094E-01	3.173E-03	1.350E-01
	21	5.822	3.026E-02	8.781E-04	3.735E-02
	22	2.470	1.284E-02	3.725E-04	1.584E-02
	23	1.666	8.657E-03	2.512E-04	1.068E-02
	24	0.426	2.216E-03	6.430E-05	2.735E-03
	25	0.368	1.912E-03	5.547E-05	2.359E-03
	26	0.560	2.910E-03	8.444E-05	3.592E-03
	27	1.320	6.858E-03	1.990E-04	8.464E-03
	28	2.131	1.107E-02	3.213E-04	1.367E-02
	90	27.099	1.408E-01	4.087E-03	1.738E-01
	91	63.230	3.286E-01	9.536E-03	4.056E-01

Table IV

HEAT-TRANSFER DATA

RUN	POS	Q	Q/Q(REF)	C(H)	H/H(REF)
40	29	104.485	5.587E-01	1.619E-02	6.897E-01
	30	8.900	4.759E-02	1.379E-03	5.875E-02
	31	7.965	4.259E-02	1.234E-03	5.258E-02
	32	5.163	2.761E-02	7.998E-04	3.408E-02
	33	27.252	1.457E-01	4.222E-03	1.799E-01
	34	21.391	1.144E-01	3.314E-03	1.412E-01
	35	29.120	1.557E-01	4.511E-03	1.922E-01
	36	11.525	6.163E-02	1.785E-03	7.608E-02
	37	24.946	1.334E-01	3.864E-03	1.647E-01
	38	24.868	1.330E-01	3.852E-03	1.642E-01
	39	22.012	1.177E-01	3.410E-03	1.453E-01
	40	17.309	9.256E-02	2.681E-03	1.143E-01
	41	17.316	9.260E-02	2.682E-03	1.143E-01
	42	19.504	1.043E-01	3.021E-03	1.287E-01
	1	10.105	5.404E-02	1.565E-03	6.670E-02
	2	9.355	5.003E-02	1.449E-03	6.175E-02
	3	4.758	2.544E-02	7.371E-04	3.141E-02
	4	19.507	1.043E-01	3.022E-03	1.288E-01
	6	5.228	2.796E-02	8.098E-04	3.451E-02
	10	2.404	1.285E-02	3.724E-04	1.587E-02
	11	0.901	4.817E-03	1.395E-04	5.946E-03
	12	1.257	6.721E-03	1.947E-04	8.296E-03
	13	115.515	6.177E-01	1.790E-02	7.625E-01
	14	115.652	6.185E-01	1.792E-02	7.634E-01
	15	118.536	6.339E-01	1.836E-02	7.825E-01
	16	5.474	2.927E-02	8.480E-04	3.613E-02
	17	2.113	1.130E-02	3.273E-04	1.395E-02
	18	2.269	1.213E-02	3.514E-04	1.497E-02
	19	0.097	5.195E-04	1.505E-05	6.412E-04
	20	13.692	7.322E-02	2.121E-03	9.038E-02
	21	3.370	1.802E-02	5.221E-04	2.225E-02
	23	0.196	1.046E-03	3.030E-05	1.291E-03
	24	0.256	1.369E-03	3.967E-05	1.690E-03
	25	0.430	2.301E-03	6.667E-05	2.841E-03
	26	0.403	2.155E-03	6.243E-05	2.660E-03
	27	0.606	3.242E-03	9.392E-05	4.002E-03
	28	1.758	9.404E-03	2.724E-04	1.161E-02
	90	30.382	1.625E-01	4.707E-03	2.006E-01
	91	68.759	3.677E-01	1.065E-02	4.539E-01

Table IV

HEAT-TRANSFER DATA

RUN	POS	Q	Q/Q(REF)	C(H)	H/H(REF)
41	29	92.041	5.449E-01	1.598E-02	6.747E-01
	30	34.912	2.067E-01	6.062E-03	2.559E-01
	31	20.015	1.185E-01	3.475E-03	1.467E-01
	32	12.567	7.441E-02	2.182E-03	9.213E-02
	33	17.271	1.023E-01	2.999E-03	1.266E-01
	34	33.390	1.977E-01	5.797E-03	2.448E-01
	35	17.915	1.061E-01	3.110E-03	1.313E-01
	36	13.206	7.819E-02	2.293E-03	9.681E-02
	37	5.786	3.425E-02	1.005E-03	4.241E-02
	38	18.593	1.101E-01	3.228E-03	1.363E-01
	39	27.633	1.636E-01	4.798E-03	2.026E-01
	40	20.182	1.195E-01	3.504E-03	1.480E-01
	41	16.881	9.995E-02	2.931E-03	1.237E-01
	42	8.571	5.075E-02	1.488E-03	6.283E-02
	1	11.832	7.006E-02	2.054E-03	8.674E-02
	2	7.227	4.279E-02	1.255E-03	5.298E-02
	3	16.861	9.983E-02	2.928E-03	1.236E-01
	4	6.967	4.125E-02	1.210E-03	5.107E-02
	5	1.952	1.156E-02	3.390E-04	1.431E-02
	6	3.202	1.896E-02	5.559E-04	2.347E-02
	10	0.458	2.712E-03	7.953E-05	3.358E-03
	11	0.698	4.135E-03	1.213E-04	5.120E-03
	12	1.096	6.491E-03	1.903E-04	8.037E-03
	13	125.999	7.460E-01	2.188E-02	9.237E-01
	14	154.501	9.147E-01	2.683E-02	1.133E 00
	16	5.621	3.328E-02	9.759E-04	4.120E-02
	17	2.007	1.188E-02	3.485E-04	1.471E-02
	18	5.633	3.335E-02	9.780E-04	4.129E-02
	19	0.124	7.334E-04	2.151E-05	9.081E-04
	20	20.113	1.191E-01	3.492E-03	1.474E-01
	21	6.770	4.008E-02	1.175E-03	4.963E-02
	22	3.045	1.803E-02	5.287E-04	2.232E-02
	23	1.923	1.138E-02	3.338E-04	1.409E-02
	24	1.307	7.738E-03	2.269E-04	9.581E-03
	25	0.214	1.265E-03	3.711E-05	1.567E-03
	26	0.671	3.975E-03	1.166E-04	4.922E-03
	27	1.276	7.555E-03	2.216E-04	9.355E-03
	28	1.739	1.030E-02	3.020E-04	1.275E-02
	90	20.090	1.189E-01	3.488E-03	1.473E-01
	91	44.586	2.640E-01	7.741E-03	3.268E-01

Table IV

HEAT-TRANSFER DATA

RUN	POS	Q	Q/Q(REF)	C(H)	H/H(REF)
42	29	107.067	5.468E-01	1.553E-02	6.748E-01
	30	39.475	2.016E-01	5.727E-03	2.488E-01
	31	24.477	1.250E-01	3.551E-03	1.543E-01
	32	14.414	7.362E-02	2.091E-03	9.085E-02
	33	20.774	1.061E-01	3.014E-03	1.309E-01
	34	38.546	1.969E-01	5.592E-03	2.429E-01
	35	21.508	1.098E-01	3.120E-03	1.356E-01
	36	15.928	8.135E-02	2.311E-03	1.004E-01
	37	6.148	3.140E-02	8.919E-04	3.875E-02
	38	22.373	1.143E-01	3.246E-03	1.410E-01
	39	32.767	1.674E-01	4.754E-03	2.065E-01
	40	23.000	1.175E-01	3.337E-03	1.450E-01
	41	20.325	1.038E-01	2.949E-03	1.281E-01
	42	9.702	4.955E-02	1.407E-03	6.115E-02
	1	15.403	7.867E-02	2.235E-03	9.708E-02
	2	8.884	4.537E-02	1.289E-03	5.599E-02
	3	21.253	1.085E-01	3.083E-03	1.340E-01
	4	7.999	4.085E-02	1.160E-03	5.041E-02
	5	2.424	1.238E-02	3.516E-04	1.528E-02
	6	4.031	2.059E-02	5.847E-04	2.540E-02
	10	0.513	2.622E-03	7.447E-05	3.235E-03
	11	0.859	4.385E-03	1.246E-04	5.412E-03
	12	1.251	6.391E-03	1.815E-04	7.888E-03
	13	150.944	7.709E-01	2.190E-02	9.514E-01
	14	180.576	9.222E-01	2.620E-02	1.138E 00
	15	212.554	1.086E 00	3.084E-02	1.340E 00
	16	5.463	2.790E-02	7.924E-04	3.443E-02
	17	2.327	1.188E-02	3.376E-04	1.467E-02
	18	6.676	3.409E-02	9.684E-04	4.207E-02
	19	0.084	4.288E-04	1.218E-05	5.292E-04
	20	26.582	1.358E-01	3.856E-03	1.675E-01
	21	7.937	4.053E-02	1.151E-03	5.002E-02
	22	3.538	1.807E-02	5.133E-04	2.230E-02
	23	2.402	1.227E-02	3.485E-04	1.514E-02
	24	1.520	7.762E-03	2.205E-04	9.580E-03
	25	0.289	1.478E-03	4.198E-05	1.824E-03
	26	0.735	3.753E-03	1.066E-04	4.631E-03
	27	1.566	7.997E-03	2.272E-04	9.869E-03
	28	2.093	1.069E-02	3.036E-04	1.319E-02
	90	23.287	1.189E-01	3.378E-03	1.468E-01
	91	61.080	3.120E-01	8.861E-03	3.850E-01

Table IV

HEAT-TRANSFER DATA

RUN	POS	Q	Q/Q(REF)	C(H)	H/H(REF)
43	29	146.463	7.283E-01	2.084E-02	8.984E-01
	30	37.253	1.852E-01	5.302E-03	2.285E-01
	31	32.561	1.619E-01	4.634E-03	1.997E-01
	32	23.124	1.150E-01	3.291E-03	1.418E-01
	33	17.667	8.785E-02	2.514E-03	1.084E-01
	34	33.907	1.686E-01	4.825E-03	2.080E-01
	35	31.473	1.565E-01	4.479E-03	1.931E-01
	36	16.866	8.387E-02	2.400E-03	1.035E-01
	37	6.888	3.425E-02	9.803E-04	4.225E-02
	38	20.251	1.007E-01	2.882E-03	1.242E-01
	39	23.046	1.146E-01	3.280E-03	1.414E-01
	40	26.438	1.315E-01	3.763E-03	1.622E-01
	41	23.120	1.150E-01	3.290E-03	1.418E-01
	42	8.571	4.262E-02	1.220E-03	5.257E-02
	1	15.674	7.794E-02	2.231E-03	9.615E-02
	2	8.693	4.323E-02	1.237E-03	5.332E-02
	3	20.273	1.008E-01	2.885E-03	1.244E-01
	4	7.343	3.651E-02	1.045E-03	4.504E-02
	5	2.044	1.016E-02	2.909E-04	1.254E-02
	6	3.117	1.550E-02	4.436E-04	1.912E-02
	10	0.445	2.213E-03	6.334E-05	2.730E-03
	11	0.546	2.714E-03	7.769E-05	3.348E-03
	12	1.262	6.277E-03	1.797E-04	7.743E-03
	13	177.228	8.813E-01	2.522E-02	1.087E 00
	14	242.546	1.206E 00	3.452E-02	1.488E 00
	15	284.092	1.413E 00	4.043E-02	1.743E 00
	16	4.510	2.243E-02	6.418E-04	2.766E-02
	17	3.863	1.921E-02	5.498E-04	2.370E-02
	18	7.585	3.772E-02	1.079E-03	4.653E-02
	19	0.226	1.125E-03	3.218E-05	1.387E-03
	20	27.725	1.379E-01	3.946E-03	1.701E-01
	21	9.542	4.745E-02	1.358E-03	5.853E-02
	22	4.146	2.061E-02	5.900E-04	2.543E-02
	23	2.812	1.398E-02	4.002E-04	1.725E-02
	24	1.855	9.224E-03	2.640E-04	1.138E-02
	25	0.464	2.309E-03	6.608E-05	2.848E-03
	26	0.971	4.831E-03	1.382E-04	5.959E-03
	27	1.666	8.283E-03	2.371E-04	1.022E-02
	28	2.112	1.050E-02	3.005E-04	1.295E-02
	90	23.253	1.156E-01	3.309E-03	1.426E-01
	91	48.969	2.435E-01	6.969E-03	3.004E-01

Table IV

HEAT-TRANSFER DATA

RUN	POS	Q	Q/Q(REF)	C(H)	H/H(REF)
44	29	121.695	6.109E-01	1.740E-02	7.541E-01
	30	42.062	2.112E-01	6.013E-03	2.606E-01
	31	39.148	1.965E-01	5.597E-03	2.426E-01
	32	35.980	1.806E-01	5.144E-03	2.229E-01
	33	16.974	8.521E-02	2.427E-03	1.052E-01
	34	27.700	1.391E-01	3.960E-03	1.716E-01
	35	34.256	1.720E-01	4.897E-03	2.123E-01
	36	16.595	8.331E-02	2.373E-03	1.028E-01
	37	7.500	3.765E-02	1.072E-03	4.647E-02
	38	19.501	9.790E-02	2.788E-03	1.208E-01
	39	30.159	1.514E-01	4.312E-03	1.869E-01
	40	20.857	1.047E-01	2.982E-03	1.292E-01
	41	16.431	8.249E-02	2.349E-03	1.018E-01
	42	14.863	7.462E-02	2.125E-03	9.210E-02
	1	18.341	9.207E-02	2.622E-03	1.136E-01
	2	11.056	5.550E-02	1.581E-03	6.850E-02
	3	18.403	9.238E-02	2.631E-03	1.140E-01
	4	7.210	3.619E-02	1.031E-03	4.467E-02
	5	2.140	1.074E-02	3.060E-04	1.326E-02
	6	4.127	2.072E-02	5.900E-04	2.557E-02
	10	0.254	1.277E-03	3.638E-05	1.577E-03
	11	0.405	2.035E-03	5.797E-05	2.512E-03
	12	1.242	6.236E-03	1.776E-04	7.698E-03
	13	167.580	8.413E-01	2.396E-02	1.038E 00
	14	289.113	1.451E 00	4.133E-02	1.791E 00
	15	169.776	8.523E-01	2.427E-02	1.052E 00
	16	5.752	2.887E-02	8.223E-04	3.564E-02
	17	2.242	1.125E-02	3.205E-04	1.389E-02
	18	8.964	4.500E-02	1.282E-03	5.554E-02
	19	0.324	1.626E-03	4.630E-05	2.007E-03
	20	27.295	1.370E-01	3.902E-03	1.691E-01
	21	8.926	4.481E-02	1.276E-03	5.531E-02
	22	4.033	2.025E-02	5.766E-04	2.499E-02
	23	2.948	1.480E-02	4.215E-04	1.827E-02
	24	1.247	6.258E-03	1.782E-04	7.724E-03
	25	0.438	2.199E-03	6.262E-05	2.714E-03
	26	0.556	2.792E-03	7.951E-05	3.446E-03
	27	1.372	6.890E-03	1.962E-04	8.504E-03
	28	2.331	1.170E-02	3.332E-04	1.444E-02
	90	24.927	1.251E-01	3.564E-03	1.545E-01
	91	16.876	8.472E-02	2.413E-03	1.046E-01

Table IV

HEAT-TRANSFER DATA

RUN	POS	Q	Q/Q(REF)	C(H)	H/H(REF)
45	29	121.467	6.076E-01	1.727E-02	7.492E-01
	30	11.327	5.666E-02	1.610E-03	6.986E-02
	31	10.964	5.485E-02	1.559E-03	6.762E-02
	32	9.379	4.692E-02	1.333E-03	5.785E-02
	33	50.097	2.506E-01	7.122E-03	3.090E-01
	34	21.013	1.051E-01	2.987E-03	1.296E-01
	35	31.469	1.574E-01	4.474E-03	1.941E-01
	36	26.315	1.316E-01	3.741E-03	1.623E-01
	37	27.516	1.376E-01	3.912E-03	1.697E-01
	38	30.981	1.550E-01	4.404E-03	1.911E-01
	39	21.982	1.100E-01	3.125E-03	1.356E-01
	40	15.832	7.920E-02	2.251E-03	9.765E-02
	41	22.607	1.131E-01	3.214E-03	1.394E-01
	42	24.365	1.219E-01	3.464E-03	1.503E-01
	1	13.051	6.529E-02	1.855E-03	8.049E-02
	2	11.818	5.912E-02	1.680E-03	7.289E-02
	3	7.296	3.650E-02	1.037E-03	4.500E-02
	4	26.149	1.308E-01	3.717E-03	1.613E-01
	5	7.082	3.543E-02	1.007E-03	4.368E-02
	6	7.820	3.912E-02	1.112E-03	4.823E-02
	10	2.696	1.349E-02	3.832E-04	1.663E-02
	11	1.840	9.206E-03	2.616E-04	1.135E-02
	12	1.429	7.148E-03	2.032E-04	8.813E-03
	13	127.428	6.375E-01	1.812E-02	7.859E-01
	14	122.030	6.105E-01	1.735E-02	7.526E-01
	15	120.484	6.027E-01	1.713E-02	7.431E-01
	16	5.595	2.799E-02	7.954E-04	3.451E-02
	17	2.868	1.435E-02	4.078E-04	1.769E-02
	18	2.320	1.161E-02	3.298E-04	1.431E-02
	19	0.138	6.889E-04	1.958E-05	8.494E-04
	20	13.659	6.833E-02	1.942E-03	8.424E-02
	21	3.474	1.738E-02	4.939E-04	2.143E-02
	22	0.416	2.082E-03	5.915E-05	2.566E-03
	23	0.214	1.070E-03	3.042E-05	1.320E-03
	24	0.325	1.624E-03	4.615E-05	2.002E-03
	25	0.390	1.951E-03	5.545E-05	2.405E-03
	26	0.430	2.151E-03	6.113E-05	2.652E-03
	27	0.406	2.030E-03	5.770E-05	2.503E-03
	28	1.268	6.342E-03	1.802E-04	7.819E-03
	90	30.430	1.522E-01	4.326E-03	1.877E-01
	91	21.937	1.097E-01	3.119E-03	1.353E-01

Table IV

HEAT-TRANSFER DATA

RUN	POS	Q	Q/Q(REF)	C(H)	H/H(REF)
46	29	112.290	6.369E-01	1.372E-02	7.817E-01
	30	11.735	6.656E-02	1.434E-03	8.169E-02
	31	8.119	4.605E-02	9.922E-04	5.652E-02
	32	13.155	7.462E-02	1.608E-03	9.158E-02
	33	41.754	2.368E-01	5.103E-03	2.907E-01
	34	19.824	1.124E-01	2.423E-03	1.380E-01
	35	30.555	1.733E-01	3.734E-03	2.127E-01
	36	24.725	1.402E-01	3.022E-03	1.721E-01
	37	20.852	1.183E-01	2.548E-03	1.452E-01
	38	31.266	1.773E-01	3.821E-03	2.177E-01
	39	20.081	1.139E-01	2.454E-03	1.398E-01
	40	14.215	8.063E-02	1.737E-03	9.896E-02
	41	21.467	1.218E-01	2.623E-03	1.494E-01
	42	17.614	9.991E-02	2.153E-03	1.226E-01
	1	13.576	7.701E-02	1.659E-03	9.452E-02
	2	12.607	7.151E-02	1.541E-03	8.777E-02
	3	6.134	3.479E-02	7.497E-04	4.271E-02
	4	20.687	1.173E-01	2.528E-03	1.440E-01
	5	7.675	4.353E-02	9.379E-04	5.343E-02
	6	4.570	2.592E-02	5.585E-04	3.182E-02
	10	1.679	9.523E-03	2.052E-04	1.169E-02
	11	1.102	6.250E-03	1.347E-04	7.671E-03
	12	0.867	4.920E-03	1.060E-04	6.038E-03
	13	118.179	6.703E-01	1.444E-02	8.227E-01
	14	115.014	6.524E-01	1.406E-02	8.007E-01
	15	115.329	6.542E-01	1.409E-02	8.029E-01
	16	5.680	3.222E-02	6.942E-04	3.955E-02
	17	1.992	1.130E-02	2.434E-04	1.386E-02
	18	2.029	1.151E-02	2.480E-04	1.413E-02
	19	0.092	5.236E-04	1.128E-05	6.427E-04
	20	12.907	7.321E-02	1.577E-03	8.986E-02
	21	3.282	1.862E-02	4.011E-04	2.285E-02
	22	1.473	8.356E-03	1.800E-04	1.026E-02
	23	0.389	2.207E-03	4.756E-05	2.709E-03
	24	0.160	9.077E-04	1.956E-05	1.114E-03
	25	0.546	3.094E-03	6.666E-05	3.798E-03
	26	0.278	1.574E-03	3.392E-05	1.932E-03
	27	0.600	3.403E-03	7.332E-05	4.177E-03
	28	1.633	9.262E-03	1.996E-04	1.137E-02
	90	30.584	1.735E-01	3.738E-03	2.129E-01
	91	20.737	1.176E-01	2.534E-03	1.444E-01

Table IV

HEAT-TRANSFER DATA

RUN	POS	Q	Q/Q(REF)	C(H)	H/H(REF)
47	29	106.100	6.049E-01	2.522E-02	7.426E-01
	30	32.175	1.834E-01	7.649E-03	2.252E-01
	31	34.030	1.940E-01	8.089E-03	2.382E-01
	32	34.609	1.973E-01	8.227E-03	2.422E-01
	33	12.810	7.303E-02	3.045E-03	8.966E-02
	34	19.921	1.136E-01	4.735E-03	1.394E-01
	35	27.037	1.541E-01	6.427E-03	1.892E-01
	36	14.690	8.375E-02	3.492E-03	1.028E-01
	37	7.186	4.097E-02	1.708E-03	5.030E-02
	38	15.262	8.701E-02	3.628E-03	1.068E-01
	39	22.430	1.279E-01	5.332E-03	1.570E-01
	40	17.561	1.001E-01	4.175E-03	1.229E-01
	41	14.772	8.422E-02	3.511E-03	1.034E-01
	42	19.494	1.111E-01	4.634E-03	1.364E-01
	1	18.453	1.052E-01	4.386E-03	1.292E-01
	2	11.047	6.298E-02	2.626E-03	7.732E-02
	3	14.080	8.028E-02	3.347E-03	9.855E-02
	4	7.373	4.203E-02	1.753E-03	5.161E-02
	5	3.141	1.791E-02	7.466E-04	2.198E-02
	6	7.846	4.473E-02	1.865E-03	5.492E-02
	10	0.138	7.893E-04	3.291E-05	9.689E-04
	11	0.313	1.784E-03	7.438E-05	2.190E-03
	12	0.522	2.976E-03	1.241E-04	3.654E-03
	13	182.585	1.041E 00	4.340E-02	1.278E 00
	14	170.789	9.737E-01	4.060E-02	1.195E 00
	15	175.981	1.003E 00	4.183E-02	1.232E 00
	16	5.413	3.086E-02	1.287E-03	3.789E-02
	17	4.008	2.285E-02	9.527E-04	2.805E-02
	18	6.647	3.789E-02	1.580E-03	4.652E-02
	19	0.271	1.547E-03	6.450E-05	1.899E-03
	20	25.786	1.470E-01	6.130E-03	1.805E-01
	21	8.130	4.635E-02	1.933E-03	5.691E-02
	22	3.390	1.933E-02	8.059E-04	2.373E-02
	23	2.341	1.335E-02	5.565E-04	1.639E-02
	24	1.651	9.410E-03	3.924E-04	1.155E-02
	25	0.375	2.139E-03	8.919E-05	2.626E-03
	26	0.950	5.417E-03	2.258E-04	6.650E-03
	27	1.336	7.614E-03	3.175E-04	9.348E-03
	28	2.167	1.236E-02	5.152E-04	1.517E-02
	90	21.468	1.224E-01	5.103E-03	1.503E-01
	91	13.204	7.528E-02	3.139E-03	9.242E-02

Table IV

HEAT-TRANSFER DATA

RUN	POS	Q	Q/Q(REF)	C(H)	H/H(REF)
48	29	134.465	7.822E-01	3.123E-02	9.602E-01
	30	31.442	1.829E-01	7.302E-03	2.245E-01
	31	32.465	1.889E-01	7.540E-03	2.318E-01
	32	28.524	1.659E-01	6.624E-03	2.037E-01
	33	12.378	7.201E-02	2.875E-03	8.839E-02
	34	21.597	1.256E-01	5.016E-03	1.542E-01
	35	31.231	1.817E-01	7.253E-03	2.230E-01
	36	14.038	8.166E-02	3.260E-03	1.002E-01
	37	6.466	3.762E-02	1.502E-03	4.618E-02
	38	14.648	8.521E-02	3.402E-03	1.046E-01
	39	24.183	1.407E-01	5.616E-03	1.727E-01
	40	14.402	8.378E-02	3.345E-03	1.028E-01
	41	18.461	1.074E-01	4.287E-03	1.318E-01
	42	10.747	6.252E-02	2.496E-03	7.675E-02
	1	16.916	9.840E-02	3.928E-03	1.208E-01
	2	9.518	5.537E-02	2.210E-03	6.797E-02
	3	14.583	8.483E-02	3.387E-03	1.041E-01
	4	6.449	3.752E-02	1.498E-03	4.606E-02
	5	2.483	1.444E-02	5.766E-04	1.773E-02
	6	4.993	2.904E-02	1.159E-03	3.565E-02
	10	0.289	1.679E-03	6.703E-05	2.061E-03
	11	0.352	2.047E-03	8.172E-05	2.513E-03
	12	0.720	4.190E-03	1.673E-04	5.143E-03
	13	206.604	1.202E 00	4.798E-02	1.475E 00
	14	231.036	1.344E 00	5.365E-02	1.650E 00
	15	167.343	9.735E-01	3.886E-02	1.195E 00
	16	6.465	3.761E-02	1.501E-03	4.616E-02
	17	4.144	2.411E-02	9.624E-04	2.959E-02
	18	6.248	3.635E-02	1.451E-03	4.462E-02
	19	0.228	1.326E-03	5.294E-05	1.628E-03
	20	28.468	1.656E-01	6.611E-03	2.033E-01
	21	8.868	5.159E-02	2.059E-03	6.333E-02
	22	3.550	2.065E-02	8.245E-04	2.535E-02
	23	2.295	1.335E-02	5.330E-04	1.639E-02
	24	1.741	1.013E-02	4.044E-04	1.243E-02
	25	0.342	1.988E-03	7.937E-05	2.440E-03
	26	1.089	6.338E-03	2.530E-04	7.780E-03
	27	1.555	9.046E-03	3.611E-04	1.110E-02
	28	2.273	1.322E-02	5.280E-04	1.623E-02
	90	21.873	1.272E-01	5.080E-03	1.562E-01
	91	12.078	7.026E-02	2.805E-03	8.625E-02

Table IV

HEAT-TRANSFER DATA

RUN	POS	Q	Q/Q(REF)	C(H)	H/H(REF)
49	29	95.322	5.456E-01	2.248E-02	6.696E-01
	30	8.783	5.028E-02	2.071E-03	6.170E-02
	31	7.986	4.571E-02	1.883E-03	5.610E-02
	32	7.391	4.231E-02	1.743E-03	5.192E-02
	33	29.538	1.691E-01	6.965E-03	2.075E-01
	35	33.712	1.930E-01	7.950E-03	2.368E-01
	36	9.148	5.236E-02	2.157E-03	6.426E-02
	37	19.285	1.104E-01	4.548E-03	1.355E-01
	38	27.736	1.588E-01	6.540E-03	1.948E-01
	39	26.394	1.511E-01	6.224E-03	1.854E-01
	40	14.627	8.373E-02	3.449E-03	1.028E-01
	41	20.651	1.182E-01	4.870E-03	1.451E-01
	42	16.762	9.595E-02	3.953E-03	1.178E-01
	1	12.037	6.890E-02	2.838E-03	8.456E-02
	2	11.470	6.566E-02	2.705E-03	8.058E-02
	3	4.905	2.807E-02	1.157E-03	3.445E-02
	4	18.586	1.064E-01	4.383E-03	1.306E-01
	5	8.345	4.777E-02	1.968E-03	5.862E-02
	6	3.813	2.183E-02	8.991E-04	2.679E-02
	10	1.846	1.056E-02	4.352E-04	1.297E-02
	11	0.659	3.775E-03	1.555E-04	4.633E-03
	12	1.037	5.935E-03	2.445E-04	7.284E-03
	13	124.731	7.140E-01	2.941E-02	8.762E-01
	14	122.118	6.990E-01	2.880E-02	8.579E-01
	15	119.411	6.835E-01	2.816E-02	8.389E-01
	16	6.027	3.450E-02	1.421E-03	4.234E-02
	17	1.584	9.069E-03	3.736E-04	1.113E-02
	18	1.897	1.086E-02	4.473E-04	1.333E-02
	19	0.235	1.345E-03	5.540E-05	1.650E-03
	20	13.702	7.843E-02	3.231E-03	9.626E-02
	21	3.543	2.028E-02	8.354E-04	2.489E-02
	22	1.505	8.614E-03	3.548E-04	1.057E-02
	23	0.712	4.074E-03	1.678E-04	5.000E-03
	24	0.278	1.590E-03	6.551E-05	1.952E-03
	25	0.382	2.188E-03	9.012E-05	2.685E-03
	26	0.300	1.715E-03	7.066E-05	2.105E-03
	27	0.866	4.955E-03	2.041E-04	6.082E-03
	28	1.836	1.051E-02	4.330E-04	1.290E-02
	90	32.912	1.884E-01	7.761E-03	2.312E-01
	91	19.728	1.129E-01	4.652E-03	1.386E-01

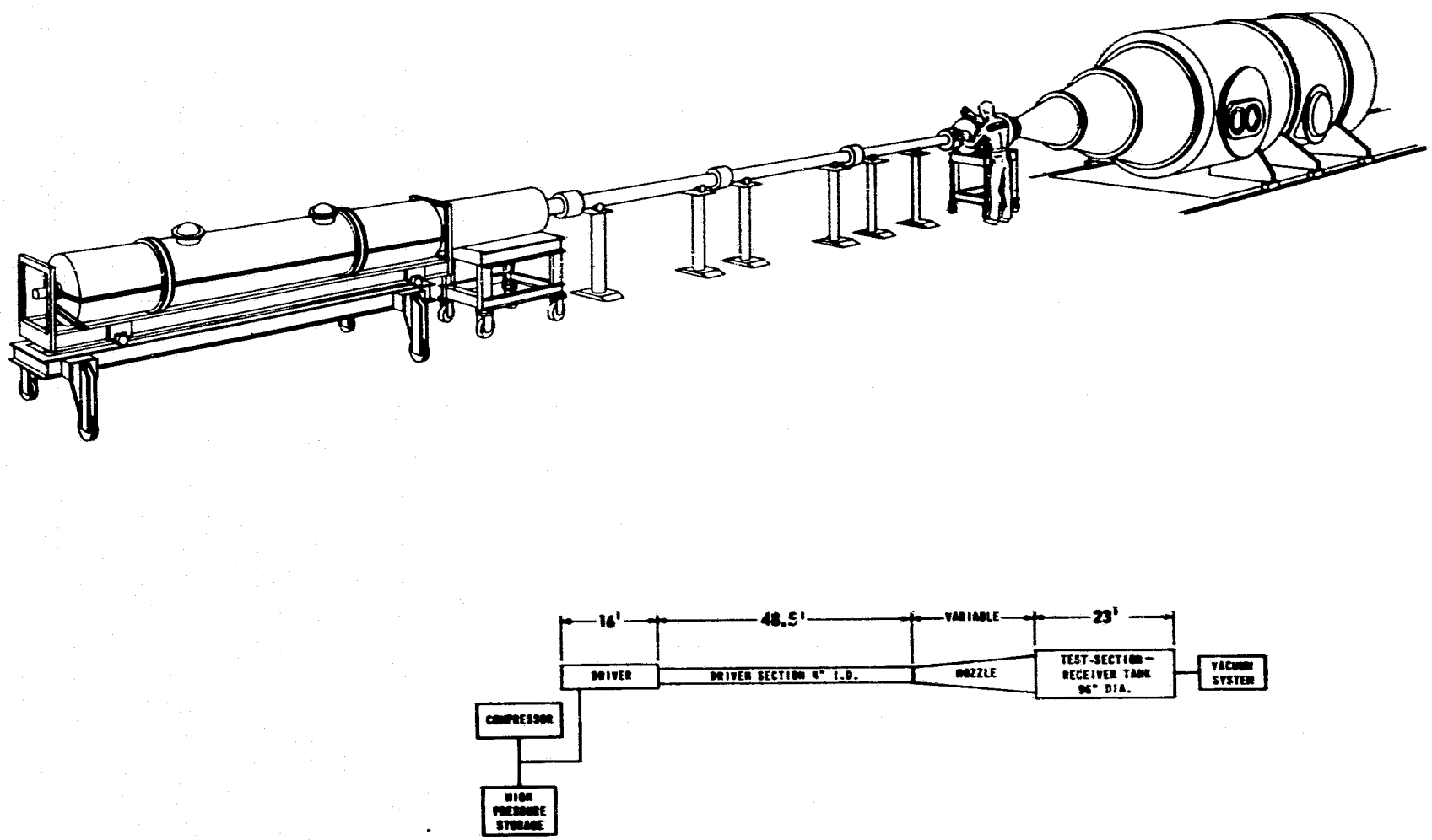

Figure 1 BASIC COMPONENTS OF THE CALSPAN 96" HYPERSONIC SHOCK TUNNEL

ORIGINAL PAGE
BLACK AND WHITE PHOTOGRAPH

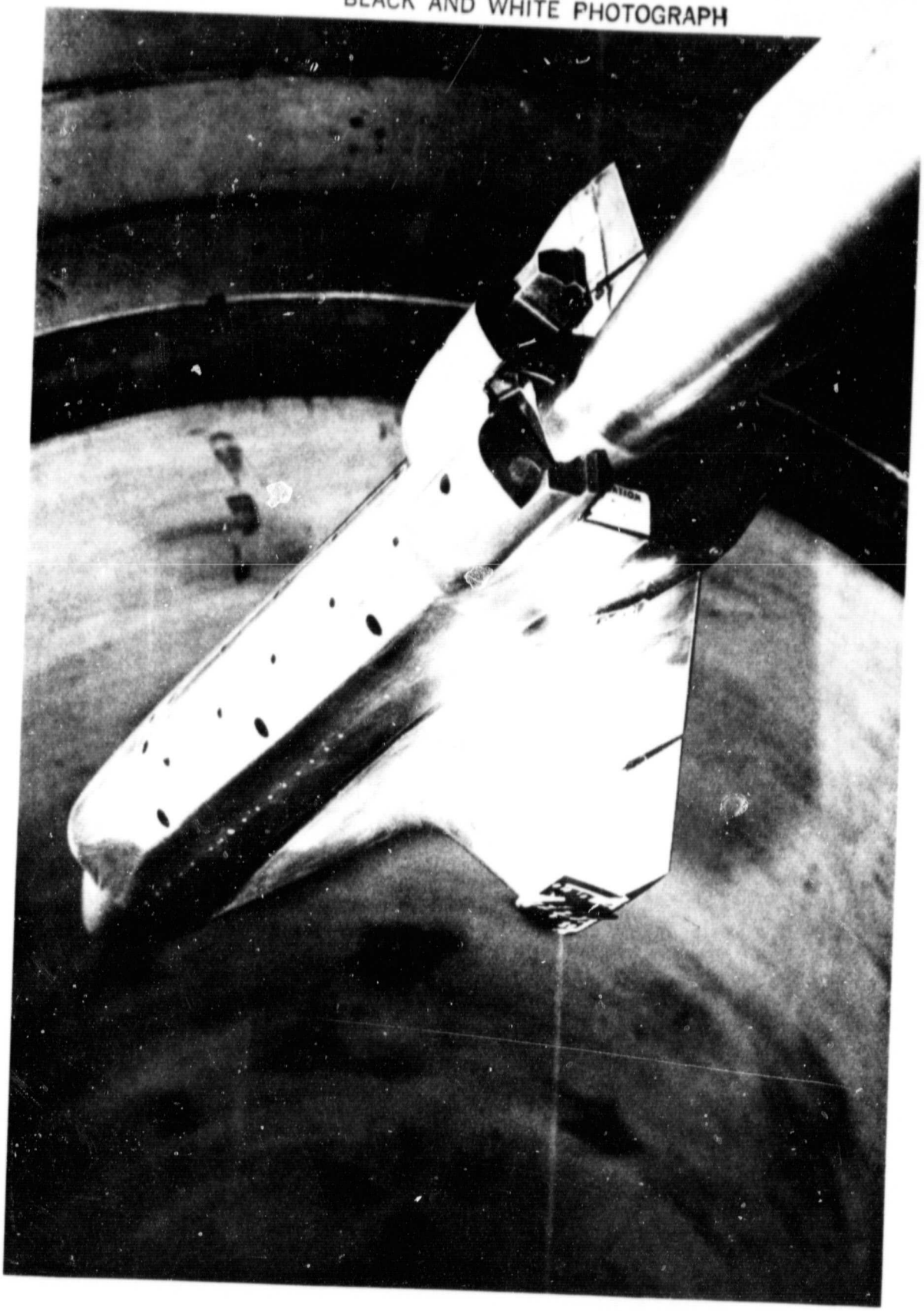

Figure 2 TIP-FIN CONTROLLER MODEL INSTALLED IN 96" HST

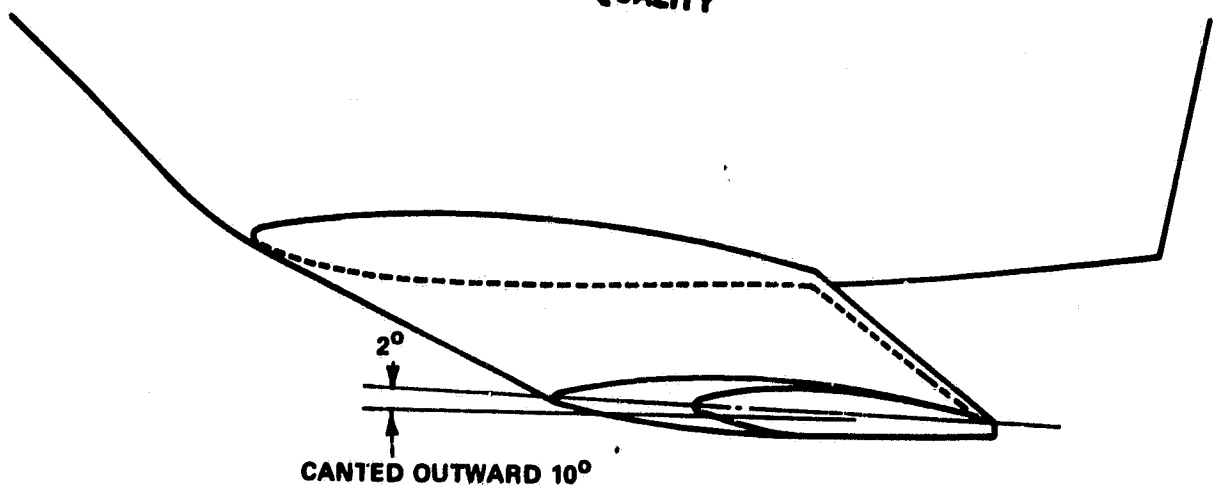

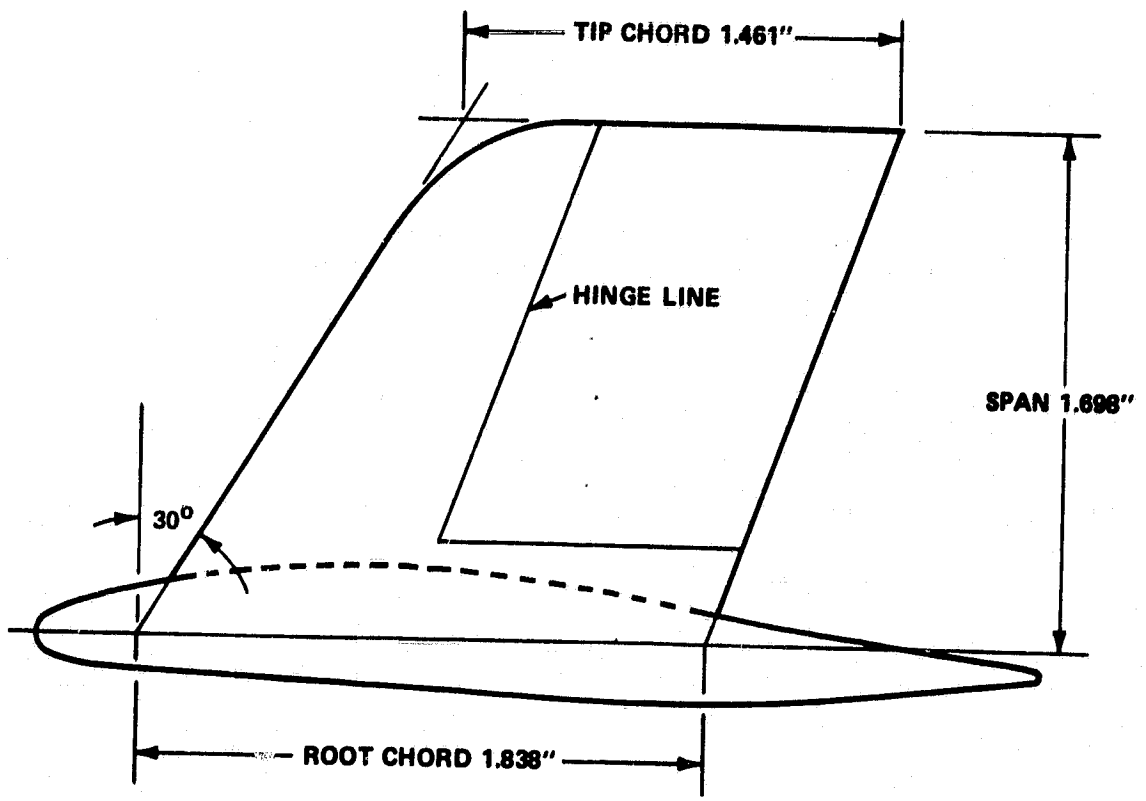

Figure 3 DETAILS OF TIP-FIN CONTROLLER

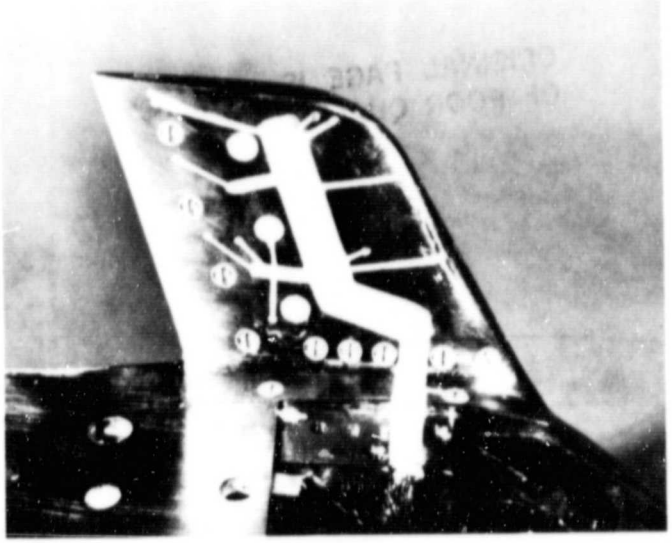

(a) INBOARD SURFACE

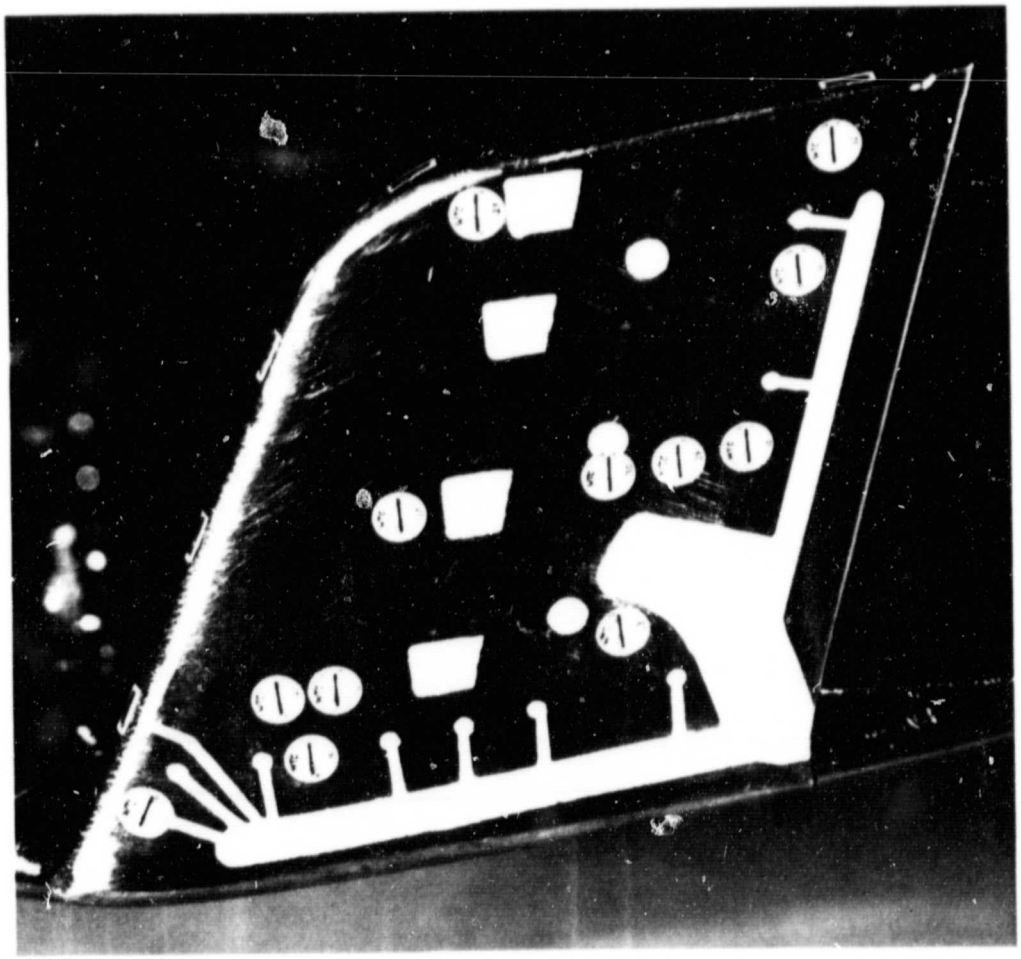

(b) OUTBOARD SURFACE

Figure 4 TIP-FIN CONTROLLER WITH UNDEFLECTED CONTROL SURFACE

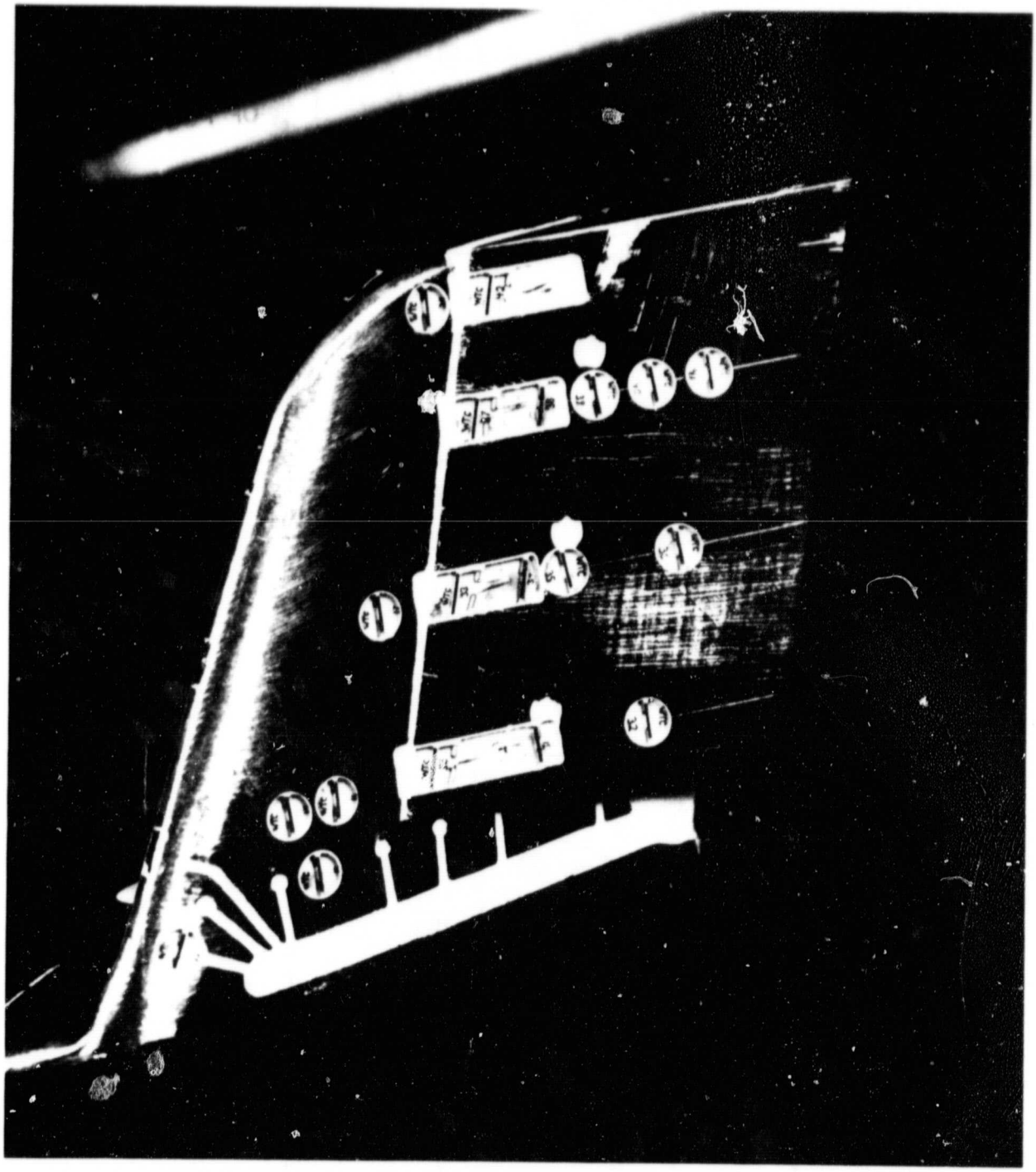

Figure 5 TIP-FIN CONTROLLER DEFLECTED 20°

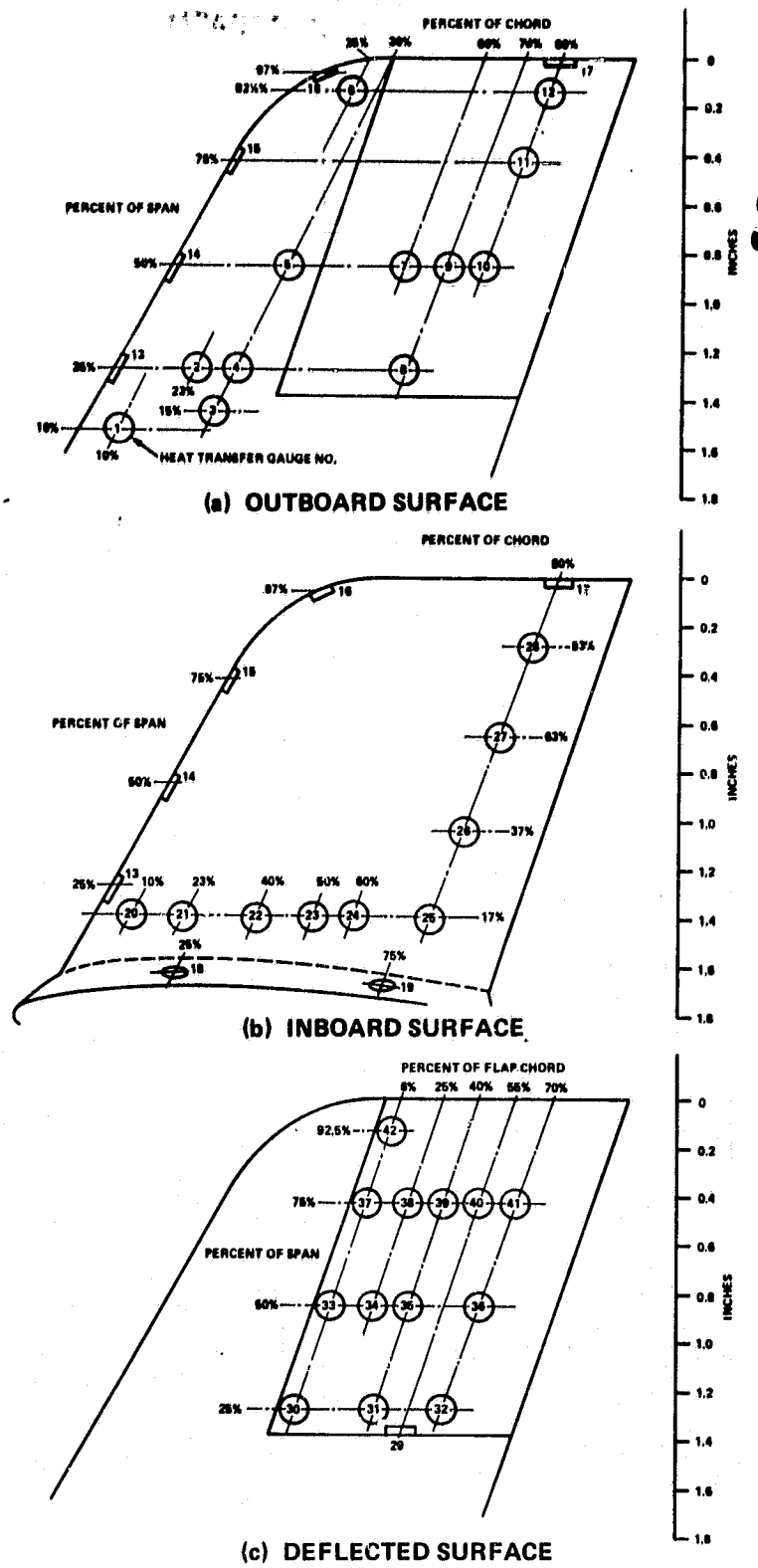

Figure 6 SKETCH SHOWING HEAT-TRANSFER GAUGE LOCATIONS

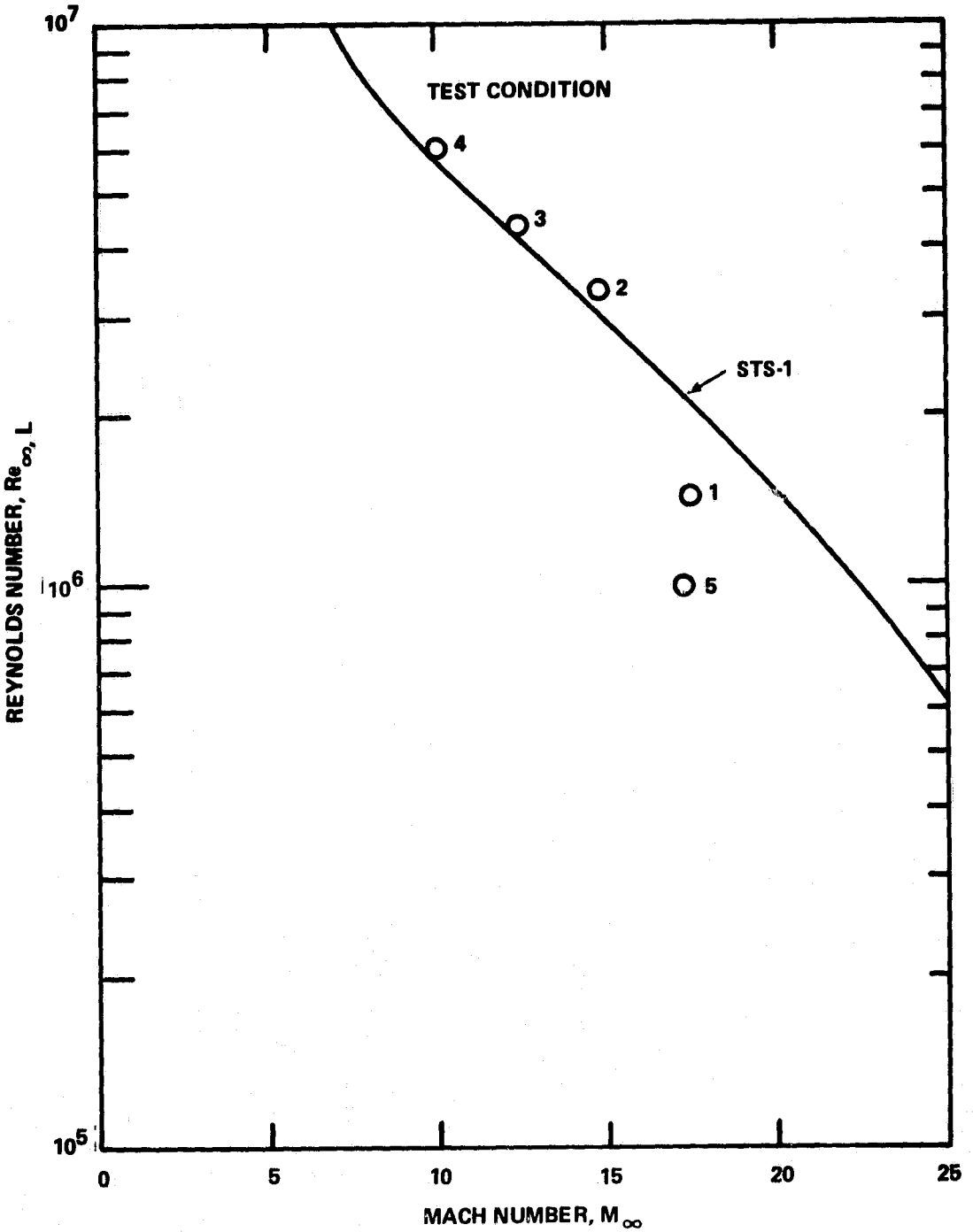

Figure 7 COMPARISON OF TEST CONDITIONS WITH STS-1 ENTRY TRAJECTORY

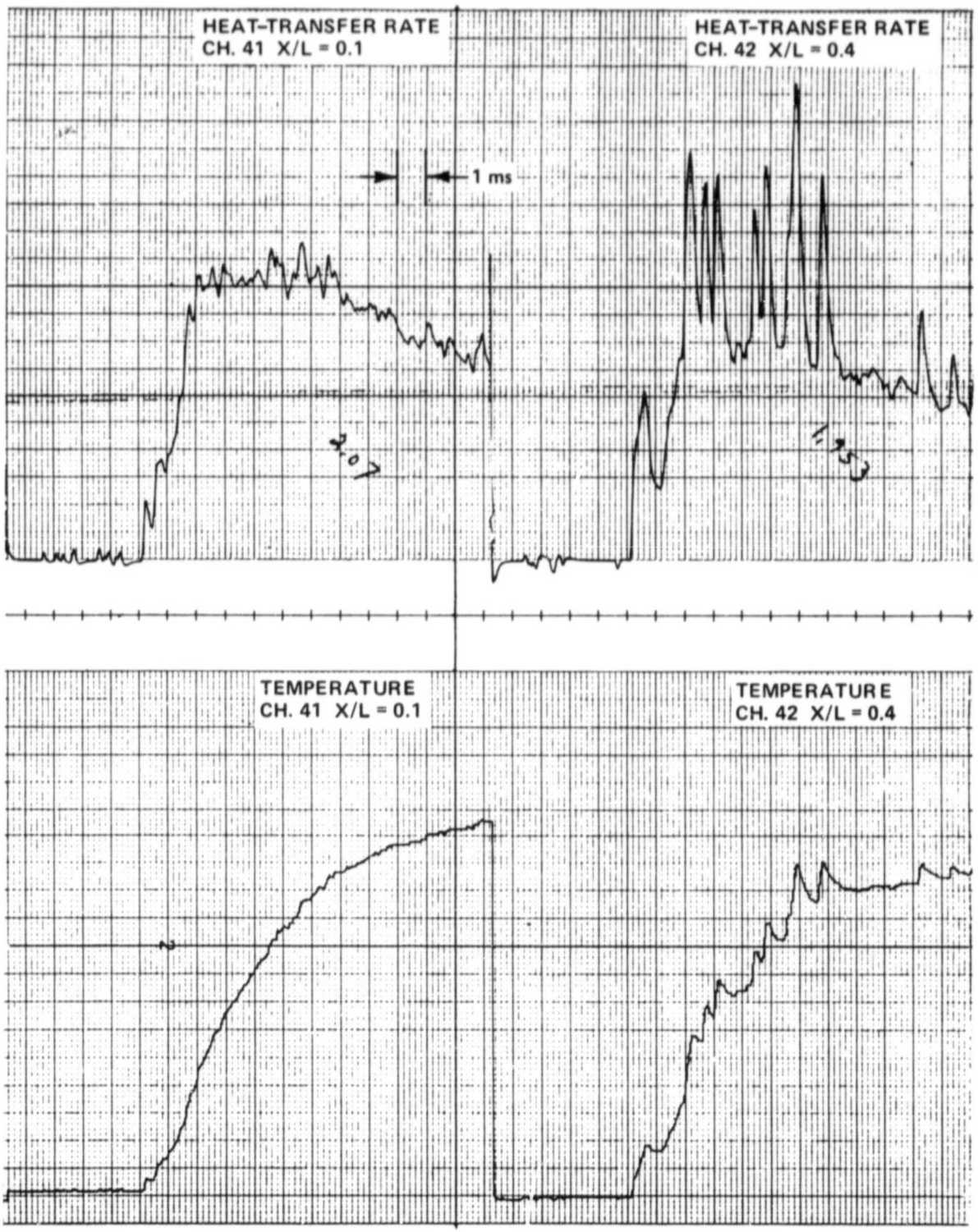

Figure 8 TEMPERATURE AND HEAT-TRANSFER RATES, RUN 1, PHASE I

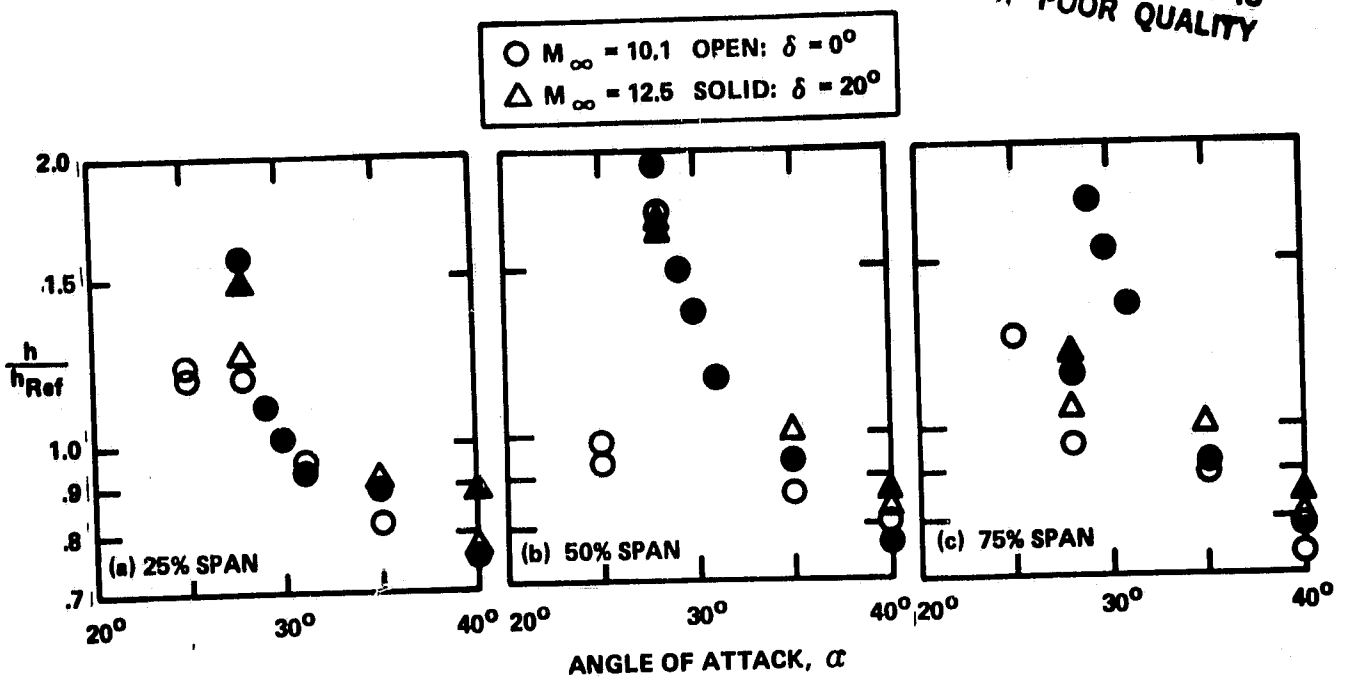

Figure 9 VARIATION OF LEADING-EDGE HEAT TRANSFER WITH ANGLE OF ATTACK

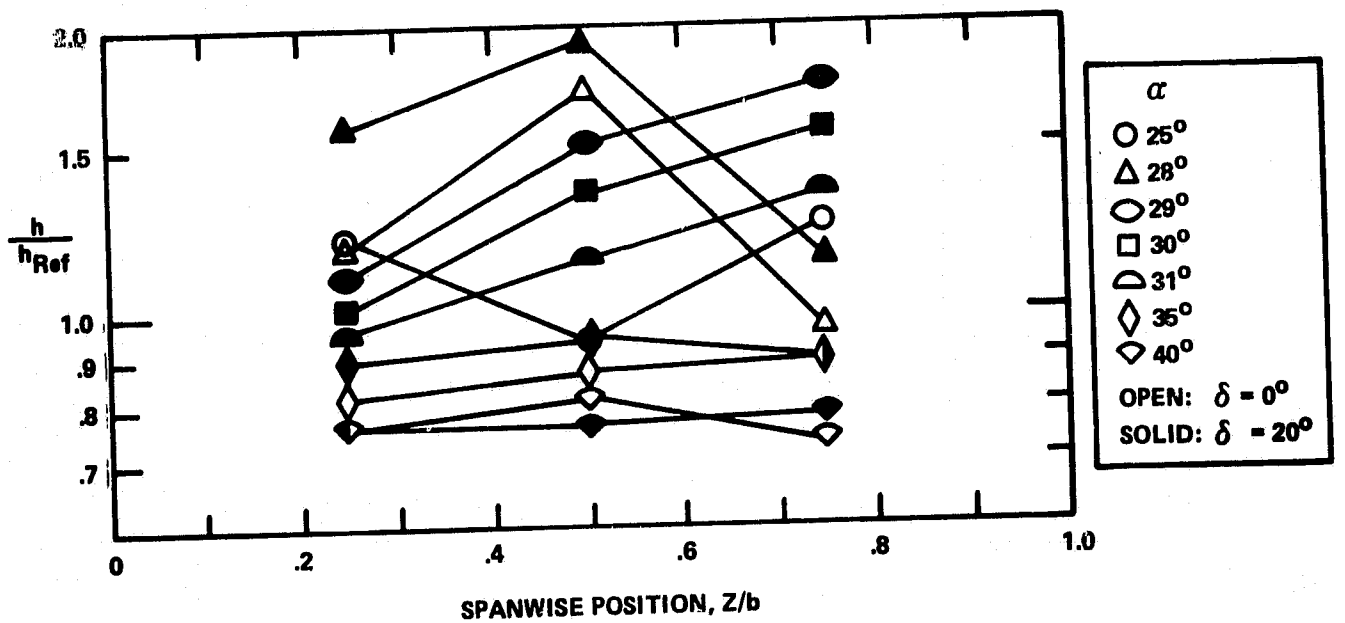

Figure 10 VARIATION OF HEAT TRANSFER ALONG LEADING EDGE AT M_∞ = 10.1, β = 0°

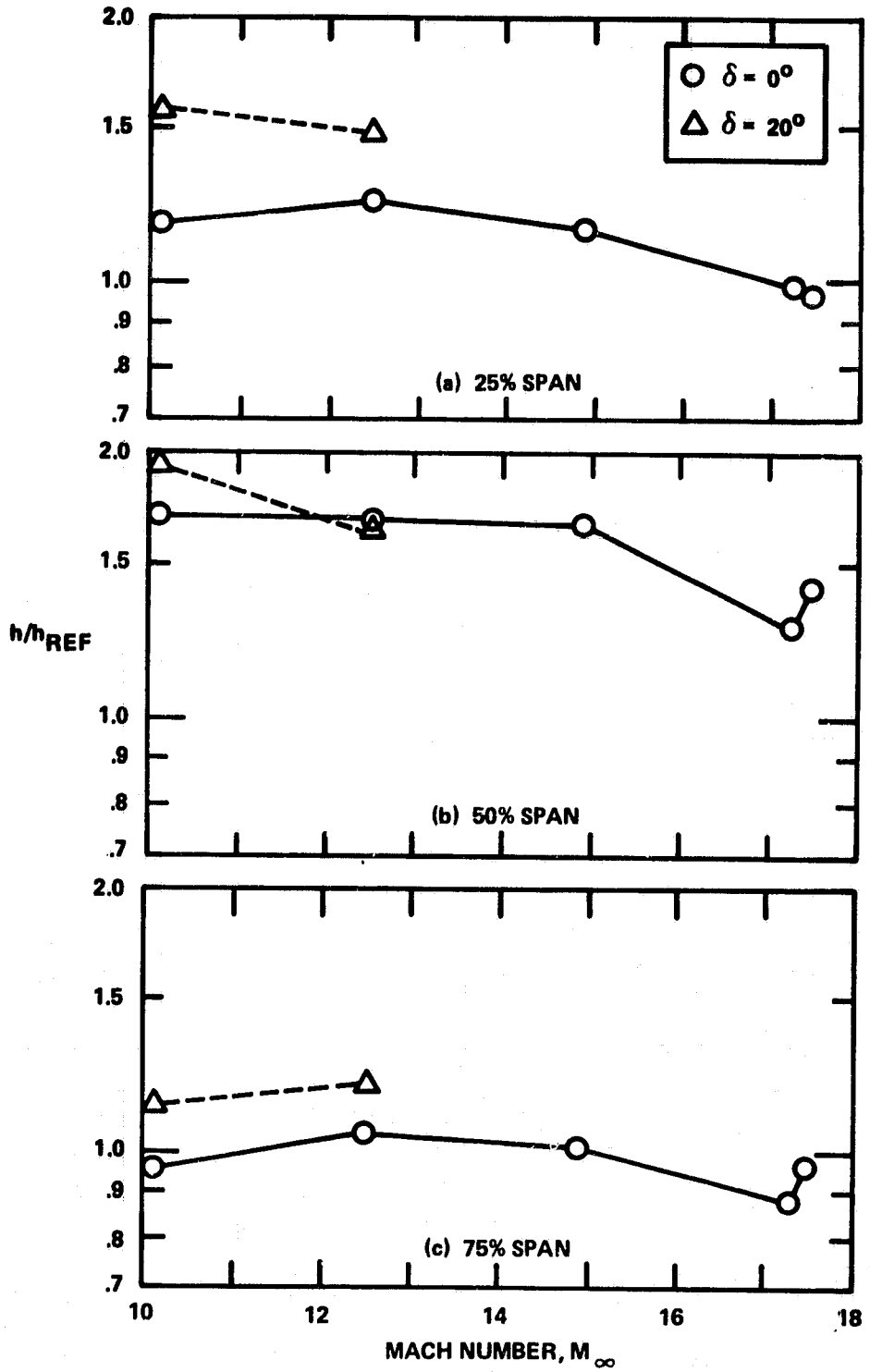

Figure 11 VARIATION OF LEADING EDGE HEAT TRANSFER WITH MACH NUMBER AT $\alpha = 28^{o}$, $\beta = 0^{o}$

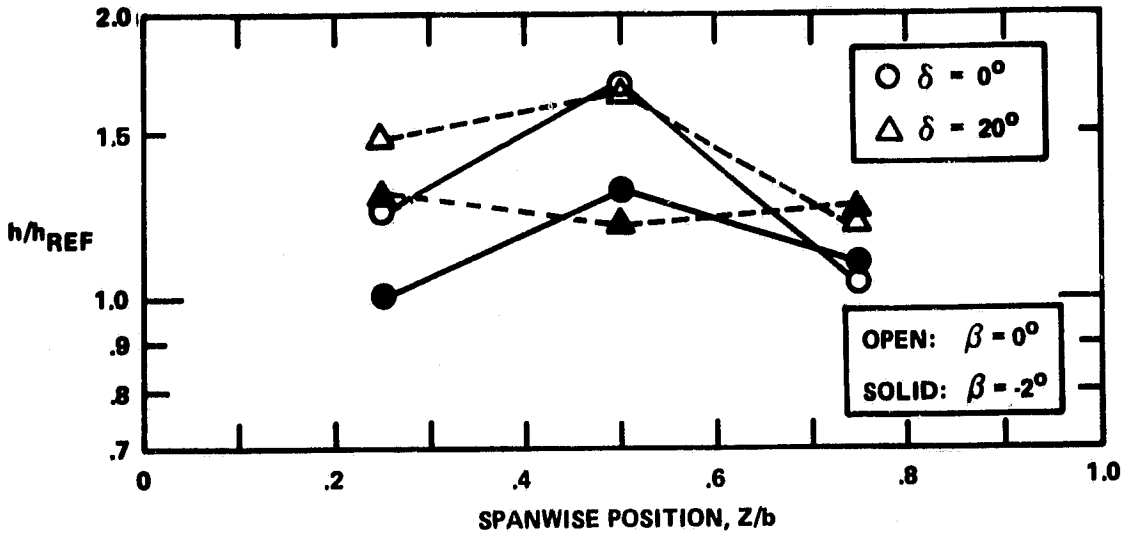

Figure 12 VARIATION OF LEADING EDGE HEAT TRANSFER WITH SIDESLIP AT M_∞ = 12.5, α = 28°

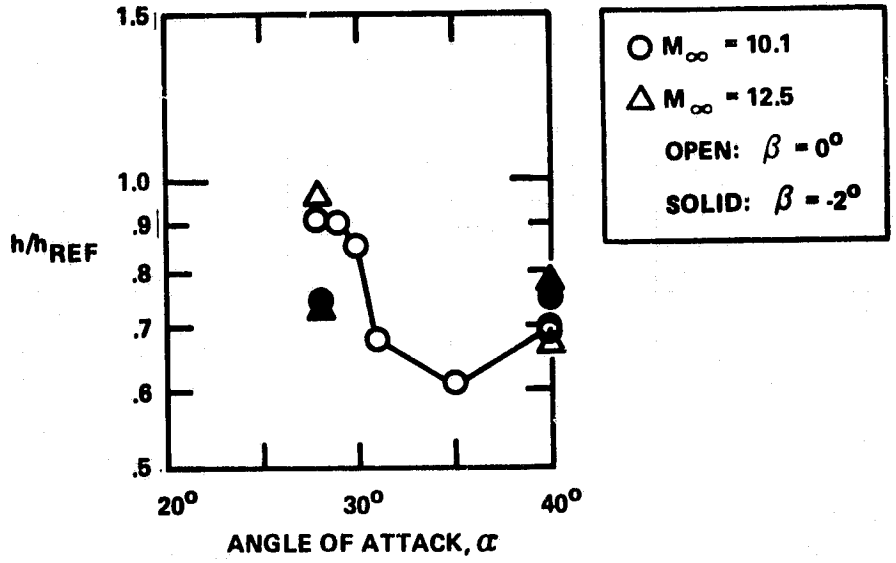

Figure 13 HEAT TRANSFER TO BOTTOM EDGE OF DEFLECTED CONTROLLER - 55% CHORD

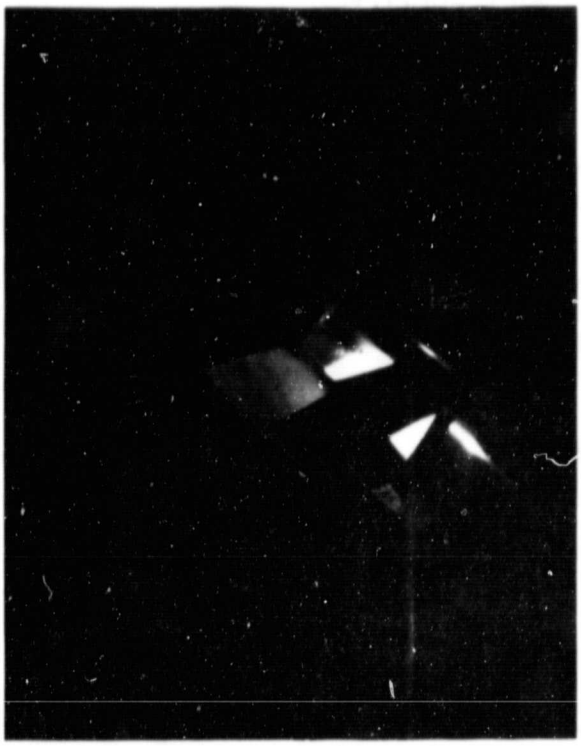

(a) TARE PICTURE

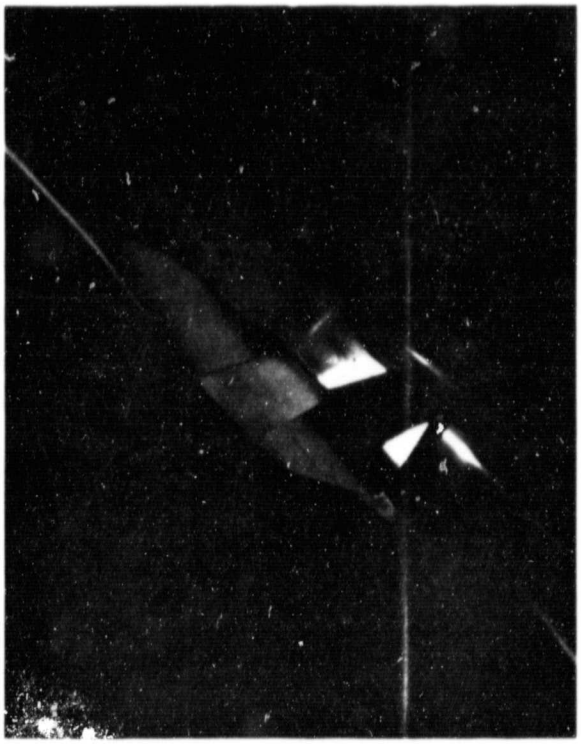

(b) TEST PICTURE

Figure 14 PHOTOGRAPHS FROM PHASE I RUN 9; M_∞ = **14.8,** α = **40°**

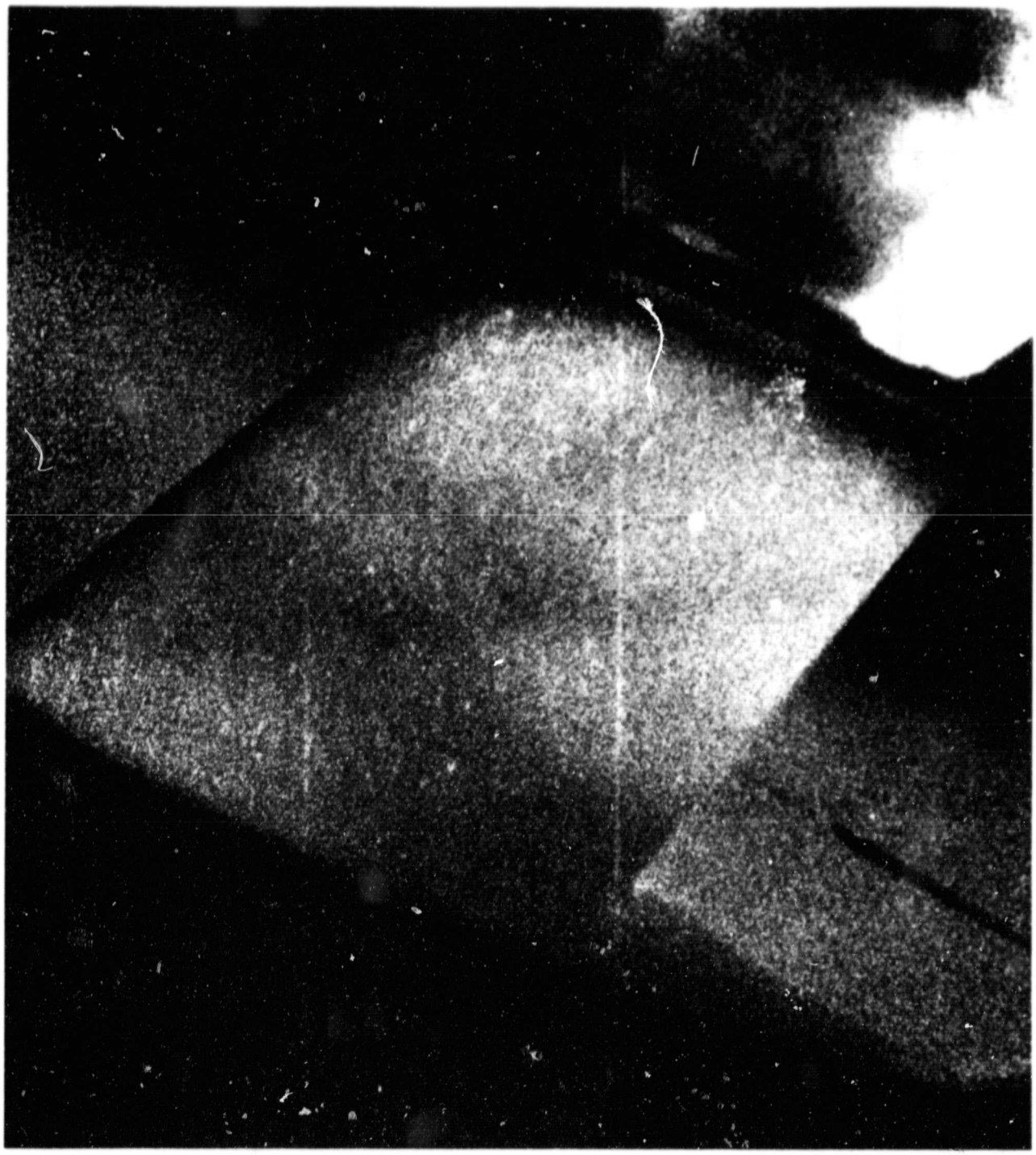

Figure 15 THERMOGRAPHIC PHOSPHOR PHOTOGRAPH OF UNDEFLECTED TIP-FIN CONTROLLER; $M_\infty = 14.8$, $\alpha = 40^o$

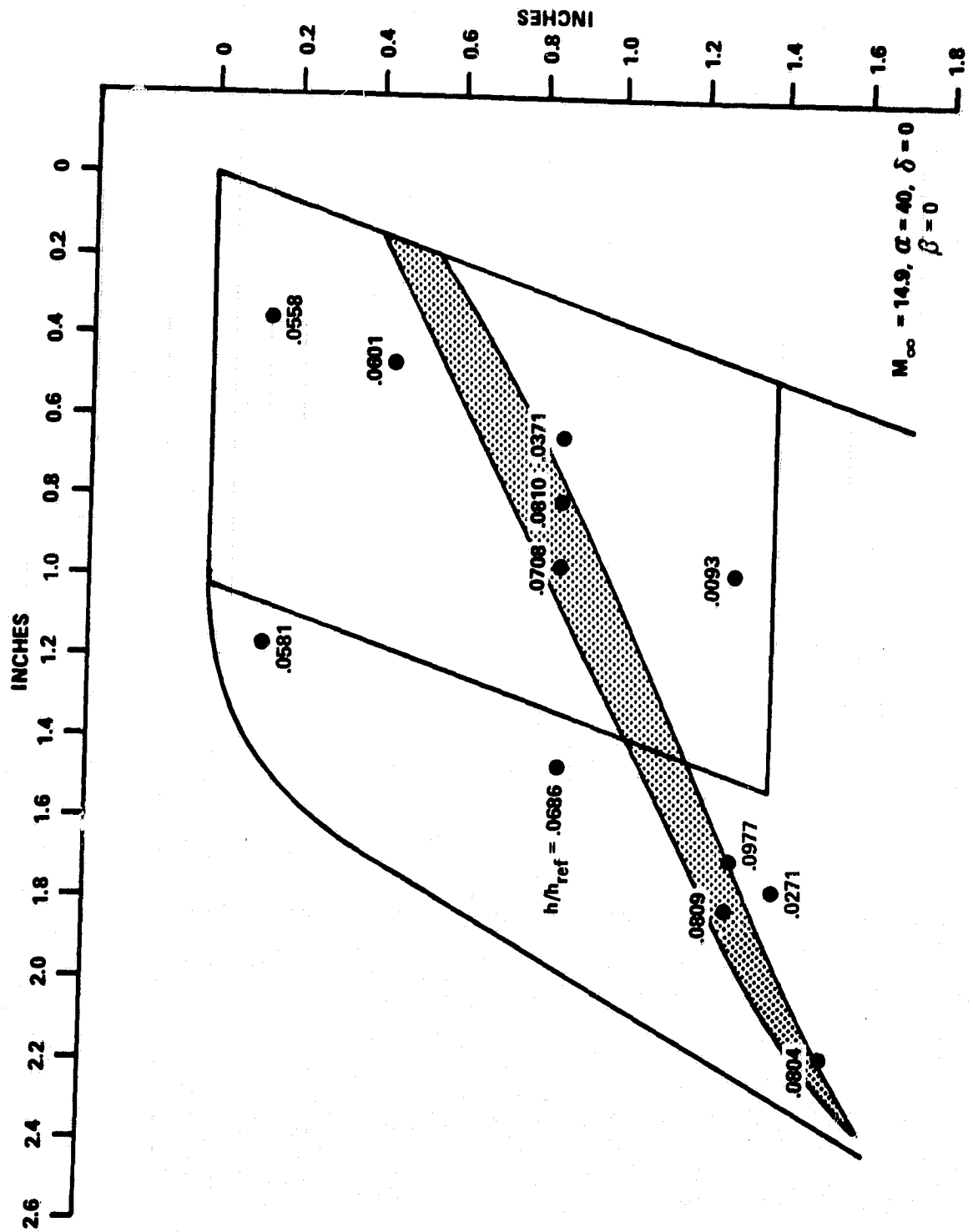

Figure 16 COMPARISON OF PHASE I AND PHASE II RESULTS FOR $\delta = 0^0$

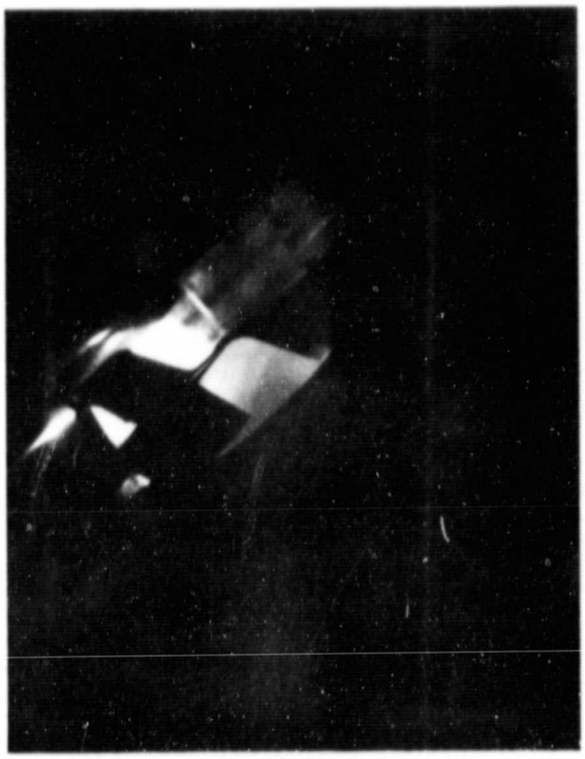

(a) TARE PICTURE

(b) TEST PICTURE

Figure 17 PHOTOGRAPHS FROM PHASE I RUN 5; $M_\infty = 10$, $\alpha = 40^o$

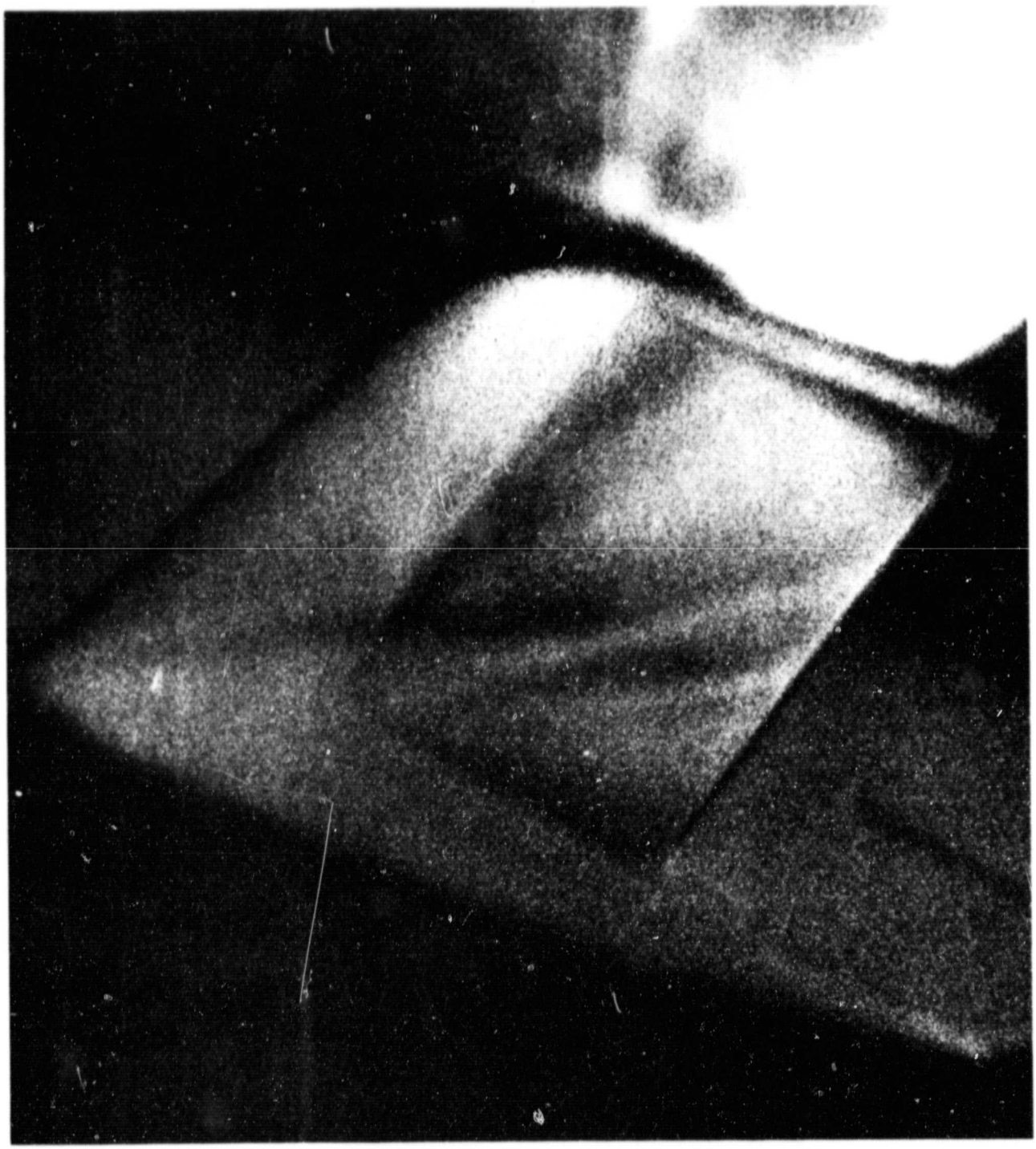

Figure 18 THERMOGRAPHIC PHOSPHOR PHOTOGRAPH OF TIP-FIN CONTROLLER DEFLECTED 20^{o}; M_{∞} = 10, = 40^{o}

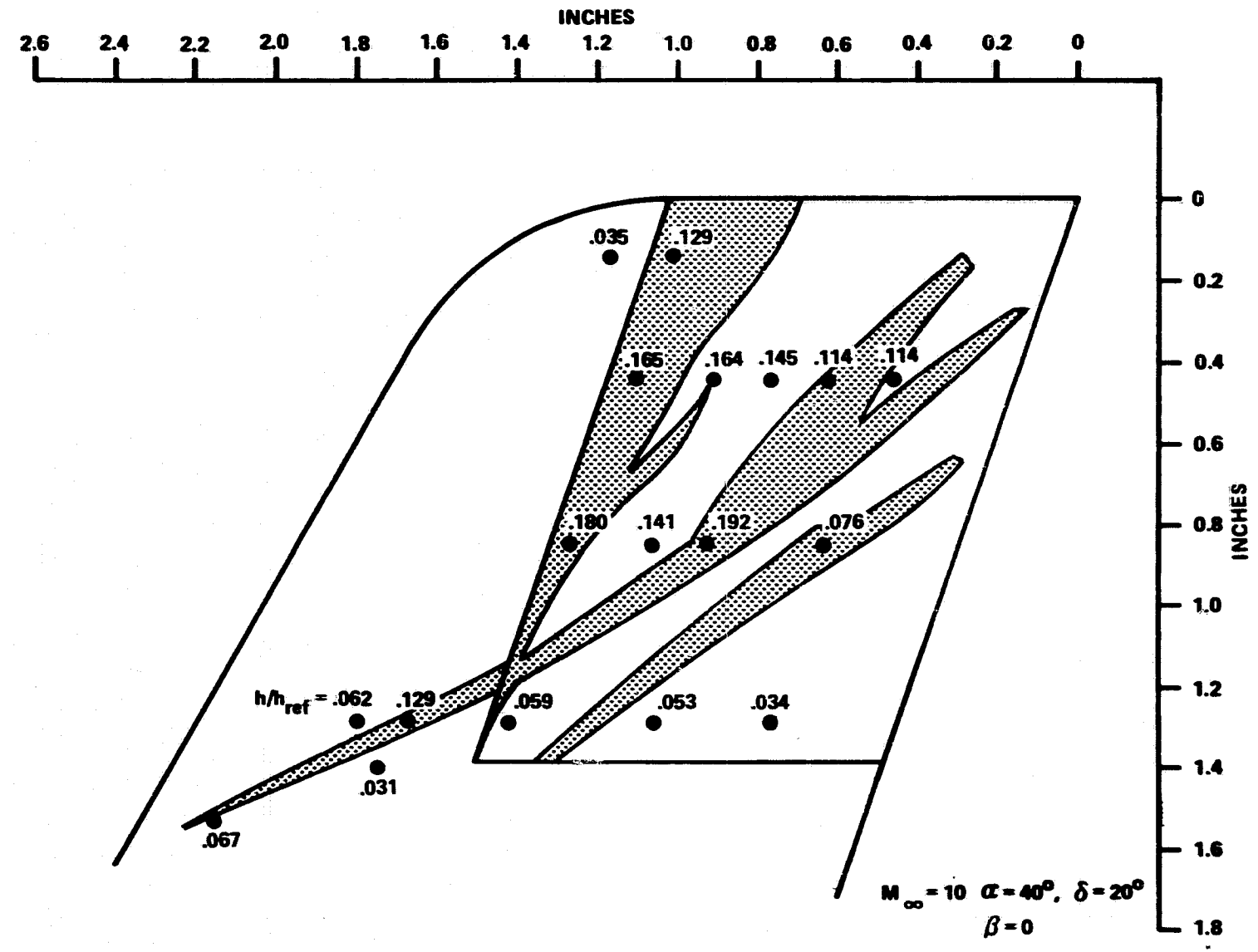

Figure 19 COMPARISON OF PHASE I AND PHASE II RESULTS FOR $\delta = 20^{o}$

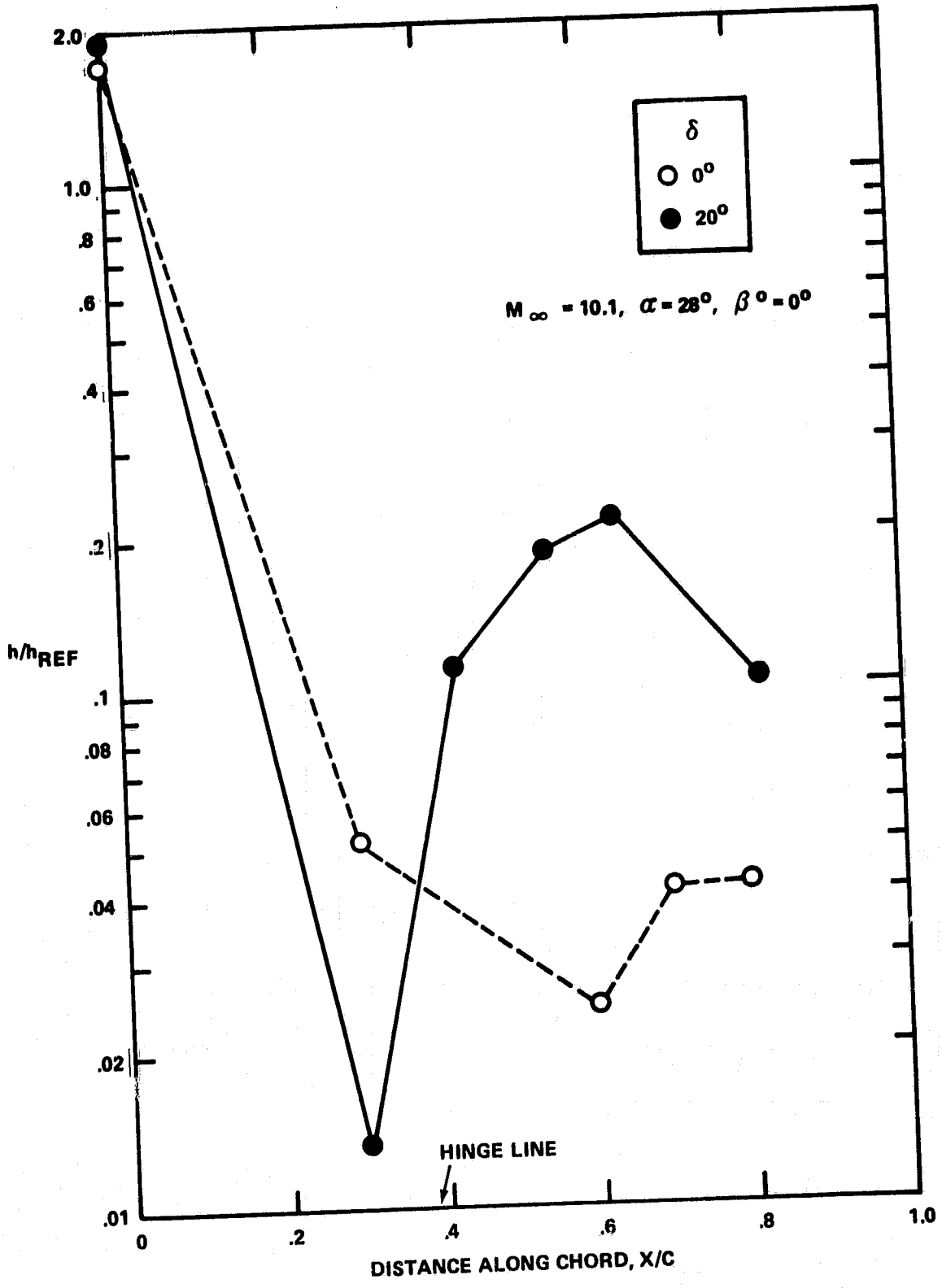

Figure 20 COMPARISON OF HEAT TRANSFER AT 50% SPAN FOR $\delta = 0^{o}$ AND 20^{o}

C-2

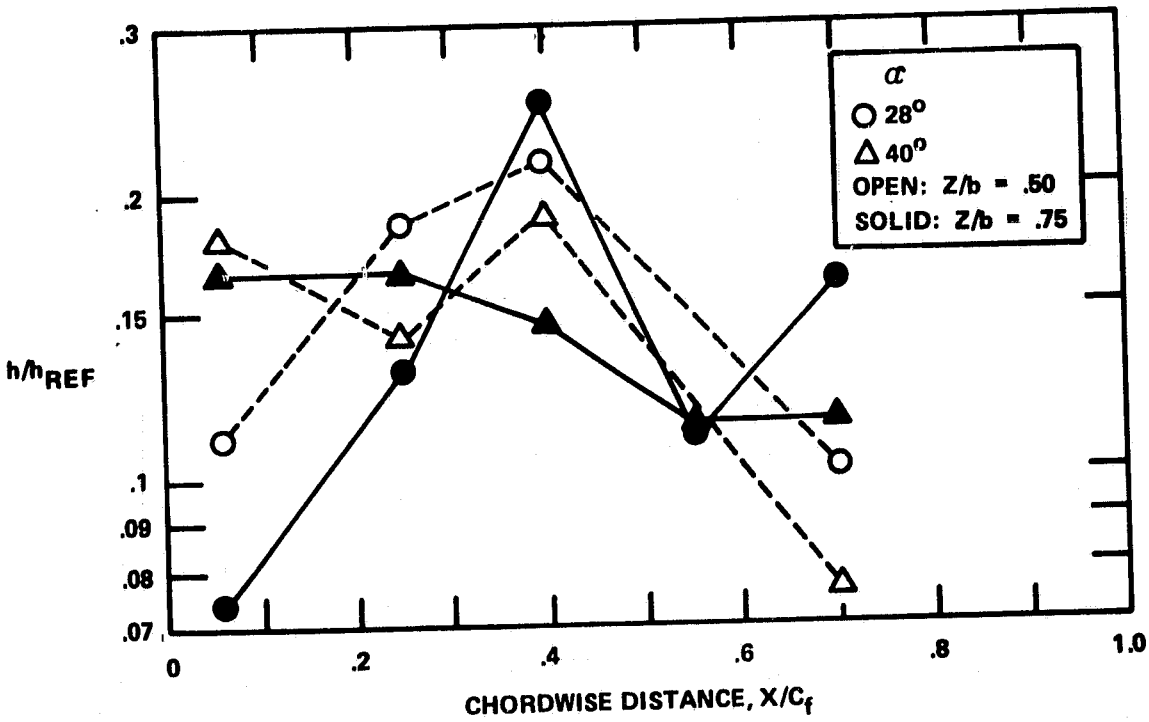

Figure 21 HEAT-TRANSFER DISTRIBUTION ON DEFLECTED CONTROLLER AT $M_\infty = 10.1$, $\beta = 0^o$

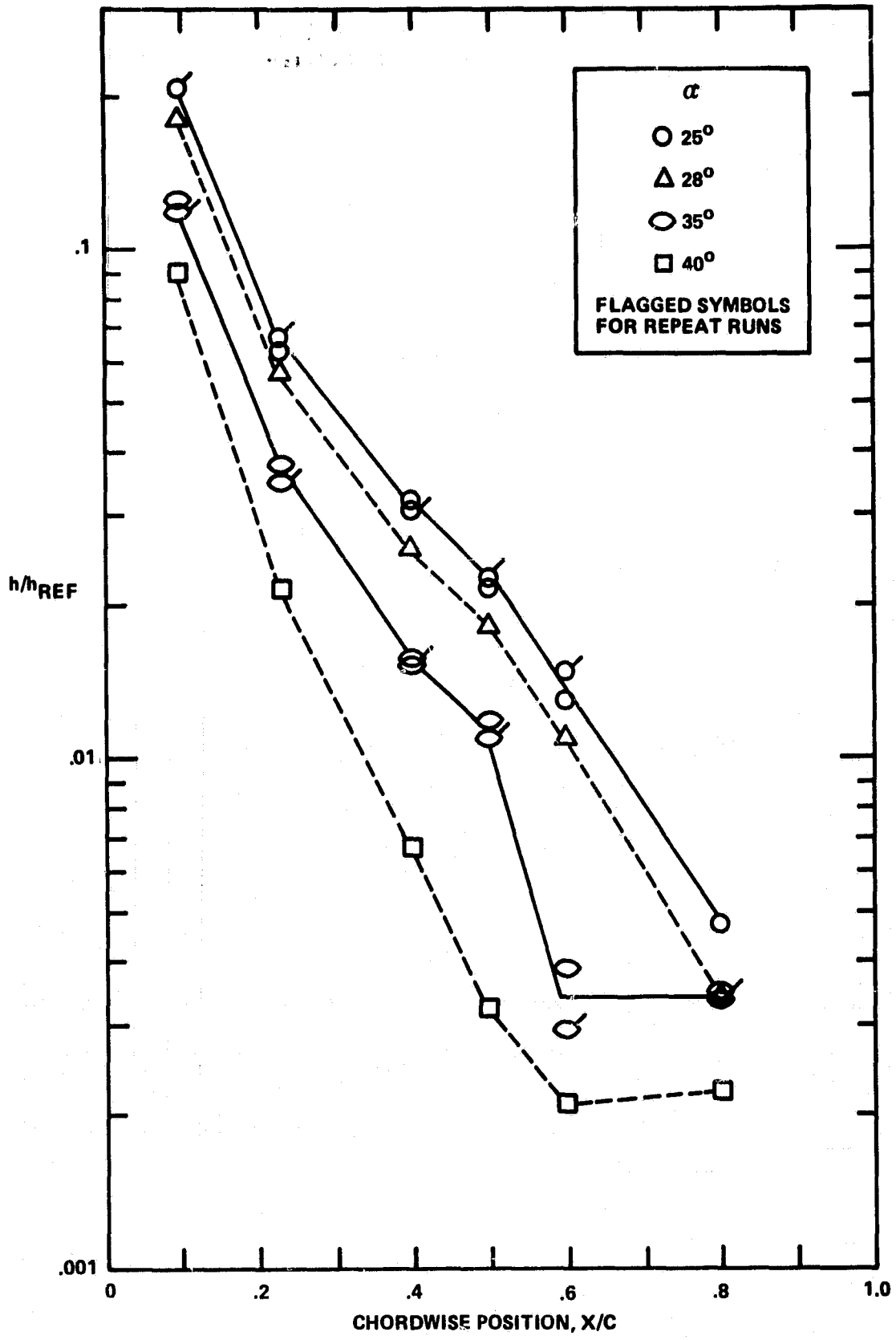

Figure 22 HEAT-TRANSFER DISTRIBUTION TO INBOARD SURFACE AT Z/b = 0.17 AND M_∞ = 10.1

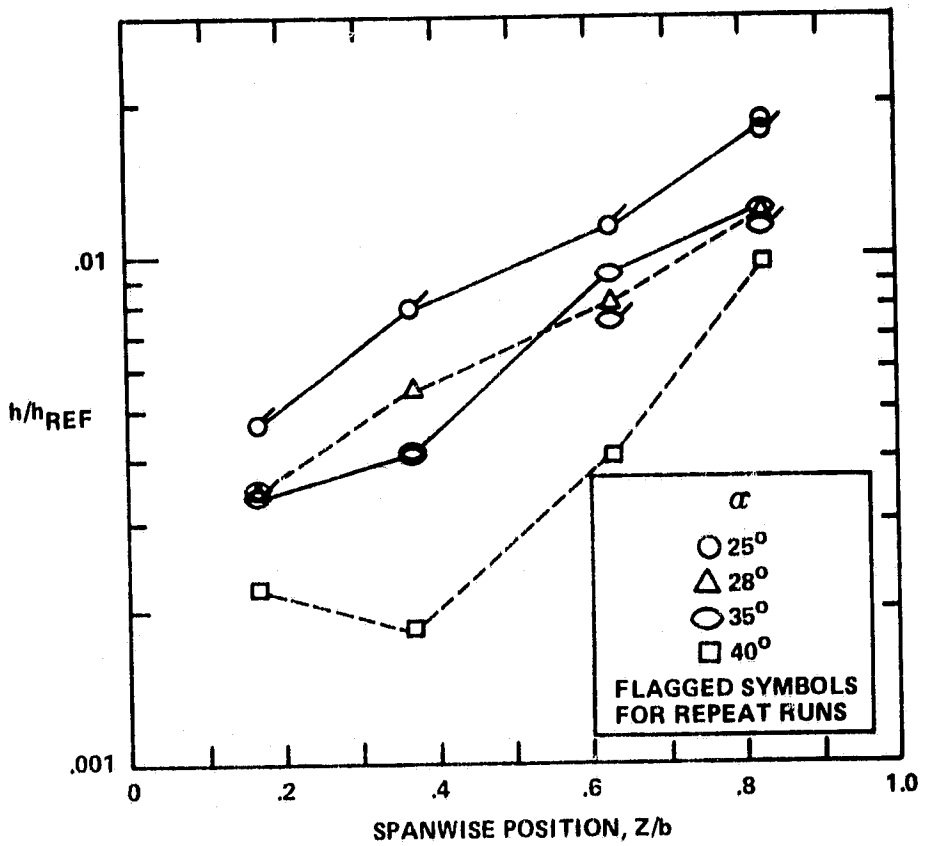

Figure 23 HEAT-TRANSFER DISTRIBUTION TO INBOARD SURFACE AT X/C = 0.80 AND M_∞ = 10.1

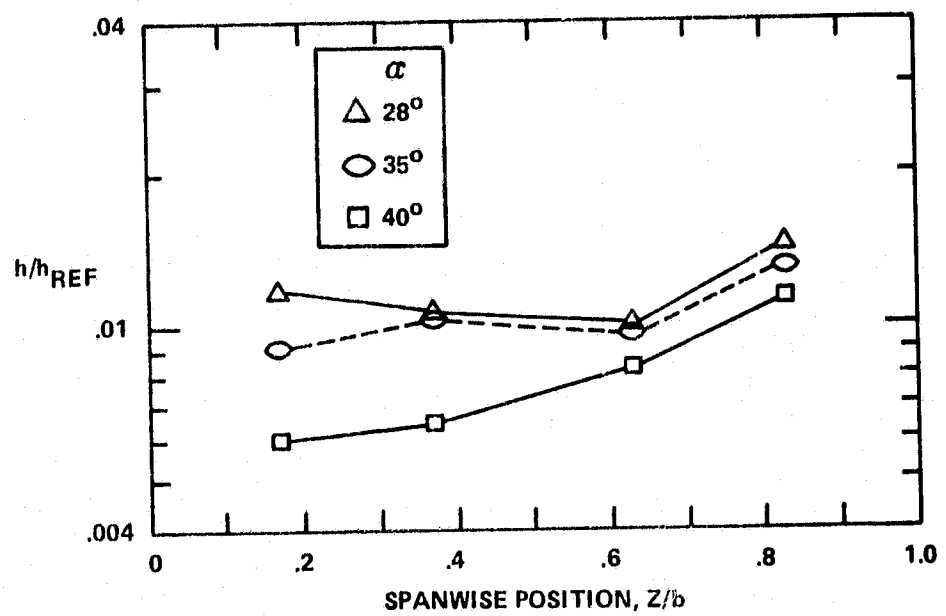

Figure 24 HEAT-TRANSFER DISTRIBUTION TO INBOARD SURFACE AT X/C = 0.80 AND M_∞ = 17.5